ANALYSIS OF TELOMERE MAINTENANCE MECHANISMS IN THE ROUNDWORM
CAENORHABDITIS ELEGANS

Ludmila Shtessel

A dissertation submitted to the faculty of the University of North Carolina at Chapel Hill in partial fulfillment of the requirements for the degree of Doctor of Philosophy in the Curriculum of Genetics and Molecular Biology.

Chapel Hill
2012

Approved by:

Shawn Ahmed, Ph.D.

Christopher Counter, Ph.D.

Jeff Sekelsky, Ph.D.

Michael Jarstfer, Ph.D.

Dale Ramsden, Ph.D.

ABSTRACT

LUDMILA SHTESSEL: Analysis of telomere maintenance mechanisms in the roundworm
Caenorhabditis elegans
(Under the direction of Dr. Shawn Ahmed)

The ends of linear chromosomes are composed of repetitive hexameric sequences called

telomeres. Because canonical DNA polymerases cannot fully replicate the ends of linear

chromosomes, they shorten with each cycle of replication. Once telomeres become critically

short, cells stop replicating and enter a state of replicative arrest—senescence. In this way,

telomere length limits the replicative potential of all cells. The enzyme telomerase can maintain

telomere length by adding *de novo* telomeric repeats via reverse transcription from an associated

RNA template. Although telomerase expression is exclusive to human somatic and germ stem

cells, its expression in somatic stem cells is not sufficient to prevent telomere erosion. Therefore,

telomeres shorten with age, effectively serving as a mitotic clock. As in mammals, components of

the *C. elegans* 9-1-1 (HPR-9/MRT-2/HUS-1) DNA damage response complex and its clamp

loader, HPR-17, are necessary for telomerase-mediated telomere repeat addition *in vivo.* Here we

present the mapping and characterization of three new telomerase-defective alleles of *mrt-2*, *hpr-*

17, and *hpr-9*, and a mutation in a novel gene, all of which possess defects in repairing ionizing

radiation- and interstrand crosslink-induced DNA damage. In addition to telomerase, several

canonical telomere-binding proteins and other associated proteins maintain telomere length

homeostasis and protect chromosome ends from exacerbated erosion and erroneous DNA damage

responses in humans. *C. elegans* harbors four homologs of the human Protection of Telomeres 1

(POT1) telomere capping protein, POT-1, POT-2, POT-3 and MRT-1. Here I identify POT-1 and

POT-2 as negative regulators of telomerase-mediated telomere repeat addition *in vivo*. I demonstrate that POT-1, but not POT-2, protects telomeres from exacerbated erosion. I employ several biochemical strategies to assess whether POT-1 or POT-2 interact with telomerase *in vivo*. Although an epitope-tagged *pot-1* transgene rescued the telomere elongation phenotype of the *pot-1* mutant, it exacerbated the onset of senescence in mutants defective for telomerase-mediated telomere repeat addition. We suggest that alterations in telomere capping proteins may drive telomere dysfunction in telomerase-negative cells, which may help to define causal mutations for patients suffering from diseases of premature aging with undefined etiologies.

DEDICATION

Given that I am now not only a self-proclaimed geneticist but also a UNC-proclaimed one, I cannot ignore the reason for who I am, why I am, and where I am today: my genes. And until 3 decades ago, my parents were the sole protectors of those genes, which were clearly well maintained until my arrival. During the pursuit of my doctorate, I became even more enamored with the genome and its simplicity and self-preservation. During that time I also entered into a compromise, with the help of Matt Ridley's *Nature via Nurture*, with the rest of the world— acknowledging that, yes, you too have a hand in my destiny. However, as it turns out, my parents also raised me, pushing me towards positive experiences and protecting me from nasty ones. So, without a doubt, I attribute most of my talents, successes, and personal proclivities to my parents—the nature *and* the nurture—who risked so much. I dedicate this doctorate to them with the hope that this can be one piece of assurance that their struggle was not for nothing.

PREFACE

The successes of my efforts presented in this thesis have greatly benefited from several collaborators. A technician, Yan Liu, and a graduate student, Dr. Julie Hall, participated in the *Mortal germline* screens, including passaging animals for sterility and assessing for the presence of end-to-end fusions, that yielded the mutants discussed in Chapter 1. Yan Liu mapped the initial, approximate locations of *yp7* and *222g*, and Dr. Hall mapped the initial, approximate location of *279* as well as analyzed telomeres of *279* mutants, shown in Figure 1.2C. In the later stages of *279* mapping, an extremely hard-working and persevering undergraduate-turned-PharmD UNC student, Ashley Hedges, participated in the SNP mapping that narrowed the ultimate *279* candidate list to 29 genes. The mapping of *yp8* appears in the following publication and is reproduced with the permission of the publisher:

> Chen Cheng, Ludmila Shtessel, Megan M. Brady, and Shawn Ahmed. Caenorhabditis elegans POT-2 telomere protein represses a mode of alternative lengthening of telomeres with normal telomere lengths. Proc Natl Acad Sci USA. 2012

I employed many transgenic animals in the biochemistry and mutant analysis presented in Chapters 2 and 3. A graduate student, Matt Simon, and a technician, Kyle Wang, participated in the construction of all the transgenes and their insertion into animals.

Chapter 3 describes the analysis of several mutants, which was initially performed by a graduate student, Dr. Mia Lowden. Dr. Lowden genotyped the *pot-1* and *pot-2*

mutants to confirm the presence of their respective mutations and analyzed their telomeres, shown in Figure 3.1B & C. The first five figures of this chapter have been published and are reproduced with the permission of the publisher:

Ludmila Shtessel, Mia Rochelle Lowden, Chen Cheng, Matt Simon, Kyle Wang, and Shawn Ahmed. Caenorhabditis elegans POT-1 and POT-2 Repress Telomere Maintenance Pathways. G3 (Bethesda). 2013

TABLE OF CONTENTS

LIST OF TABLES

Table

LIST OF FIGURES

INTRODUCTION

Telomeres and Telomerase

   The ends of linear chromosomes, called telomeres, are comprised of repetitive sequence tracts that function in various ways to maintain chromosome fidelity. In the 1930s, forty years before telomeres were molecularly defined, Herman Muller noticed that the ends of chromosomes were resistant to the detrimental effects of X-rays. He concluded that they must be special, coining the term "telomere" from the Greek words "telos" and "meros", meaning "end part", in the process. Concurrently, Barbara McClintock's work with the variable color patterns in maize led her to define the functional importance of telomeres. She described a "breakage-fusion-bridge cycle" in maize as a continuous loop initiated fusion of two chromosomes, followed by segregation-mediated breakage of dicentric chromosomes, resulting finally in a new fusion of improperly capped chromosome ends that re-enter the breakage-fusion-bridge cycle (McClintock 1939). These kinds of chromosomal dynamics illustrated the crucial function telomeres play in preventing genomic instability.

   Elizabeth Blackburn, as a post-doctoral associate in John Gall's laboratory, was the first to molecularly define the ends of chromosomes in 1978, revealing mysterious repetitive hexameric sequences in *Tetrahymena*, a single-celled ciliate (Blackburn & Gall 1978). Four years later, in collaboration with Jack Szostak, Blackburn cloned telomeres, demonstrating that terminal *Tetrahymena* repeats (TTGGGG) retained their chromosome capping function when placed onto the ends of a linearized yeast chromosome (Szostak & Blackburn 1982). Since then, telomeres from a myriad of organisms have been cloned, comprising different repeats and tract sizes. *Oxytricha* ciliates harbor T_4G_4 tracts spanning 20 bp (Klobutcher *et al.* 1981), TTAGGG repeats

in mice and humans span up to 80 kb and 5-15 kb, respectively (Moyzis *et al.* 1988; Harley *et al.* 1990; Kipling & Cooke 1990; Prowse & Greider 1995; Zhu *et al.* 1998), *Arabidopsis* plants exhibit 2-4 kb-long TTTAGGG tracts (Richards & Ausubel 1988; Riha *et al.* 1998), TTAGGC tracts span 4-9 kb in the roundworm *C. elegans* (Wicky *et al.* 1996), and more complicated TTAC(A)(C)G(1-8) or G(2-3)(TG)(1-6)T repeats comprise telomeric tracts of approximately 300 base pairs (bp) in fission and budding yeasts, respectively (Shampay *et al.* 1984; Murray *et al.* 1986).

Organisms that package their DNA into linear chromosomes are burdened by incomplete replication of chromosome termini. Because conventional DNA polymerases cannot initiate synthesis *de novo* and instead rely on small RNA primers, an obligate gap remains at the 5' ends once the primers are removed (reviewed in Levy *et al.* 1992). This "end-replication problem" results in loss of telomeric DNA with each cell division, along with additional nuclease-mediated telomere processing, until a critically short telomere triggers senescence—a non-dividing state of arrest (Bodnar *et al.* 1998; Hemann *et al.* 2001; Sfeir *et al.* 2005). The enzyme telomerase is tasked with maintaining telomeres by adding telomeric repeats *de novo* via reverse transcription using an RNA template (Greider & Blackburn 1985; Greider & Blackburn 1989). Most human somatic cells do not express telomerase and thus exhibit telomere shortening during cellular replication, which limits their replicative lifespan *in vitro* (Sharma *et al.* 1995; Hayflick & Moorhead 1961; Harley *et al.* 1990). Telomere length is not only indicative of *in vitro* replicative lifespan but also decreases as a function of age *in vivo* (Harley *et al.* 1990; Allsopp *et al.* 1992; Aubert & Lansdorp 2008). Therefore, human lifespans are not actually defined by a temporal clock but rather a "mitotic clock" based on the replicative potential of cells.

Telomere maintenance is the lynchpin in the delicate battle between cancer and organismal aging. While limiting amounts of telomerase result in telomere attrition and eventual cellular senescence, a hallmark of aging tissues, the uncontrolled expression of telomerase that occurs in most cancer cell lines is one of the necessary steps to unabated replication (reviewed in

Shay & Wright 2011; Kim *et al.* 1994). Proper telomere length homeostasis is maintained in part by canonical telomere-binding proteins and other associated components.

In mammals, the shelterin complex, composed of the six canonical telomere proteins TRF1, TRF2, POT1, TIN2, TPP1, and RAP1, maintains the integrity and length of telomeres (reviewed in Palm & de Lange 2008 and in Diotti & Loayza 2011). TRF1 and TRF2 both bind the duplex telomeric DNA and negatively regulate telomere length (van Steensel & de Lange 1997, Smogorzewska *et al.* 2000). While over-expression of TRF2 drives telomere attrition in culture, it also protects telomeres from fusion, underscoring both critical roles of TRF2 in telomere biology (Karlseder *et al.* 2002; Richter *et al.* 2007). TRF2 conditional and dominant negative alleles in mammals induce end-to-end chromosomal fusions, extrachromosomal circles, telomere rapid deletion events, and an increase in sister chromosome exchange (reviewed in Longhese 2008; Wang *et al.* 2004; Li *et al*. 2008). A TRF2 binding partner, RAP1 also exerts a negative force on telomere length but does not bind DNA directly (Li *et al*. 2003; O'Connor *et al.* 2004). Curiously, over-expression of wildtype RAP1, or RAP1 truncation mutants that do not localize to telomeres, prompted telomere elongation in cultured human cells (Li *et al*. 2000; Li *et al.* 2003), which the authors suggest as an indication that RAP1 may titrate a negative regulator of telomere length away from the telomere when present in excess.

Although TRF1 and TRF2 do not directly bind each other, they are both bound by TIN2, which connects the single-stranded telomeric binding protein POT1 to the telomeric duplex via an interaction with TPP1 (Ye *et al.* 2004; Kim *et al.* 2004). TIN2 also negatively regulates telomere length, and can dramatically affect the stability of the shelterin complex on telomeres via its direct interactions with multiple components (Kim *et al.* 1999; Kim *et al.* 2004). TPP1, which bridges POT1 and TIN2, exerts regulation on telomere length through its interaction with POT1 and TIN2 (Liu *et al.* 2004). Knock-down of TPP1, as well as expression of TPP1 mutants unable to bind either POT1 or TIN2, results in telomere elongation in cultured human cells (Ye *et al.* 2004; Liu *et al.* 2004; O'Connor *et al.* 2006), suggesting that TPP1 must localize to telomeres to

3

inhibit elongation, which it does so via POT1. POT1 binds single stranded telomeric DNA and TIN2 directly and exerts both positive and negative regulation on telomere length (Liu *et al.* 2004; Lei *et al.* 2005). Critically, POT1 also protects telomeres from eliciting a DNA damage response, which requires TIN2-mediated recruitment (Takai *et al.* 2011).

C. elegans has four proteins with homology to human POT1: POT-1, POT-2, POT-3, and MRT-1. MRT-1 positively regulates telomere length, while POT-3 appears dispensable. My work in Chapter 3 describes the roles of *C. elegans* POT-1 and POT-2, which are negative regulators of telomere length, in telomere maintenance. Surprisingly, I show that an epitope-tagged *pot-1* transgene rescues *pot-1* mutant defects but exacerbates the onset of senescence in telomerase mutants. This work is the basis for the remainder of this introduction, where we propose the existence of two telomere dysfunction-associated disease states—one that is directly caused by mutations in proteins that promote telomerase activity, including telomerase itself and one that is accompanied by telomere shortening that remains to be directly attributable to dysfunctional telomere biology, the pathologies of which we hypothesize may occur due to dysfunction specifically in telomerase-deficient cells.

Human diseases of telomere dysfunction

Dyskerin was the first telomerase component to be causally identified in human disease (Heiss *et al.* 1998). Dyskerin participates in the stability and maturation of small nucleolar RNAs (snoRNAs) by binding to an H/ACA motif, and its binding to this motif at the 3' end of human telomerase RNA (hTR) is required for hTR's biogenesis and stability (Mitchell *et al.* 1999a; Mitchell *et al.* 1999b). This disease, dyskeratosis congenita (DC), was the first disease with a molecularly defined cause seeded in telomere biology (Heiss *et al.* 1998). DC is diagnosed predominantly within the first 10-20 years of life by the presence of two of three classical symptoms—nail dystrophy, skin hyperpigmentation, and oral leucoplakia—and bone marrow

failure (reviewed in Dokal 2011). The vast majority of patients die prematurely from bone marrow failure, followed by pulmonary disease and cancer.

DC patients without mutations in dyskerin harbor mutations in other proteins that function directly in telomere biology, including heterozygous, homozygous and biallelic mutations in the telomerase reverse transcriptase (TERT) (Vulliamy et al. 2005; Marrone *et al.* 2007), heterozygous mutations in the telomerase RNA (encoded by *TERC*) (Vulliamy *et al.* 2001), homozygous mutations in both NOP and NHP2, which are similar to dyskerin in their RNA-binding and telomerase stabilization functions (Walne *et al.* 2007; Vulliamy *et al.* 2008), heterozygous mutations in *TINF2,* which encodes the shelterin component TIN2 (Savage *et al.* 2008; Walne *et al.* 2008), biallelic mutations in a trafficking protein, TCAB1, which transports the telomerase holoenzyme to sites of RNA processing called Cajal bodies (Zhong *et al.* 2011; Venteicher *et al.* 2009), and homozygous mutations in the gene *C16orf*57*,* which remains poorly characterized (Walne *et al.* 2010).

Several other syndromes, including Hoyeraal-Hreidarsson (HH), Revesz, Rothmund-Thomson (RTS), PN (p̲oikiloderma with n̲eutropenia), Coats' plus, and myelodysplastic syndrome (MDS) are characterized by a subset of pathologies seen in DC patients. HH is considered a severe form of DC, where patients exhibit DC-like symptoms, such as bone marrow failure, at an earlier age accompanied by intrauterine growth retardation, microcephaly, and cerebellar hypoplasia, resulting in premature mortality within the first decade of life (Touzot *et al.* 2011; reviewed in Dokal 2011). RTS patients characteristically exhibit poikiloderma (a skin rash) and short stature that typically present within the first 2 years of life (reviewed in Larizza *et al.* 2010). A myriad of other heterogeneous features, including thin hair, cataracts and retinal defects, dental abnormalities, nail dystrophy, and skeletal abnormalities, also can appear at a prematurely young age. Strikingly, RTS patients do not live shorter lives if cancer is avoided. Coats' plus disease is marked by telangectasias (small blood vessels) in the eye, cataracts and even eventual blindness, growth retardation, brain calcifications, and other bone abnormalities quite similar to

RTS. Some patients also exhibit coarse and sparse hair with eventual premature hair graying, dystrophic nails, aplastic anemia, and ataxia (reviewed in Crow *et al.* 2004; Savage *et al.* 2012).

Identification of dyskerin, *TINF2,* and *TERT* mutations in Hoyeraal-Hreidarsson (HH) patients underlines the molecular connection among these complex and heterogeneous pathologies (Knight *et al.* 1999; Marrone *et al.* 2007; Walne *et al.* 2008). Additionally, heterozygous mutations in *TINF2* have been observed in Revesz syndrome patients (Walne *et al.* 2008; Sasa *et al.* 2012). Causal heterozygous mutations in *TERC* and *TERT* have been identified in patients with AA and MDS (Vulliamy *et al.* 2002; Yamaguchi *et al.* 2003; Yamaguchi *et al.* 2005) as well as in patients with idiopathic pulmonary fibrosis, liver cirrhosis, and leukemia (Tsakiri *et al.* 2005; Armanios *et al.* 2007; Diaz *et al.* 2010; Calado *et al.* 2009; Dokal 2011). RTS and PN patients also harbor homozygous mutations in *C16orf57* (Volpi *et al.* 2010; Walne *et al.* 2010; Clericuzio *et al.* 2011). Most recently, biallelic mutations in *CTC1*, a single-stranded telomeric DNA-binding protein, were identified in 16 Coats' plus patients (Anderson *et al.* 2012). Mammalian CTC1 forms a heterotrimeric complex with STN1 and TEN1, which localizes to telomeres in mice and human cells and binds ssDNA telomeric DNA *in vitro* (Miyake *et al.* 2009).

While these diseases are separable, they exhibit vast overlaps in pathologies. Moreover, although these diseases can be distinguished molecularly, overlap there exists as well. This overlap in etiology suggests an underlying pathology that may be caused from directly perturbing telomere maintenance, whether by mutation of telomerase holoenzyme components or by mutations in telomere-binding proteins. In particular, telomere dysfunction appears to affect a specific subset of tissues, such as blood cells (red and white), the lungs, liver, skin, bones and hair. These tissues may represent somatic stem cells that harbor the highest levels of telomerase activity or the highest rates of cell turnover (Chiu *et al.* 1996; Kilian *et al.* 1997; Kolquist *et al.* 1998) and thus are most sensitive to perturbations to telomere maintenance. In fact, families segregating *TERC* or *TERT* mutations can display anticipation, where the next generation exhibits

an earlier and more severe onset of symptoms due to inheriting both the *TERC* or *TERT* mutation and short telomeres, indicating that telomere maintenance is affected in germ cells (Vulliamy *et al.* 2004; Armanios *et al.* 2005; Goldman *et al.* 2005; Basel-Vanagaite et al. 2008). Given the molecular and pathological overlaps between DC and these other diseases, the 40% of DC cases that remain molecularly undefined are likely attributable to components with major functions in telomere biology (reviewed in Dokal 2011).

Human diseases of accelerated aging

Several human diseases of premature aging, such as Werner syndrome (WS) and Hutchinson-Gilford progeria, are accompanied by short telomeres, but proteins with canonical functions in telomere biology have yet to be implicated in their etiology (Ishikawa *et al.* 2011; Decker *et al.* 2009; Allsopp *et al.* 1992). Cultured fibroblasts from Werner and HGPS patients exhibit telomere shortening and senesce prematurely (Faragher *et al.* 2003; Huang *et al.* 2008), which can be overcome with telomerase expression (Wyllie *et al.* 2000; Choi *et al.* 2001; Benson *et al.* 2010), providing a compelling argument for telomere involvement in the pathology of these syndromes. Moreover, telomerase-positive cells from WS patients do not senesce prematurely (James *et al.* 2000), again indicating that telomerase activity may participate in mechanisms that regulate the premature cellular senescence observed in WS patients.

Homozygous mutations in *WRN*, a homolog of the RecQ family of DNA helicases, are responsible for the majority of WS cases (Yu *et al.* 1996; Oshima *et al.* 1996; Sogabe *et al.* 2004; Huang *et al.* 2006). WRN is a DNA helicase, one of several human homologs of the *E. coli* RecQ DNA helicase, that also harbors exonuclease activity (Gray *et al.* 1997; Huang *et al*. 1998). WRN has a myriad of roles in mediating the repair of and response to DNA damage, and it does so through acting at several targets, such as stalled replication forks, Holliday junctions, and G-quadruplex structures (Patro *et al.* 2011; Machwe *et al.* 2011; Phillips & Sale 2010; Constantinou et al. 2000; Fry & Loeb 1999; Baynton *et al.* 2003; Ghosh *et al.* 2009). WRN also associates with

known telomeric proteins, such as Ku, TRF2, and POT1 (Cooper *et al.* 2000; Li & Comai 2000; Opresko *et al.* 2002; Ghosh *et al.* 2009; Machwe *et al.* 2004) and participates in some aspects of telomere biology, such as excision of loops of telomeric DNA (t-loops) from chromosome ends and suppressing telomeric sister chromatid exchanges (t-sce) (Opresko *et al.* 2004; Opresko *et al.* 2005; Machwe *et al.* 2004; Hagelstrom *et al.* 2010; Li *et al.* 2008). WS patients are characterized by short stature in their teens and typically begin to manifest other features, including thinning and graying hair, skin atrophy, cataracts, osteoporosis, diabetes, atherosclerosis and mesenchymal or epithelial cancer after the third decade of life (reviewed in Muftuoglu *et al.* 2008). Cancer and heart attack are the predominant causes of premature death in patients in their 50s.

Although numerous studies have shown short telomeres in WS cells and patients, whether telomere length or shortening rate is causal to WS pathologies is still contentious (Schulz *et al.* 1996; Baird *et al.* 2004). Work in *Wrn*-deficient mice supports a role for telomeres in WS pathology. Mice lacking *Wrn* not display overt premature aging phenotypes (Lebel & Leder 1998; Lombard *et al.* 2000), but telomerase mutants do after multiple generations (Lee *et al.* 1998). Strikingly, introducing deficiencies for *Wrn* into mice lacking the telomerase RNA, *Terc*, dramatically exacerbated the pathologies of $Terc^{-/-}$ mice, including early-onset sterility, reduction in lifespan, growth retardation, gastrointestinal defects, wound healing defects, and increased cancer incidence (Du *et al.* 2004; Chang *et al.*). Moreover, splenocytes cultured from $Wrn^{-/-}$ mice do not prematurely senesce in culture, whereas $Wrn^{-/-}$ fibroblasts do, perhaps indicating a telomerase-dependent effect (Lebel & Leder 1998; Lombard *et al.* 2000). Thus, pathologies of human WS patients are likely affected by telomere shortening, but current models suggest that this is not the sole form of age-related stress that is repressed by WRN.

Approximately 20% of WS patients do not carry any identifiable mutations in WRN and instead are said to exhibit atypical Werner syndrome. Of these atypical WS cases, 15% harbor mutations in *LMNA* (Chen *et al.* 2003; Doh *et al.* 2009; Renard *et al.* 2009; reviewed in Muftuoglu *et al.* 2008). *LMNA* encodes two primary lamin isoforms—A and C, which are major

structural components of the nuclear envelope. Lamin A is initially translated into the precursor prelamin A, which is modified and consequently processed by the metalloprotease ZMPSTE24 into mature lamin A (reviewed in Bertrand *et al.* 2011). Most mutations interfere with its processing, resulting in a persistent and toxic prelamin that dominantly interferes with wildtype lamin A. Expression of known *LMNA* mutations in human fibroblasts has been shown to drive premature senesce in culture (Huang *et al.* 2008).

To date, there are 458 different mutations in *LMNA* (http://www.umd.be/LMNA/) that cause nine clinically distinct diseases in addition to WS, including HGPS, Emery–Dreifuss muscular dystrophy (EDMD), limb-girdle muscular dystrophy type 1B (LGMD1B), Charcot–Marie–Tooth axonal neuropathy (CMT2B1), familial partial lipodystrophy of Dunnigan type (FPLD), mandibuloacral dysplasia (MAD), LIRLLC, restrictive dermopathy (RD), and fetal akinesia (reviewed in Bertrand *et al.* 2011). While these diseases exhibit distinct pathologies, several are shared among two or more diagnoses, including cardiac defects, muscle degeneration, abnormal fat distribution, insulin resistance, skin defects, and osteolysis (reviewed in Bertrand et al. 2011).

The vast majority of HGPS patients harbor mutations in *LMNA* (De Sandre-Giovannoli *et al.* 2003; Eriksson *et al.* 2003; reviewed in Bertrand *et al.* 2011). One patient, displaying symptoms of HGPS as well as MAD and RD, harbored biallelic mutations in *ZMPSTE24*, which effectively resulted in the lack of prelamin A maturation (Shackleton *et al.* 2005). Patients are diagnosed with HGPS as toddlers predominantly due to their failure to thrive and the presence of hair loss, skin defects, lipodystrophy, and characteristic bird-like facial features (reviewed in Hennekam 2006). Additionally, height and weight is dramatically stunted, nails are poorly formed (dystrophic), joint mobility erodes, and teeth decay. Although overt cardiac defects are not apparent in most patients, heart attacks are the primary cause of death at about 13 years. MAD characteristics most closely resemble HGPS, and both *LMNA* and *ZMPSTE24* mutations have been observed in MAD patients, also called non-classical or atypical HGPS (Agarwal *et al.*

2003). Although MAD patients exhibit similar pathologies to HGPS patients, these are alleviated—MAD patients live longer lives, are bigger, and display less severe hair loss, lipodystrophy and osteolysis (bone breakdown) later in life (reviewed in Hennekam 2006). Curiously, osteolysis is more severe in these patients than classical HGPS.

Two disease states separated by telomerase status

My work in Chapter 3 describes a premature onset of senescence in worms deficient for telomere maintenance in the presence of an epitope tagged telomere-binding protein, POT-1. However, in the context of telomerase proficiency, *pot-1::mCherry* animals appear and behave as wildtype. As *C. elegans* POT-1 is homologous to the bona fide telomere-capping protein POT1 in mammals, and perturbing the telomere cap has clinical relevance, we were prompted to consider two scenarios of human disease that may be dictated by the presence or absence of telomere maintenance.

In the first scenario, as illustrated by defects in telomerase holoenzyme components and telomere-binding proteins, it appears that tissues that typically express telomerase or turn over rapidly are affected. In this context, telomerase deficiencies manifest as defects in hematopoietic, pulmonary, and hepatic lineages, and most patients die of bone marrow failure. Moreover, diseases caused by telomerase defects can display genetic anticipation, where the next generation is sicker earlier, indicating that germ cells are also affected. However, instances of severe defects observed suddenly in one generation also exist, where patients that harbor homozygous mutations in telomerase or heterozygous mutations in *TINF2* display extremely short telomeres and other pathologies within the first decade of life (Marrone *et al.* 2007; Walne *et al.* 2008; Sarper *et al.* 2010; Sasa *et al.* 2012). Studies assessing how *TINF2* mutations promote such severe dysfunction suggest that they do so, in part, through defects in telomerase-mediated telomere maintenance (Yang *et al.* 2011; Canudas *et al.* 2011; Houghtaling *et al.* 2012). Thus, except for one known

case (Touzot *et al.* 2010), clinical diagnoses of DC-related defects are due to mutations in proteins that directly affect telomerase activity at telomeres.

In contrast, pathologies in the second scenario, as illustrated by mutations in *WRN* and *LMNA*, manifest in distinct tissues, such as the skin, eyes, bones, and vasculature, and most patients die of a heart attack. Because the presence of telomerase alleviated cellular senescence of telomerase-negative cells from patients *in vitro*, the tissues that exhibit defects in these patients may represent telomerase-deficient environments that are sensitized to the additional stresses caused by losing *WRN*. Defects caused by a *WRN* deficiency, such as poorly replicated telomeres or recombination-mediated telomere loss, perhaps could be healed by the presence of telomerase in somatic and germ stem cells but would persist in cells that naturally lack telomerase or express it at low levels. Since WS patients do not display the more severe and life-threatening pathologies until their 30s or 40s, extensive information about familial inheritance of WS-causing mutations is available. However, we were not able to find any description of genetic anticipation, highlighting the possibility that WS pathologies may be due to defects in telomerase-negative cells, where germ cells, which express extremely high levels of telomerase, would be immune.

Biallelic mutations in *RECQL4*, another member of the RecQ DNA helicase family with some roles in telomere biology, have been identified in RTS patients (Ghosh *et al.* 2012; Kitao *et al.* 1998; Kitao *et al.* 1999), who display a subset of DC-like symptoms, indicating that distinct molecular pathways could manifest as similar defects in humans. As approximately 20% of WS patients remain molecularly undefined, we propose that mutations in proteins with major functions in telomere biology represent ideal candidates and thus could definitively illustrate the role of telomere biology in WS and other diseases marked by accelerated aging. In particular, because WRN has cooperative functions at telomeres with both TRF2 and POT1, mutations in neither of which have been identified in any disorders, these canonical telomere proteins could be the molecular culprits in undefined cases of progeroid syndromes.

CHAPTER 1:

Genetic mapping and characterization of *C. elegans* telomere maintenance-defective mutants

To understand the mechanisms governing telomerase-mediated telomere maintenance in multicellular organisms, we employed the roundworm *Caenorhabditis elegans*. Genetic approaches bypass temporal and physical limitations of biochemical purification schemes, which may be limited by transient interactions as well as small concentrations of proteins or accessory factors that might be required for telomerase activity *in vitro*. While the *in vivo* and *in vitro* data from budding yeast lend a nice model of telomerase action, the level of analogy with metazoan telomerase is unclear. A forward mutagenesis genetic screen to identify genes required for maintaining germline immortality was performed in the laboratory prior to my arrival. Numerous animals were mutagenized with ethyl methanesulfonate (EMS), and approximately 7,000 F2 animals, likely homozygous for hundreds of mutations, were passaged once weekly for 15 weeks, where one week accounted for two generations of growth. Animals that harbored mutations in genes necessary for germline maintenance, termed *mortal germline (mrt)* mutants, eventually became sterile. Because starved stage one larvae (L1) animals can survive freezing and thawing, all strains were frozen as stocks prior to passaging for sterility. To determine which animals became sterile due to defects in telomere maintenance, all mutants were assayed for the presence of chromosomal fusions, a hallmark of dysfunctional telomeres. Of over 400 *mrt* mutants, six displayed late-onset chromosomal fusions, assayed by DAPI staining and fluorescence microscopy.

Mapping mutations in *C. elegans* relies heavily on physical markers to select for recombination events in a restricted area of the genome. *C. elegans* harbors hundreds of genes

that, when mutated, yield relatively easily discernible phenotypes, such as short and fat worms, "dumpy" or "Dpy", immobile or slow moving worms, "uncoordinated" or "Unc", and worms that roll in circles, "roller" or "Rol". For example, if a mutant animal is suspected to harbor a mutation in a gene that lies on the right arm of chromosome *I,* those animals can be crossed to hermaphrodites that harbor mutations in genes that flank that region, such as *dpy-5 unc-29* animals. *dpy-5 unc-29* animals harbor a mutation in *dpy-5*, which is at the center of chromosome *I*, also referred to as genetic position 0, and *unc-29*, which is at genetic map distance +3.3 on chromosome *I* (all six chromosomes are defined as roughly 50 genetic map units in length). Progeny from these crosses, referred to as the F1 generation, will be heterozygous for the mutant allele on one chromosome and the *dpy-5, unc-29* alleles on the other, and selection for Dpy-non-Unc or Unc-non-Dpy F2 progeny indicates that a recombination event has occurred necessarily between these two markers. The number of recombinants that harbor the mutant phenotype being mapped indicates where the mutation lies relative to *dpy-5* or *unc-29*.

Using such genetic mapping techniques, two of the six *mrt* mutants with chromosomal fusions were identified as mutations in the telomerase reverse transcriptase, *trt-1(yp1)*, and in a nuclease, *mrt-1(yp2)* (Meier *et al.* 2006; Meier *et al.* 2009). This chapter describes the efforts taken to map and characterize the remaining four telomere maintenance-defective *mrt* mutants, three of which are novel alleles of components of the Rad9/Rad1/Hus1 (9-1-1) DNA damage response (DDR) complex and its clamp loader, Rad17.

The structure of the 9-1-1 complex resembles the proliferating nuclear cell antigen (PCNA) sliding clamp of DNA polymerase and mediates the DNA damage checkpoint by inducing cycle arrest when chromosomes are damaged or improperly replicated (Weinert & Hartwell 1988; St Onge *et al.* 1999; Caspari *et al.* 2000; reviewed in Parilla-Castellar *et al.* 2004). Fidelity of this checkpoint is vital for maintaining chromosomal integrity. Sites of stalled replication or DNA damage harbor single-stranded DNA coated with RPA, which is necessary for recruiting ATR, a PI3K-like kinase, and its binding partner ATRIP (Zou & Elledge 2003). 9-1-1

is loaded onto junctions of single-stranded and double-stranded DNA adjacent to these sites by Rad17, initiating a signaling cascade that primarily hinges on CHK1, a kinase with a myriad of targets (reviewed in Cimprich & Cortez 2008). Moreover, 9-1-1 participates in establishing a DNA double strand break-induced signaling cascade via ATM and CHK2 (Chen *et al.* 2001). Work in yeast has also suggested that 9-1-1 components may function directly in repair of DNA damage (Lydall & Weinert 1995).

While several canonical telomere proteins function to protect telomeres from DDR-mediated repair processes, effective telomere maintenance relies on DNA damage repair proteins, including the 9-1-1 complex. The mammalian 9-1-1 complex has been shown to localize to telomeres as well as associate with catalytically active telomerase (Francia *et al*. 2006). Moreover, human and mouse cells deficient for Rad9 display an increase in end-to-end chromosome fusions and loss of fluorescent telomere-specific signals (Pandita *et al*. 2006). Fission yeast *rad1, rad3* (ATR in humans), *rad17,* and *rad26* (ATRIP in humans) mutants and budding yeast *ddc1* (Rad9 in humans) and *rad17* (Rad1 in humans) mutants exhibit short telomeres after prolonged growth (Dahlen *et al.* 1998; Longhese *et al.* 2000; Nakamura *et al.* 2002).

C. elegans homologs of Rad1, Hus1 and Rad17 have been previously shown to be necessary for telomere maintenance *in vivo* (Ahmed & Hodgkin 2000; Hofmann *et al.* 2002; Boerckel *et al.* 2007). In addition to novel alleles of *mrt-2* (hRad1) and *hpr-17 (*hRad17), here I describe the identification and characterization of the Rad9 homolog, *hpr-9*, which I reveal is also required for *in vivo* telomere maintenance.

Mapping and characterization of hpr-17(yp7)

Prior to my arrival to the laboratory, the *yp7* mutation was mapped to the right arm of chromosome *II* using linkage analysis. To test whether *yp7* was located near the middle of chromosome *I*, *yp7* males were crossed to *dpy-5* hermaphrodites, and F1 progeny were singly

placed onto new plates ("singled") and allowed to self-fertilize. Next, non-Dpy F2 progeny were singled and allowed to self-fertilize, and F2 lines that did not segregate Dpy F3 progeny were propagated weekly to assay for progressive sterility. If the *yp7* mutation is in a gene close to *dpy-5*, then most of the F2 lines should become sterile. However, if the *yp7* mutation is on a different chromosome or close to the ends of chromosome *I*, then approximately 25% of the F2 lines should become sterile. In this way, an approximately left, middle, or right chromosomal location is assigned to each mutation.

I employed three-factor mapping to refine its position. *yp7* males were crossed to *rol-6 unc-52* or *rol-1 unc-52* hermaphrodites, F1 progeny were singled and allowed to self-fertilize, Rol-non-Unc F2 recombinant progeny were singled and allowed to self-fertilize, Rol-non-Unc F3 progeny were singled and allowed to self-fertilize, and F3 lines that did not segregate Unc F4 progeny were propagated weekly to assay for progressive sterility (Figure 1.1A). Seven out of ten *rol-6 non-unc-52* recombination events picked up *yp7*, and 24/67 *rol-1 non-unc-52* recombination events picked up *yp7*, indicating a genetic map position between +13 and +16 on chromosome *II* (Figure 1.1B).
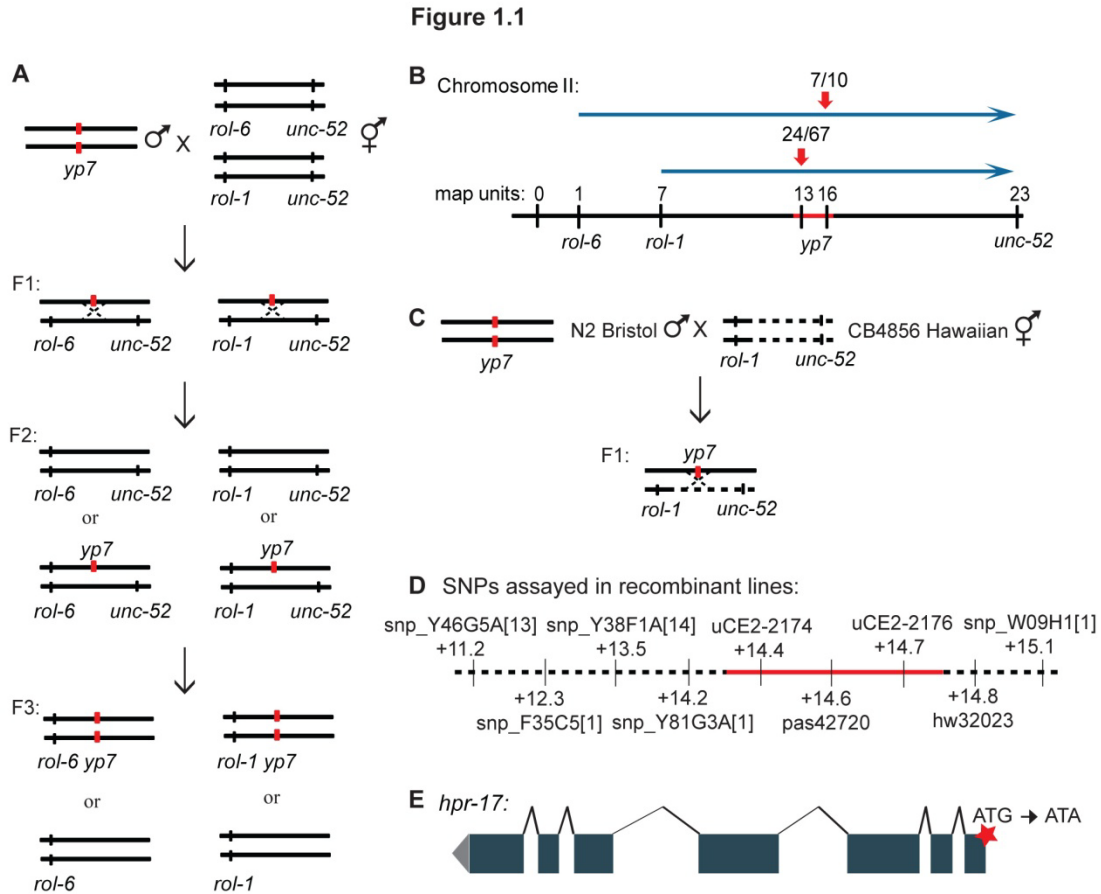
Figure 1.1

Figure 1.1 A novel mutation that displayed hallmarks of telomerase deficiency, *yp7*, was mapped to the hpr-17 gene on Chromosome *II*. A) *yp7* males were crossed to *rol-6 unc-52* or *rol-1 unc-52* hermaphrodites, F1 progeny were singled and allowed to self-fertilize, Rol-non-Unc F2 and F3 recombinant progeny were singled and allowed to self-fertilize, and F3 lines that did not segregate Unc F4 progeny were propagated weekly to assay for progressive sterility. B) Seven out of ten *rol-6 non-unc-52* and 24/67 *rol-1 non-unc-52* became sterile, indicating a genetic map position between +13 and +16 on chromosome II. C) N2 Bristol males, homozygous for yp7, were crossed to *rol-1 unc-52* with intervening Hawaiian sequence, and F1 heterozygotes were singled and allowed to self-fertilize. D) Nine SNPs were genotyped in 50 Rol-non-Unc recombinants, revealing a candidate region between +14.2 and +14.8 on chromosome II, including *hpr-17*, a gene previously identified to be required for *in vivo* telomere maintenance. E) PCR amplification and sequencing of *hpr-17* using genomic DNA from *yp7* as a template revealed a G to A mutation that changes the predicted methionine start codon to an isoleucine, likely resulting in either a complete absence of the HPR-17 protein or a truncated mutant that is translated from an internal ATG codon, resulting in an N-terminal truncation.

16

To more precisely identify the position of *yp7*, single nucleotide polymorphism (SNP) mapping was employed. SNP mapping utilizes the frequent single nucleotide differences that occur between the genomes of two *C. elegans* wildtype strains isolated from Bristol, UK, called N2 Bristol, and from Hawaii, USA, called CB4856 Hawaiian. A SNP occurs approximately once every 1,000 base pairs between these two strains (Fay & Bender 2008). Thousands of these SNPs yield restriction fragment length polymorphisms (RFLPs). These RFLPs cause a change in a restriction enzyme recognition site, thereby removing or creating a restriction site at that locus (Wicks *et al.*, 2001). Instead of genotyping via sequencing, these enzyme digestion products can easily be visualized by gel electrophoresis. A CB4856 Hawaiian strain for mapping was constructed by crossing Hawaiian males to N2 Bristol *rol-1 unc-52* hermaphrodites, and F3 Rol-non-Unc plates that did not segregate Unc F4 progeny, selected analogously as previously described (Figure 1.1A), were analyzed for the presence of Hawaiian DNA between *rol-1* and *unc-52*. N2 Bristol males, homozygous for *yp7*, were crossed to *rol-1 unc-52* hermaphrodites that harbored CB4856 Hawaiian sequence in between the two genes, and analogous F1, F2, and F3 progeny were selected as described above (Figure 1.1C). Fifty *rol-1* non-*unc-52* F3 lines were genotyped for the presence of the N2 Bristol vs. CB4856 Hawaiian SNP at each indicated locus (Figure 1.1D).

The genotyping revealed that *yp7* was located between +14.2 and +14.8, a region that harbors approximately 15 genes, including *hpr-17*, a gene we have previously shown to be required for telomerase-mediated telomere repeat addition *in vivo* (Figure 1.1D) (Boerckel *et al.* 2007). PCR amplification and sequencing of *hpr-17*, using genomic DNA from *yp7* mutants as the template, revealed a G to A mutation that changes the predicted methionine start codon to an isoleucine, likely resulting in either a complete absence of the HPR-17 protein or a truncated mutant that is transcribed from a secondary ATG, leading to a shorter, incomplete transcript (Figure 1.1E).

17

I crossed *yp7* males to *rol-1 unc-52* hermaphrodites and maintained *yp7* animals as heterozygotes for several generations to remove additional mutations that may lie in the *yp7* background. I re-isolated several *yp7* homozygote lines and analyzed them for characteristic features of *hpr-17* mutants. *yp7* animals exhibited defects in repairing DNA damage, illustrated as embryonic lethality, induced by interstrand crosslink (ICL) agents (Figure 1.2D) and ionizing radiation (IR), consistent with the other previously identified mutant allele of *hpr-17(tm1579)* and mutant 9-1-1 complex components (Boerckel *et al.* 2007; Meier *et al.* 2009). Although I did not analyze the telomere dynamics of this mutant, it likely exhibits progressive telomere attrition based on the similarities with the other mutant allele of *hpr-17*, including late onset end-to-end fusions, progressive drops in brood size, a Mortal Germline phenotype, a High incidence of males (Him) phenotype (due to end-to-end fusion between the X chromosome and an autosome and the resulting high frequency of mis-segregation of the X chromosome), and hypersensitivity to DNA damaging agents.

Mapping and characterization of mrt-2(yp8)

Genome-wide SNP mapping was undertaken to obtain an approximate, initial position for *yp8*. N2 Bristol males, homozygous for *yp8*, were crossed to CB4856 Hawaiian hermaphrodites, F1 heterozygotes were singled and allowed to self-fertilize, and 100 F2 progeny were passaged for sterility (Figure 1.3A). All F2 lines were genotyped for the presence of the N2 Bristol vs. CB4856 Hawaiian SNP at several loci on each chromosome, as previously described (Davis *et al.* 2005). Genotyping F2 lines that became progressively sterile, indicative of a homozygous *yp8* genotype, placed *yp8* in the middle of Chromosome *III* (Figure 1.3B). To refine this position, *yp8* males were crossed to *unc-32 vab-7* hermaphrodites, and F1 progeny were singled and allowed to self-fertilize. Twenty F2 Vab-non-Unc recombinants were propagated for sterility, which was never attained. Therefore, *yp8* must be to the right of *vab-7* (Figure 1.3C).

Figure 1.2
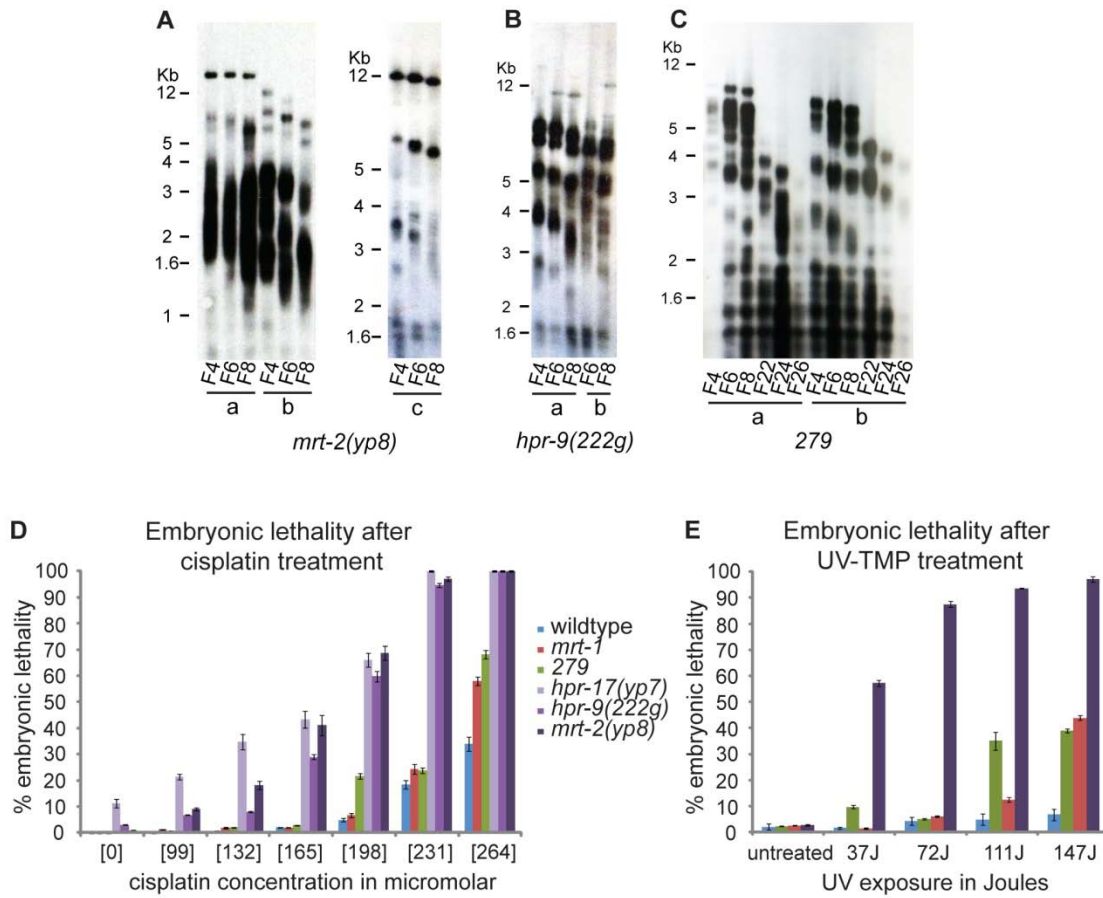
Figure 1.2 Characterization of novel telomere maintenance-defective mutants. A-C) Terminal restriction fragment analysis of DNA from consecutive generations of *yp8*, *222g*, and *279* mutant lines indicates progress telomere shortening. *yp7*, *222g*, and *yp8* mutants are hypersensitive to interstrand crosslinking agents, cisplatin (D) and UV-TMP (E), whereas *279* is moderately sensitive (D & E).

19

Figure 1.3

A

N2 Bristol ♂ X CB4856 Hawaiian ♀

yp8

F1:

yp8

F2:

yp8   *yp8*   *yp8*   *yp8* → Mrt

yp8   *yp8* → wildtype
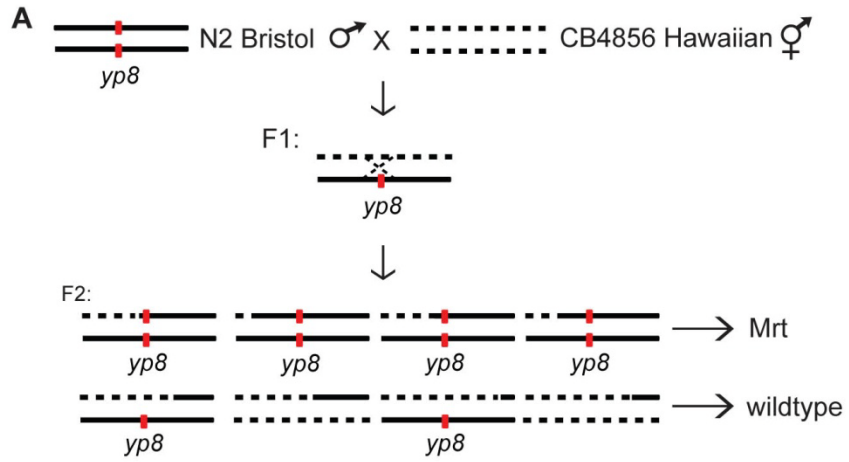
B   genome-wide SNP mapping of F2 homozygotes

Chromosome:

I
II
III
IV
V
X

C

♂ X   *unc-32*   *vab-7* ♀

yp8

F1:   *yp8*

unc-32   *vab-7*

F2:

0/20

Chromosome *III*:
map units: 0   5.6   12.1

unc-32   *vab-7*   *mrt-2*

D

mrt-2:

yp8

AA**ATGA**[365 nucleotides deleted]AACAAA
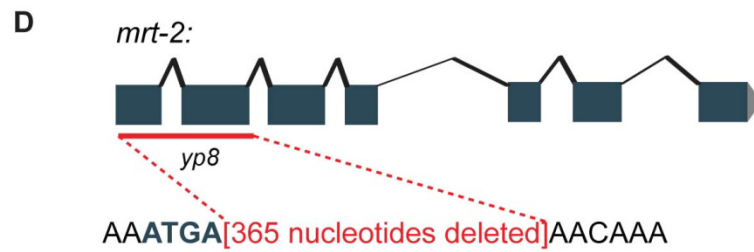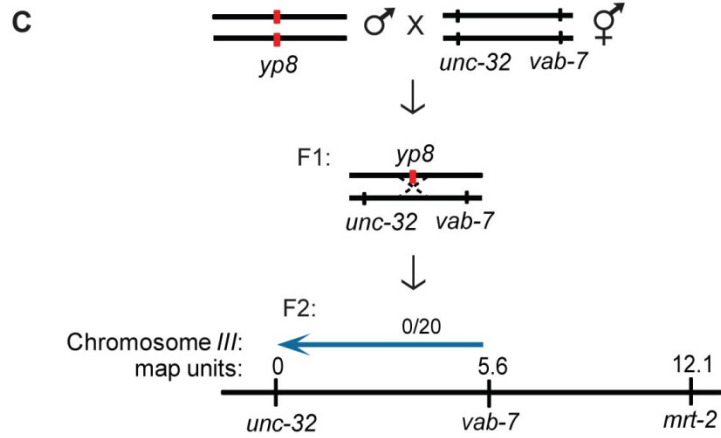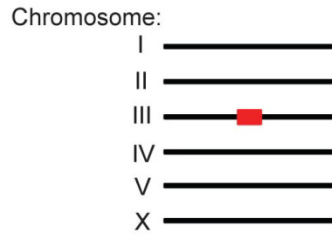
Figure 1.3 A novel mutation that displayed hallmarks of telomerase deficiency, *yp8*, was mapped to the *hpr-17* gene on Chromosome *III*. A) N2 Bristol males, homozygous for *yp8*, were crossed to CB4856 Hawaiian hermaphrodites, F1 heterozygotes were singled and allowed to self-fertilize, and 100 F2 lines were propagated weekly to assay for sterility. B) F2 lines were genotyped for the presence of the N2 Bristol vs. CB4856 Hawaiian SNP at several loci on each chromosome, as described in Davis *et al*. 2005. Genotyping of F2 lines that became progressively sterile, indicative of a homozygous *yp8* genotype, placed *yp8* in the middle of Chromosome III. C) *yp8* males were crossed to *unc-32 vab-7* hermaphrodites, and F1s were singled and allowed to self-fertilize. Twenty F2 Vab-non-Unc recombinants were propagated for sterility, which was never attained. Therefore, *yp8* must be to the right of *vab-7*. D) Because *mrt-2*, a gene previously identified to be required for telomere replication, is located at +12 map units on chromosome III, we sequenced this gene in *yp8* animals. A 365-nucleotidedeletion, starting with the fifth base pair of the first exon and ending after the second exon, was identified, likely precluding a functional protein product.

Because *mrt-2*, a gene previously identified to be required for telomerase-mediated telomere repeat addition (Ahmed & Hodgkin 2000), is located to the right of *vab-7* at +12 map units on chromosome *III*, I sequenced this gene in *yp8* animals. A 365-nucleotide-deletion, starting with the fifth base pair of the first exon and ending after the second exon, was identified, likely precluding a functional protein product (Figure 1.3D).

We crossed *yp8* males to *dpy-18 unc-64* hermaphrodites and maintained *yp8* animals as heterozygotes for several generations to remove additional mutations that may lie in the *yp8* background. I re-isolated several *yp8* homozygote lines and analyzed them for characteristic features of *mrt-2* mutants. To assess telomere length in *yp8* animals, DNA was collected from several *yp8* mutant lines during several weeks of growth and subjected to terminal restriction fragment analysis. Southern blotting revealed progressive telomere attrition for all *yp8* lines (Figure 1.2A). Additionally, *yp8* animals exhibited defects in repairing DNA damage, illustrated by scoring embryonic lethality after exposure to IR or ICL agents, consistent with the other previously identified mutant allele of *mrt-2(e2663)* (Figure 1.2D & E) (Ahmed & Hodgkin 2000; Meier *et al.* 2009).

Mapping and characterization of hpr-9(222g)

Prior to my arrival to the laboratory, *222g* was roughly mapped to the right arm of chromosome *III* using genome-wide linkage analysis as described for *yp7*. To refine this position, I constructed the following double mutants for three-factor mapping: *dpy-1 unc-93, dpy-17 unc-32, unc-32 dpy-18,* and *dpy-18 unc-64*. I crossed *222g* males to *dpy-1 unc-93* hermaphrodites, and Dpy-non-Unc F3 lines, generated analogously as previously described (Figure 1.1A), that did not segregate Unc F4 progeny were propagated weekly to assay for progressive sterility. Dpy-non-Unc and Unc-non-Dpy F3 lines were established analogously from crosses between *222g* males and *dpy-17 unc-32* hermaphrodites, Dpy-non-Unc and Unc-non-Dpy F3 lines were established analogously from crosses between *222g* males and *unc-32 dpy-18* hermaphrodites, Dpy-non-Unc

and Unc-non-Dpy F3 lines were established analogously from crosses between *222g* males and *dpy-18 unc-64* hermaphrodites, and all were propagated for sterility (Figure 1.4A). The location of the *222g* mutation, which was approximately at +4, was determined by calculating percent sterility. Because *hpr-9*, the Rad9 homolog component of the 9-1-1 complex, is located at +4 map units on chromosome *III*, I sequenced this gene in *222g* animals. A premature opal stop (TGG to TGA) was identified in the 8th exon, which likely results in either a truncated or non-functional protein product (Figure 1.4B).

I crossed *222g* males to *unc-32 vab-7* hermaphrodites and maintained *222g* animals as heterozygotes for several generations to remove additional mutations that may lie in the *222g* background. I re-isolated several *222g* homozygote lines and analyzed them for characteristic features of other 9-1-1 mutant components. To assess whether telomeres in *222g* also eroded progressively, DNA was collected from several *222g* mutant lines during several weeks of growth and subjected to terminal restriction fragment length analysis. Southern blotting revealed progressive telomere attrition for both *222g* lines (Figure 1.2B). Additionally, *222g* animals exhibited defects in repairing DNA damage, illustrated as embryonic lethality, after exposure to IR or ICL agents, consistent with the phenotypes of *mrt-2* and *hpr-17* mutants (Figure 1.2D). Lastly, to confirm that the *222g* mutation specifically was driving the onset of sterility, and not another mutation in a nearby gene, I performed complementation analysis with an independent allele of *hpr-9(ok2396)*. Both *hpr-9(222g)/hpr-9(ok2396)* trans-heterozygotes and *222g* and *ok2396* homozygous mutants were hyper-sensitive to IR. Because *hpr-9(ok2396)* did not complement *222g* for IR hyper-sensitivity, we conclude that the *222g* mutation, as opposed to independent mutations in adjacent genes, drives the telomere attrition and the resulting sterility. This allele of *hpr-9* is the first to be investigated for telomere defects, thus we are the first to definitively demonstrate that the Rad9 homolog, *hpr-9*, is required for telomere repeat addition *in vivo* in *C. elegans.*

Figure 1.4
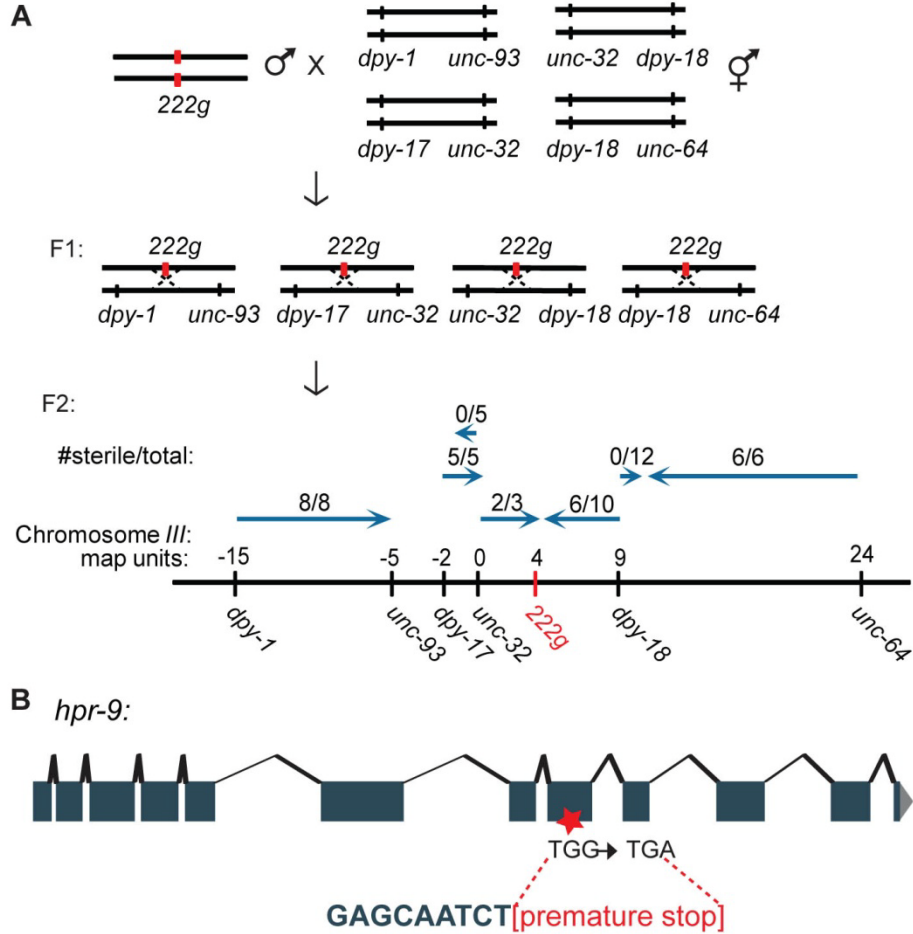
Figure 1.4 A novel mutation that displayed hallmarks of telomerase deficiency, *222g*, was mapped to the *hpr-9* gene on Chromosome *III*. A) *222g* males were crossed to d*py-1 unc-93, unc-32 dpy-18, dpy-17 unc-32*, and *dpy-18 unc-64* hermaphrodites, F1 heterozygotes were singled and allowed to self-fertilize, and F2 lines were propagated weekly to assay for sterility. The numbers of sterile animals from each cross indicate that *222g* is located at approximately +4. map units. B) Because *hpr-9*, the Rad9 homolog component of the 9-1-1 complex, is located at +4 map units on chromosome *III*, we sequenced this gene in *222g* animals. A premature opal stop (TGG to TGA) was identified in the 8th exon, which likely results in either a truncated or non-functional protein product.

Mapping and characterization of 279

Prior to my arrival to the laboratory, the *279* mutation was mapped to the right arm of chromosome *I* using genome-wide linkage analysis as previously described. To refine this position, I constructed the following double mutants for three-factor mapping: *daf-8 unc-29*, *dpy-14 unc-29*, and *dpy-5 unc-29*. Unc-non-Daf F3 lines were established analogously as previously described (Figure 1.1A) from crosses between *279* males and *daf-8 unc-29* hermaphrodites, Unc-non-Dpy F3 lines were established analogously from crosses between *279* males and *dpy-14 unc-29* hermaphrodites, Dpy-non-Unc F3 lines were established analogously from crosses between *279* males and *dpy-5 unc-29* hermaphrodites, and all lines were propagated for sterility. The cumulative map positions, based on percent sterility, placed *279* at approximately +2.3 on chromosome *I*, which is close to but likely to the left of the *mrt-1* and *trt-1* genes (Figure 1.5A).

Although the Unc-non-Daf recombinant data suggested that *279* lies in a gene to the left of *daf-8*, it is possible that *279* may also reside in a gene extremely close to the right of *daf-8*. Additionally, because genetic mapping relies on recombination frequency, it may not always be accurate if recombination is perturbed in the mapping area, thus distorting the analogy between the genetic and physical map. Therefore, I wanted to assess whether *279* may be an allele of *mrt-1* or *trt-1*, so complementation analysis was performed with *trt-1(ok410)* and *mrt-1(e2661)*. While *279, trt-1(ok410),* and *mrt-1(e2661)* homozygous mutants became sterile after multiple generations of growth, both *279/trt-1(ok410)* and *279/mrt-1(e2661)* trans-heterozygotes did not. Therefore, we can conclude that *279* does not represent a mutation in the *trt-1* or *mrt-1* gene.
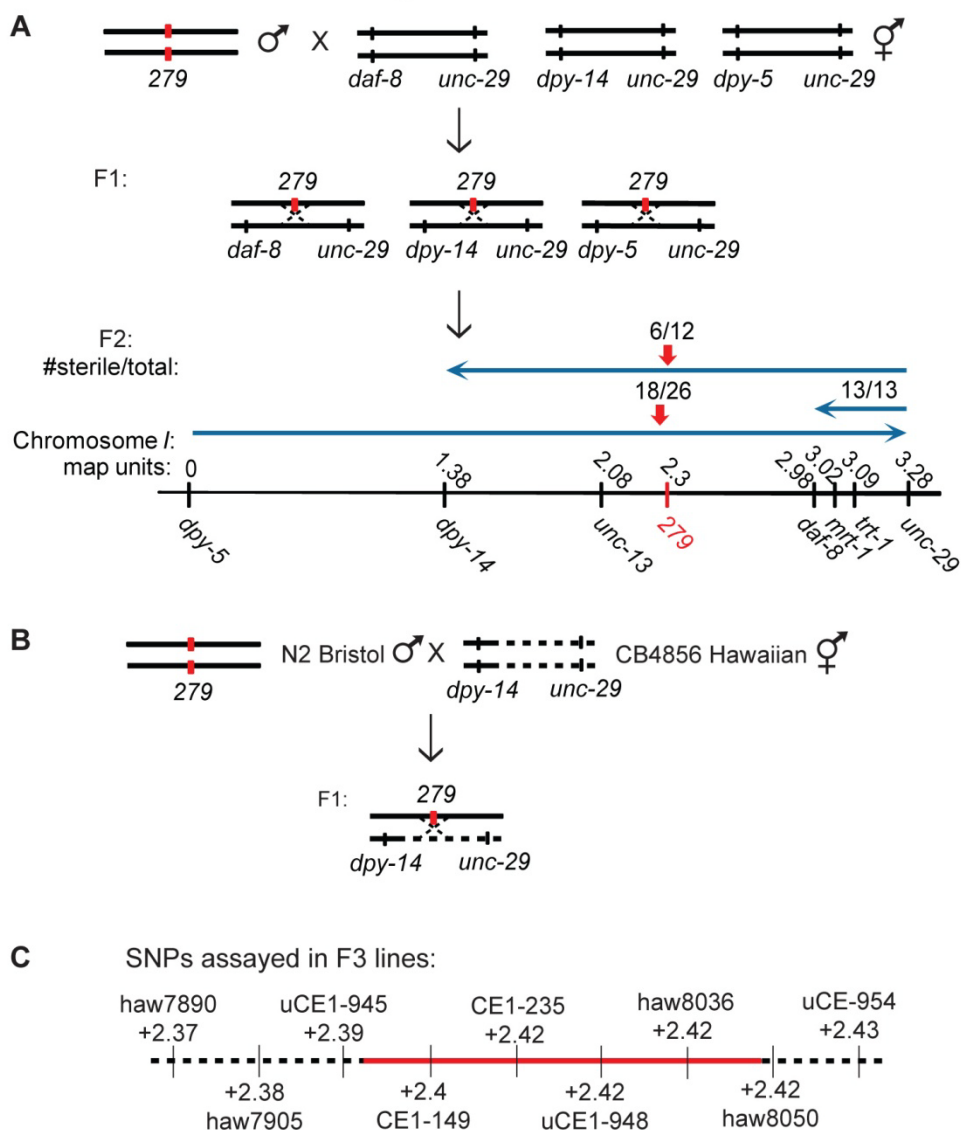
Figure 1.5 A novel mutation that displayed hallmarks of telomerase deficiency, *279*, was mapped to a candidate region of 29 genes on Chromosome *I*. A) *279* males were crossed to *daf-8 unc-29, dpy-14 unc-29*, and *dpy-5 unc-29* hermaphrodites, F1 heterozygotes were singled and allowed to self-fertilize, and F2 lines were propagated weekly to assay for sterility. The numbers of sterile animals from each cross indicate that *279* is located at approximately +2.3 map units. B) N2 Bristol males, homozygous for *279*, were crossed to *dpy-14 unc-29* hermaphrodites with intervening Hawaiian sequence, F1 heterozygotes were singled and allowed to self-fertilize, and 30 Dpy-non-Unc recombinant lines were propagated weekly to assay for sterility. C) Nine SNPs were genotyped in 30 lines, revealing a candidate region between +2.39 and +2.42 on chromosome *I*, which harbors 29 genes.

To further refine the position of *279*, I employed three-factor mapping in combination with SNP mapping. Attempts at selecting Daf-non-Unc or Unc-non-Daf recombinants from crosses between CB4856 Hawaiian males and *unc-13 daf-8* hermaphrodites failed, perhaps because introduction of the Hawaiian sequence at that locus somehow interfered with the viability of these strains or crossovers in this region. Instead, I crossed Hawaiian males with *dpy-14 unc-13* hermaphrodites, and selected Dpy-non-Unc F2 recombinant progeny as previously described. Next, *dpy-14* hermaphrodites (obligately harboring Hawaiian sequence to the right of *unc-13*) were crossed with *unc-29*/+ males, F1 progeny were singled and allowed to self-fertilize, and *dpy-14 unc-29* recombinant progeny were selected analogously, as previously described, for genotyping to assess for the presence of Hawaiian sequence in between the two genes. N2 Bristol males, homozygous for *279*, were crossed to *dpy-14 unc-29* hermaphrodites that harbored intervening CB4856 Hawaiian sequence, F1 progeny were singled and allowed to self-fertilize, and the eventual Dpy F3 lines, selected for as previously described, that did not segregate Unc F4 progeny were propagated weekly to assay for progressive sterility (Figure 1.5B). Thirty F3 lines were genotyped for the presence of the N2 Bristol vs. CB4856 Hawaiian SNP at each indicated locus (Figure 1.5C). The genotyping revealed that *279* was located between the SNPs uCE1-945 (+2.39) and haw8050 (+2.42), a region that harbors the following 29 protein-coding and non-coding genes: F55D12.1, F55D12.8 (ncRNA), F55D12.7 (miRNA), F55D12.2, F55D12.9 (ncRNA), F55D12.3 (*nhr-191*), F55D12.4 (*unc-55*), F55D12.6, F55D12.5, F20G4.2, F20G4.1 (*smgl-1*), F20G4.3 (*nmy-2*), T22C1.1, T22C1.2 (*glb-26*), T22C1.3, T22C1.4, T22C1.5, T22C1.6, T22C1.7 (*jph-1*), T22C1.15 (ncRNA), T22C1.14 (ncRNA), T22C1.13 (ncRNA), T22C1.8, T22C1.9, T22C1.12, T22C1.10 (*rgb-2*), T22C1.11, H05L14.1, and H05L14.2.

To remove additional mutations that may lie in the *279* background, *279* males were crossed to *unc-29 dpy-24* hermaphrodites and maintained as heterozygotes for several generations. Several *279* homozygote lines were re-isolated and analyzed for characteristic features of mutants deficient for telomerase-mediated telomere replication. To observe telomere

dynamics in *279* animals, DNA was collected from several *279* mutant lines during several weeks of growth and subjected to terminal restriction fragment length analysis. Southern blotting revealed progressive telomere attrition for both *279* lines (Figure 1.2C). Additionally, *279* animals exhibited defects in repairing DNA damage, illustrated as embryonic lethality, after exposure to ICL agents (Figure 1.2D & E). Curiously, *279* mutants were moderately hypersensitive to ICL agents, similar to *mrt-1* mutants that are more sensitive than wildtype but less sensitive than 9-1-1 components.

Discussion

I identify novel alleles of *hpr-17(yp7)* and *mrt-2(yp8)*, which both display telomere defects that result in late onset end-to-end chromosomal fusions and sterility. Additionally, I demonstrate for the first time that the *C. elegans* Rad9 homolog, *hpr-9*, is required for telomere repeat addition *in vivo*. Abrogating 9-1-1 complex components in mice is incompatible with life (Weiss *et al.* 2000; Hopkins *et al.* 2004), and their loss is not tolerated in culture (Francia *et al.* 2006; Hopkins *et al.* 2004), precluding analysis of telomere length dynamics. However, the progressive nature of telomere length defects in *C. elegans* 9-1-1 complex mutants allows for examination of the roles that these components play in telomere length maintenance over time. In fact, TRF analysis of human cells deficient for *Rad9* revealed normal-length telomeres (Pandita *et al.* 2006), whereas analysis of progressive growth of 9-1-1-deficient *C. elegans* clearly establishes a role for 9-1-1 components in promoting telomere maintenance.

Work with mammalian 9-1-1 suggests that its components may promote telomere elongation through direct effects on telomerase. Mouse Hus1, Rad1, and Rad17 have been shown to associate with telomerase and telomeres *in vivo*, and both mouse and human components are necessary for telomere repeat addition *in vitro*, suggesting that 9-1-1 may contribute to the biogenesis or stability of the holoenzyme (Francia *et al.* 2006). However, a proteomics of isolated segments (PICh) approach, using a nucleic acid probe to precipitate telomere-bound proteins,

28

identified 9-1-1 components in an exclusively human telomerase-negative cell line that maintains telomeres via a telomerase-independent mechanism, termed alternative lengthening of telomeres (ALT) (Déjardin & Kingston 2009). Additionally, Rad9 and Rad17 were shown to colocalize with telomeres only when they were associated with promyelocytic leukemia (PML) bodies, which occurs exclusively in ALT cells (ALT-associated PML bodies or APBs) (Nabetani *et al.* 2004). Consistently, we have recently shown that 9-1-1 components are necessary for survival of telomerase-deficient *C. elegans* lines (Cheng *et al.* 2012). These results suggest that while 9-1-1 components may be required for the recombination processes that drive ALT-mediated telomere maintenance, similar 9-1-1-governed processes may be necessary to stimulate telomerase-mediated telomere repeat addition in *C. elegans* and other multi-cellular organisms. More recently, 9-1-1 was shown to physically interact with WRN, a helicase with some roles in telomere maintenance (Pichierri *et al.* 2011). Although the authors suggest that 9-1-1 cooperates with WRN at stalled replication forks, which have been proposed to occur at telomeres naturally (reviewed in Maizels 2006), 9-1-1's mechanism of action at telomeres remains unclear.

All of the new *mrt* mutants that displayed chromosomal fusions also experienced progressive telomere erosion, thus we can be confident that assaying for these fusions is an accurate method for identifying telomere maintenance defects in *mrt* lines. However, this kind of selection excludes mutations that may result in short, but stable telomeres or progressively shortening telomeres that are protected from end-to-end fusions. In fact, it is likely that additional genes required for telomere maintenance in *C. elegans* remain unidentified. For example, the telomerase RNA component has yet to be identified.

A candidate gene approach is one way to tackle uncovering the identity of *279.* Of the five predicted non-coding RNAs present in the candidate region, one (T22C1.13) harbors complementary base pairs to the telomeric template: 3'-cggatt-5', representing an excellent candidate for the telomerase RNA. The length of the RNA, 186 nucleotides (nt), is within a plausible range, where the human telomerase RNA is 451 nt, 397 nt in mice, between 150 and

29

159 nt in *Tetrahymena* species, and 189-191 nt in *Euplotes* species. However, telomerase RNAs identified to date harbor more than one telomere repeat of complementary sequence, which allows for primer re-alignment. A minimum of eight nucleotides are conserved throughout all vertebrates, and more complementary sequences promote telomerase processivity, where one telomere is elongated for more than one round of alignment (Chen & Greider 2003). Thus, this non-coding RNA is not likely to code for the *C. elegans* telomerase RNA subunit. However, if sequencing this non-coding RNA reveals a mutation in *279* animals, expressing this gene with mutations in the predicted template would be an appropriate next step in assessing whether it represents the telomerase RNA. Sequencing the telomeres from animals expressing a mutated construct should reveal the aberrant sequence if it does indeed serve as the telomeric template.

Because we did not recover several mutations in the same gene, the conditions used in this screen were likely not saturating. For example, approximately 7,000 F2 EMS-mutagenized animals were passaged for up to 30 generations, where an EMS concentration that yields a per gene mutation frequency of approximately 1 in 4,000 F2 mutagenized animals was used (Ahmed & Hodgkin 2000). Passaging 7,000 animals provided almost a two-fold gene coverage, predicting that a mutation in each gene would be recovered more than once in this screen. However, all of the six telomere maintenance-defective mutants we identified represent distinct genes. Additionally, mutations in genes that resulted in slower telomere attrition may have been missed if those animals became sterile at much later generations (>30). Furthermore, while the aim of this screen was to identify mutations that cause late-onset sterility, which is great for studying telomere dynamics, genes that cause drastic telomere defects when mutant, resulting in more sudden and rapid sterility, would have been missed using such an identification scheme.

In conclusion, identification of additional alleles of 9-1-1 components and its clamp loader underscores the major role this complex plays in telomere maintenance. Moreover, our efforts in mapping *279* to an area harboring only 30 genes represent a significant advance towards identifying a novel gene involved in telomere biology. Future efforts to understand the

mechanism(s) by which 9-1-1 components regulate telomere repeat addition might include the following: 1) identification of binding partners using affinity purification of epitope-tagged 9-1-1 components, 2) analysis of *in vivo* localization via fluorescence microscopy using fluorescent protein-tagged 9-1-1 components, 3) analysis of changes in telomerase *in vivo* localization in 9-1-1 mutant vs. wildtype animals using fluorescent protein-tagged telomerase, and 4) analysis of *in vitro* telomerase activity from 9-1-1 mutant vs. wildtype animals. Additionally, if any of our *mrt-1* or *9-1-1* mutant alleles cause telomere dysfunction by interfering with their binding or localization to telomeres, fusing mutant MRT-1 or 9-1-1 proteins to wildtype POT-1 or POT-2, known telomere-binding proteins, may rescue their mutant phenotypes. Similarly, if any of our *mrt-1* or *9-1-1* mutant alleles cause defects in recruitment of telomerase to telomeres, expressing a TRT-1::POT-1/2 fusion protein in *mrt-1* or *9-1-1* mutant animals may overcome such a defect. In contrast, identification of additional genes that exacerbate or rescue the phenotypes of mutant 9-1-1 animals using forward genetic screens may be more effective or yield results distinct from biochemistry. The following chapter describes biochemical efforts taken to understand how telomeres are maintained.

CHAPTER 2:

Biochemical analysis of proteins that participate in telomere length homeostasis

In addition to proteins that participate in telomere length homeostasis through their interaction with chromosome termini, the activity of the telomerase enzyme itself is regulated by several factors. Analysis of the mechanisms involved in the formation, stabilization, and activity of the telomerase holoenzyme is vital to dissecting telomerase function. A number of biochemical approaches have been employed to identify components of the telomerase holoenzyme. In 1995, a cofractionation approach identified the first two proteins to co-purify with telomerase activity in *Tetrahymena* extracts—p80 and p95 (Collins *et al.* 1995). However, these proteins were later shown to be dispensable for telomere maintenance *in vivo* and could not precipitate telomerase or telomerase activity *in vitro* or *in vivo* (Miller & Collins 2000; Mason *et al*. 2001). In fact *p80/p95* mutants exhibit telomere elongation instead (Miller & Collins 2000).

An oligonucleotide-based affinity purification of telomerase from *Euplotes* extracts successfully identified a 43-kilodalton protein, p43 (Lingner & Cech 1996). p43 directly interacts with telomerase RNA *in vivo* and *in vitro* and has been suggested to promote the RNA stability based on its role in stabilizing other SNP complexes (Aigner *et al.* 2000). Additionally, affinity purification of epitope-tagged telomerase in *Tetrahymena* effectively identified three telomerase holoenzyme subunits, p45, p65, and p75 (Witkin & Collins 2004; Witkin *et al.* 2007). These proteins are required for viability, like the telomerase catalytic and RNA subunits in *Tetrahymena*, and analysis of partial knockdowns revealed a striking decrease in telomere length in all three mutants (Witkin & Collins 2004; Witkin *et al.* 2007). Furthermore, p65 is necessary for the stability of the telomerase ribunocleoprotein (RNP), which is similar to p43's role in

Euplotes—both proteins harbor the La motif necessary for RNA binding (Witkin & Collins 2004; Aigner *et al.* 2004). In contrast, p20, which initially co-purified with p45, p65, and p75, did not co-immunoprecipitate telomerase activity or the RNA in later experiments, and *p20* mutants actually exhibit long telomeres, a phenotype strikingly similar to the p80 and p95 proteins purified a decade prior (Witkin *et al.* 2007; Collins *et al.* 1995).

In vertebrates, telomerase-mediated telomere extension *in vivo* requires not only the catalytic and RNA telomerase subunits, hTERT and hTR, but also several RNP assembly proteins. Because hTR harbors an H/ACA domain observed in small nucleolar RNAs (snoRNAs), dyskerin, one of several proteins that interacts with snoRNAs and is necessary for their maturation, was assessed for interactions with hTR. Indeed, immunoprecipitation of dyskerin also recovered co-transfected hTR from human cells (Mitchell *et al.* 1999). Furthermore, telomere repeat addition was completely abolished in cells from patients with mutated dyskerin, which had been implicated in the disease Dyskeratosis Congenita a year prior (Heiss *et al.* 1998), revealing dyskerin's crucial role in stabilizing telomerase (Mitchell *et al.* 1999).

Several previously known and novel proteins were identified through tandem affinity purification of telomerase. However, the Sm proteins, which participate in stabilizing small nuclear RNPs (snRNPs), and heterogeneous nuclear RNP (hnRNP) family RNA-binding proteins were shown to be dispensable for telomere elongation (Fu & Collins 2007). These proteins, and other identified chaperones, are proposed to perhaps bridge the interaction between a stable, active telomerase and telomeres (reviewed in Collins 2006). Ultimately, the telomerase RNP is comprised of hTERT, hTR, three hTR-stabilizing proteins, dyskerin, NHP2, and NOP10, and one additional less abundant participant GAR1, which is required for RNP function but not its stabilization (Fu & Collins 2007).

A strategy combining gradient sedimentation and dual-affinity purification of epitope-tagged telomerase identified two novel players, ATPases pontin and reptin, which interact with dyskerin in stabilizing the telomerase RNP (Venteicher *et al.* 2008). Due to the low *in vitro*

33

catalytic activity of the telomerase complex purified from pontin or reptin immunoprecipitations, the authors suggest that these ATPases promote RNP assembly but may not be retained in a final telomerase complex that locates to and actively elongates telomeres. Such a complex may indeed have been missed from purification schemes that relied on proteins co-purifying with the most active telomerase fractions, as measured by an *in vitro* assay.

Using genetics, I have identified several positive (discussed in Chapter 1) and negative (to be discussed in Chapter 3) regulators of telomere length *in vivo*, but their mechanisms of action remain largely undefined. Using epitope-based affinity purification, I aimed to assess whether these proteins affect telomere length by directly interacting with telomerase and/or by affecting its catalytic activity.

Creation of transgenic animals

Because generating highly specific antibodies to native proteins can be difficult and time-consuming, proteins were tagged with a 1xFLAG epitope or a fluorescent protein tag, for which commercial antibodies are readily available. The following transgenes were constructed: *Ppgl-3::GFP::pot-2, Ppgl-3::trt-1::FLAG::tbb-2utr, Ppie-1::trt-1::FLAG::mes-3utr, Ppie-1::FLAG::pot-1::mes-3utr*, and *Pdaz-1::pot-1::mCherry::tbb-2utr* (see Materials & Methods for details). Transgenes were incorporated into young adult animals as described in the Materials & Methods. To confirm their expression, RNA levels were assessed by reverse transcription-polymerase chain reaction (RT-PCR).

To assess whether the *GFP::pot-2, trt-1::FLAG, FLAG::pot-1*, and *pot-1::mCherry* transgenes were functional, they were crossed into backgrounds mutant for *pot-2, trt-1,* or *pot-1*, respectively. The final lines used for analysis were genotyped for the presence of both the respective transgene and the endogenous mutant gene. Southern blotting of DNA collected from several generations of *FLAG::pot-1; pot-1(tm1620)* strains revealed wildtype telomere lengths, indicating that the transgene rescues the telomere elongation phenotype of *pot-1* (discussed in

Chapter 3) (Figure 2.1A). Southern blotting of *trt-1::FLAG; trt-1(ok410)* DNA revealed

progressive telomere erosion, indicating that the *trt-1::FLAG* construct does not express a protein

that can function properly to maintain telomeres *in vivo* (Figure 2.1B). Analysis of *GFP::pot-2*

and *pot-1::mCherry* transgenes is presented in Chapter 3.

Analysis of protein expression by western blot

       I am confident of the expression of the *GFP::pot-2* and *pot-1::mCherry* constructs

because their protein product can be seen under a fluorescent microscope *in vivo* (see Chapter 3),

and *FLAG::pot-1* is expressed because it rescued the mutant phenotype of *pot-1*. Moreover, even

though *trt-1::FLAG* did not rescue the telomere defects of *trt-1* mutants, the TRT-1::FLAG

protein, if expressed, may still be functional *in vitro*. Therefore, I wanted to assess whether we

could observe their expression via western blot from whole animal extracts. Three independent

trt-1::FLAG lines, two *FLAG::pot-1* lines, and two positive control strains, *tom-*

1ΔSNARE::FLAG; *tom-1(nu468)* and *tom-1SNARE::FLAG*; *tom-1(nu468)*, were collected from

large, almost starved, 100-cm plates, washed several times, and boiled in Laemmli sample buffer.

Extracts were resolved by gel electrophoresis on a polyacrylamide gel and transferred to a

membrane for western blotting with mouse anti-FLAG primary antibodies (Sigma F3165)

followed by anti-mouse HRP-conjugated secondary antibodies (see Materials & Methods for

details). A first-look at these extracts did not reveal specific bands corresponding to TRT-

1::FLAG (~63 kDa) or FLAG::POT-1 (~39 kDa), whereas an appropriate, specific ~115-kDa

band was apparent in *tom-1ΔSNARE::FLAG* extracts exclusively, indicating that the blotting

procedure was successful (Figure 2.2A). The levels of TOM-1ΔSNARE::FLAG and TOM-

1SNARE::FLAG (17 and 23-fold over wildtype, respectively) are likely higher than telomerase

or POT-1, which are single-copy insertions. Thus, observing TOM-1, but not TRT-1 or POT-1,

via western blot does not indicate that TRT-1 or POT-1 are not expressed or recalcitrant to

detection by this specific antibody.
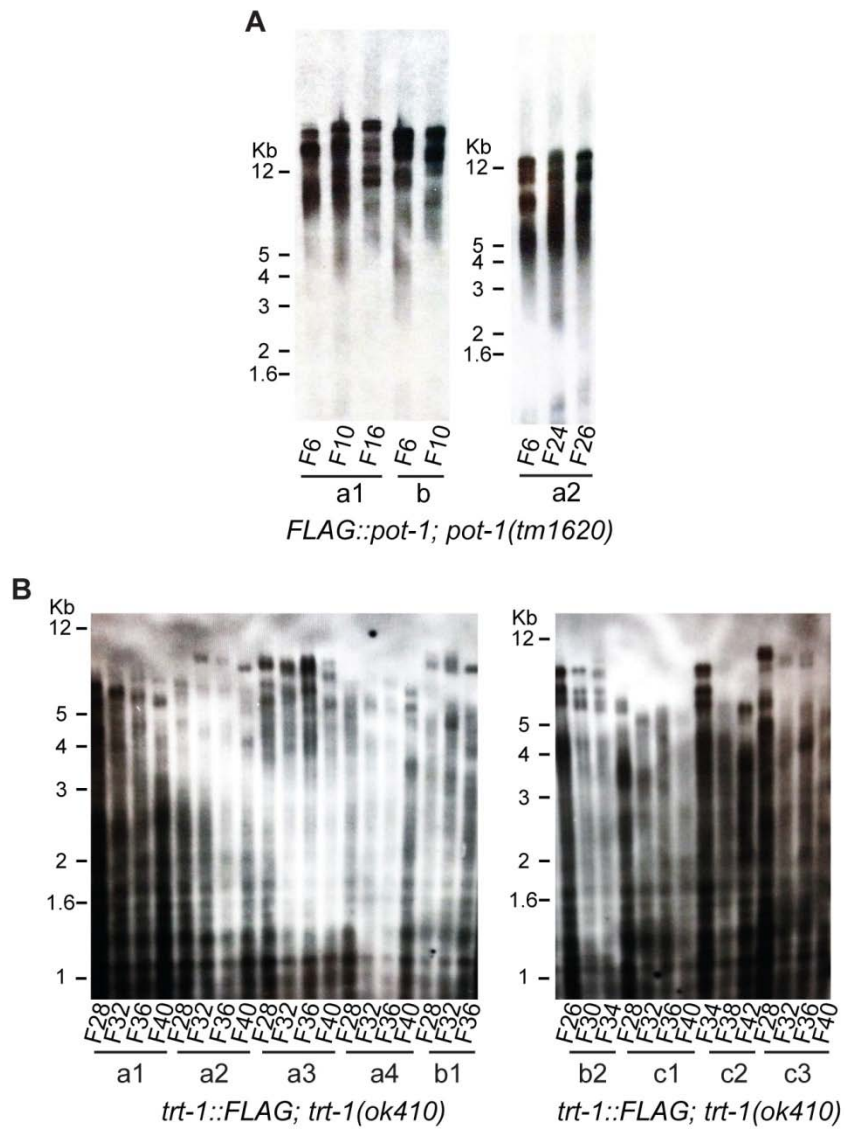
Figure 2.1 Analysis of phenotype rescue for FLAG::POT-1 and TRT-1::FLAG constructs.
Terminal restriction fragment analysis of consecutive generations of DNA collected from several
FLAG::pot-1; pot-1(tm1620) lines (A) and *trt-1::FLAG; trt-1(ok410)* lines (B).

Low levels of TRT-1 or POT-1 expression may preclude their detection by immunoblot from extracts, so I wanted to test whether immunoprecipitation (IP) of the FLAG-tagged proteins from extracts would yield successful detection by western blot. To acquire a large amount of cellular extract for immunoprecipitation, animals were grown in liquid media. Cultures were harvested, frozen in liquid nitrogen, ground by mortar and pestle, sonicated, and clarified by centrifugation (see Materials & Methods for details). Beads conjugated with anti-FLAG antibodies (Sigma F2426) were incubated with clarified extracts, washed several times, and bound protein was eluted either with heat or competing amounts of FLAG epitope. The products were resolved by gel electrophoresis on a polyacrylamide gel and then transferred to a membrane for blotting with various antibodies.

An initial precipitation using only *tom-1ΔSNARE::FLAG* and wildtype extracts yielded the appropriate ~115-kDa band in the first elution from beads incubated with *tom-1ΔSNARE::FLAG* extracts and not with wildtype extracts, indicating that the F2426 anti-FLAG antibody can successfully IP FLAG-tagged proteins (Figure 2.2B). However, multiple immunoprecipitation and western blotting experiments using anti-FLAG antibodies did not reveal the predicted bands specific for TRT-1::FLAG or POT-1::FLAG from *trt-1::FLAG* or *pot-1::FLAG* extracts, while an appropriately sized, specific band was apparent for the TOM-1SNARE::FLAG control (~7 kDa) (Figure 2.2C). Blotting for POT-1::mCherry directly from total extracts using anti-mCherry antibodies revealed a light band of appropriate size in extracts from *pot-1::mCherry* animals exclusively (Figure 2.2D). However, IPs from *pot-1::mCherry* extracts using anti-mCherry antibodies coupled to beads did not reveal any bands of appropriate size specifically in the *pot-1::mCherry* extracts compared to wildtype (assessed by western blot using anti-mCherry antibodies) (Figure 2.2E). Not having a positive control for the IP or western, I cannot be sure that the protocols were successful; although, the same protocols were used for the anti-FLAG IPs and westerns described above, which successfully precipitated and recognized the positive controls.

Figure 2.2
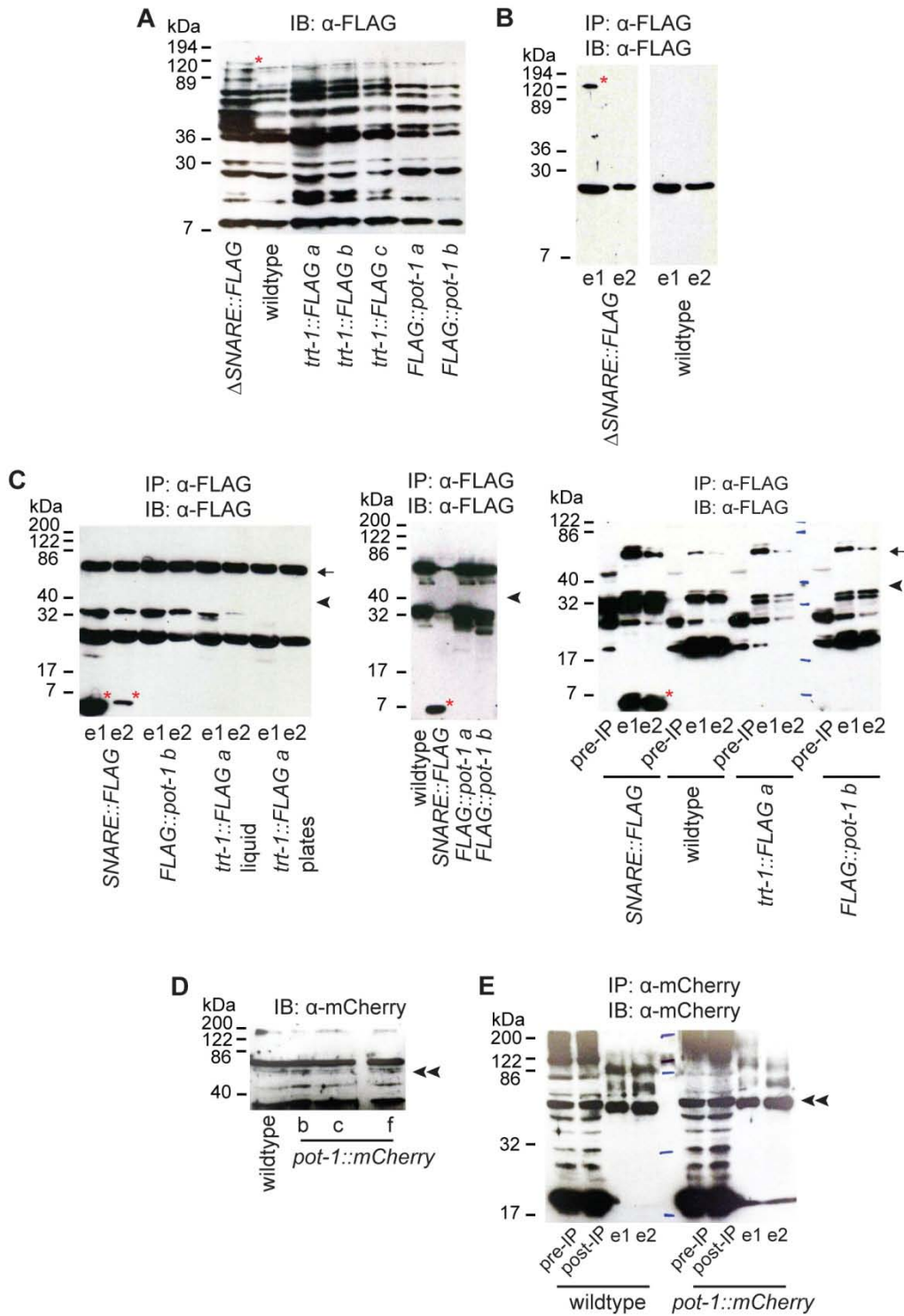
Figure 2.2 Immunodetection of proteins from whole worm extracts via western blot. A) Whole worm extracts were resolved via SDS-PAGE and immunobloted with α-FLAG antibodies. B) Immunoprecipitation from *tom-1SNARE::FLAG; tom-1(nu468)* and wildtype extracts using α-FLAG antibodies for IP and detection. C) Independent immunoprecipitations from several *tom-1SNARE::FLAG; tom-1(nu468), FLAG::pot-1*, and *trt-1::FLAG* extracts using α-FLAG antibodies for IP and detection. D) Extracts were resolved via SDS-PAGE and immunobloted with α-mCherry antibodies. E) Immunoprecipitation from *pot-1::mCherry* and wildtype extracts using α-mCherry antibodies for IP and detection. Clarified extracts (pre-IP) and extracts after incubation with α-mCherry-coupled beads (post-IP) were analyzed along with the first and second bead elutions (e1 and e2). asterisk: appropriate control band, arrow: predicted TRT-1::FLAG size, arrowhead: predicted FLAG::POT-1 size, double arrowhead: predicted POT-1::mCherry size.

To assess for the presence of POT-2::GFP via western blot, *pot-2::GFP* animals were harvested, along with a GFP-tagged histone (H2B) line as a positive control (strain TH32), and incubated with beads coupled with anti-GFP antibodies (Chromotek, gta-20). Bead elutions were probed with anti-GFP antibodies (Santa Cruz, sc-9996) via western blot. Specific bands of potentially appropriate sizes were observed in the *pot-2::GFP* (~56 kD?) and *histone::GFP* (~44 kD?) extracts (Figure 2.3A). Strikingly, western blotting with anti-GFP antibodies yielded much less background, which has been persistent with all other antibodies used. Because prominent background bands may be obstructing specific bands, performing future biochemistry using GFP tags, along with the antibodies and bead-coupled IP platforms that are available for this tag, may yield better results. To confirm that the POT-2::GFP band was accurately observed in anti-GFP blots, I stripped the membrane and incubated it with anti-MRT-1 antibody, which was previously generated against a domain that is present in both MRT-1 and POT-2 and thus could likely detect POT-2. Although POT-2::GFP is predicted to be 56 kD, a band running slightly below the 86-kD marker was detected by anti-MRT-1 in both bead elutions and pre-IP and post-IP extracts from *pot-2::GFP* animals only (Figure 2.3B). A similar-sized band was detected by the anti-GFP antibody from *pot-2::GFP* animals as well, suggesting that this band might represent POT-2::GFP (Figure 2.3A), and therefore that the anti-MRT-1 antibody might be capable of detecting the related OB2 fold domain in POT-2. However, GFP, expressed both in human cells and in worms, typically runs at the predicted size (~28 kD) on a gel (Saito *et al.* 2004; Zahn *et al.* 2004; Ropp *et al*. 1995), so this results needs to be confirmed.

While the POT-1::mCherry, FLAG::POT-1, and TRT-1::FLAG proteins may be recalcitrant to detection by antibodies via western blot, they may still have been successfully immunoprecipitated. Therefore, I wanted to assess whether POT-1::FLAG interacts with POT-2 or MRT-1, proteins whose homologs have been shown to interact with POT1 in other systems, and whether these proteins could be seen by western blot. Immunoblotting with a native anti-MRT-1 antibody, which may detect both MRT-1 and POT-2, revealed two specific bands in the

second elution for POT-1 (Figure 2.3C). The size of the higher band is in accordance with the approximate size of MRT-1 (~69 kDa), but the lower band appears significantly lower than the predicted size for POT-2 (~29 kDa). However, western blotting additional IPs with anti-MRT-1 antibodies did not reveal specific bands of the appropriate sizes from *trt-1::FLAG, pot-1::FLAG*, or *pot-1::mCherry* extracts or bead elutions (IP) (Figure 2.3D).

Finally, to assess whether anti-FLAG antibodies successfully precipitated TRT-1::FLAG but could not recognize the FLAG epitope on a membrane, I used a native anti-TRT-1 antibody on anti-FLAG IPs from *trt-1::FLAG* and *FLAG::pot-1* extracts. Although bands of the appropriate predicted size appear exclusively in TRT-1::FLAG and FLAG::POT-1 IPs (~62 kDa), this band is also apparent in the TOM-1SNARE::FLAG IP, suggesting that it is the result of non-specific recognition by the anti-FLAG antibody and not representative of TRT-1::FLAG or TRT-1 (Figure 3E). But because I lacked a positive TRT-1 control, and because I cannot be confident that POT-1 or TRT-1 were successfully precipitated, I cannot conclude anything about an interaction between POT-1 and TRT-1. To confirm that proteins were not lost in the clarification of extracts or appear in the insoluble pellet, crude extracts, extracts after one round of clarification, and pellets from the 1st and 2nd clarification rounds were assessed for the presence of FLAG-tagged proteins via western blotting using anti-FLAG antibodies. Neither FLAG::POT-1 nor TRT-1::FLAG-sized bands were apparent (Figure 2.3F).

In summary, although I observed several specific bands that may represent our proteins of interest, I cannot be confident of their identity. Moreover, while I did not see specific bands of appropriate sizes for TRT-1, those bands may be masked by prominent non-specific bands of the predicted TRT-1 size. Therefore, the possibility that I successfully precipitated TRT-1::FLAG or other tagged proteins remains.

Figure 2.3
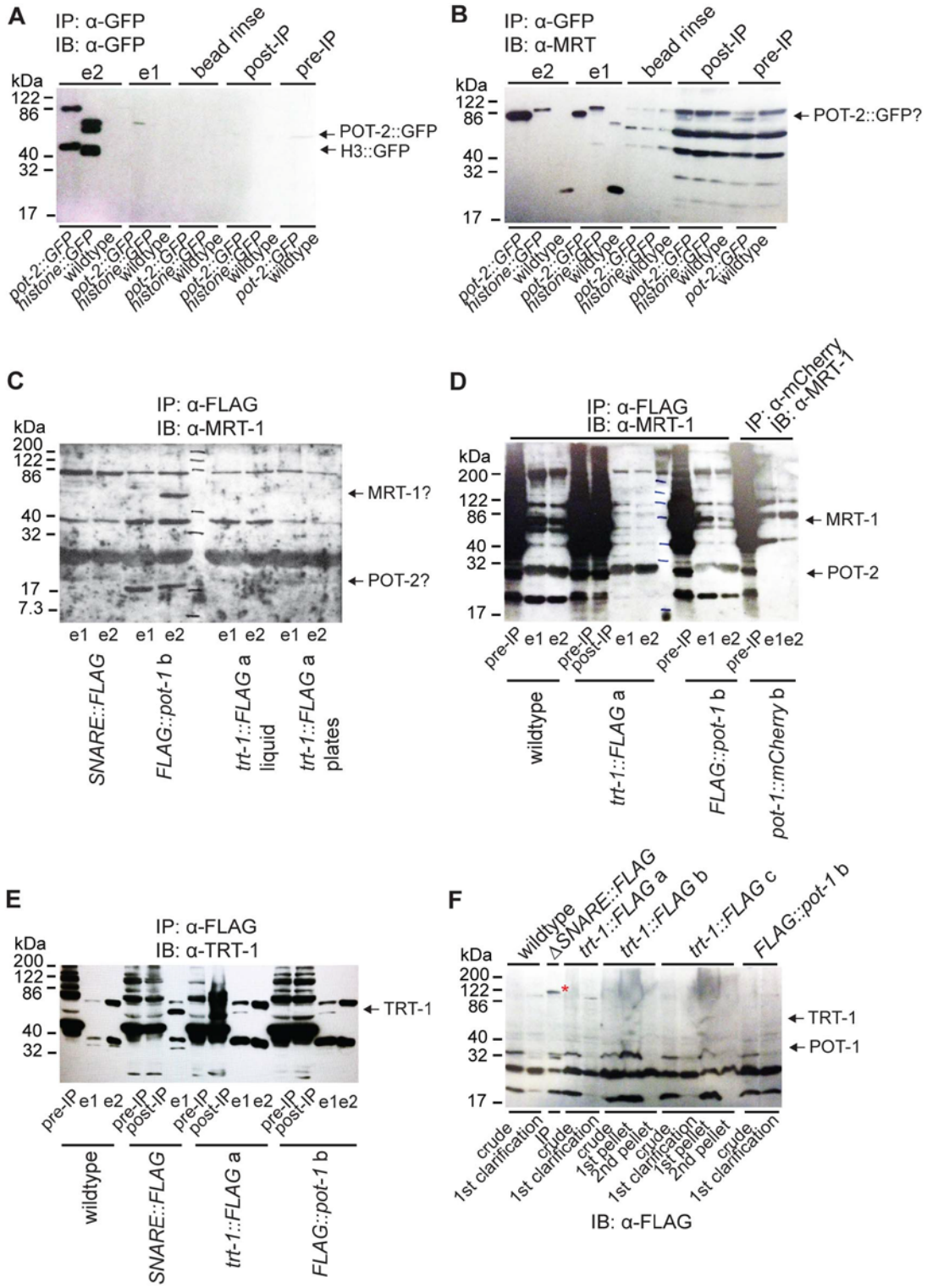
Figure 2.3 Immunodetection of proteins from whole worm extracts via western blot. A) Immunoprecipitation from *pot-2::GFP, histone::GFP* and wildtype extracts using α-GFP antibodies for IP and detection. Clarified extracts (pre-IP), extracts after incubation with α-GFP-coupled beads (post-IP), and a bead rinse were analyzed along with the first and second bead elutions (e1 and e2). Predicted sizes for POT-2::GFP (56 kD) and histone::GFP (44 kD) are shown to the right. B) Membrane from (A) was stripped and re-probed with α-MRT-1 antibodies, which likely can detect both MRT-1 and POT-2. The putative POT-2::GFP band (56 kD) is indicated to the right. C) Immunoprecipitation from *tom-1SNARE::FLAG; tom-1(nu468), FLAG::pot-1*, and *trt-1::FLAG* extracts using α-FLAG antibodies for IP and α-MRT-1 antibodies for detection. Putative MRT-1 (67 kD) and POT-2 (28 kD) bands are indicated to the right. D) Immunoprecipitations from wildtype, *trt-1::FLAG*, and *FLAG::pot-1* using α-FLAG antibodies and from *pot-1::mCherry* using α-mCherry antibodies were immunoblotted with α-MRT-1 antibodies. Predicted sizes for MRT-1 (67 kD) and POT-2 (28 kD) are shown to the right. E) Immunoprecipitations from wildtype, *tom-1SNARE::FLAG; tom-1(nu468), FLAG::pot-1*, and *trt-1::FLAG* extracts using α-FLAG antibodies were immunoblotted with α-TRT-1 antibodies. The predicted size of TRT-1 (62 kD) is shown to the right. F) Crude extracts, clarified extracts (1st clarification), and pellets from the 1st or 2nd clarifications (1st pellet or 2nd pellet) from wildtype, *FLAG::pot-1* and three lines of *trt-1::FLAG*, as well as an α-FLAG IP from *tom-1ΔSNARE::FLAG; tom-1(nu468)* animals as an α-FLAG immunoblot control, were blotted with α-FLAG antibodies. Asterisk indicates the appropriate control band, and the predicted sizes of TRT-1 (62 kD) and POT-1(38 kD) are shown to the right.

Direct telomerase activity assays

Although *trt-1::FLAG* transgenes did not prevent telomere erosion in *trt-1* mutants (Figure 1B), the fact that *trt-1::FLAG; trt-1(ok410)* animals were fertile through at least 40 generations of growth indicates that TRT-1::FLAG is capable of telomere maintenance, because *trt-1(ok410)* mutants typically become sterile within 15-30 generations (Meier *et al.* 2006). Therefore, I wanted to assess whether immunoprecipitated TRT-1::FLAG, although not clearly detectable based on the assays I performed, exhibited telomere repeat addition *in vitro*.

As *C. elegans* conditions for an *in vitro* telomerase activity assay have not yet been developed, I decided to perform the assay on IPs from *trt-1::FLAG* extracts using human or *Tetrahymena* conditions. Human telomerase activity assays performed at 30°C, 25°C, or 15°C, using all six configurations of the *C. elegans* hexameric telomere repeat (Figure 2.4A), did not yield activity for TRT-1::FLAG or FLAG::POT-1 IPs, while telomerase immunoprecipitated from human HEK 293 cells effectively elongated the human telomeric template, indicating that the assay conditions were successful (Figure 2.4B-D). Adding RNAse inhibitor (RNAsin, Promega) to the reaction to ensure telomerase RNA stability did not improve the activity, suggesting that degradation of the RNA template in our IPs is not what is preventing a lack of activity in this assay (Figure 2.4B). Curiously, addition of TRT-1::FLAG IP to the positive control reaction mixture attenuated the activity of the purified human telomerase, indicating that TRT-1::FLAG IPs either possess proteins that inhibit this reaction or the buffer itself is inhibitory (Figure 2.4D). However, several bands could be seen in the POT-1::FLAG IP that are reminiscent of the terminal transferase activity, an RNA template-independent addition of one nucleotide to the end of a telomere oligo, that has been shown for both human and yeast telomerase (Figure 2.4D) (Lue *et al.* 2005).

Figure 2.4

A *C. elegans* telomeric oligos:

T1: TTAGGCTTAGGC**TTAGGC**
T2: TAGGCTTAGGCT**TAGGCT**
T3: AGGCTTAGGCTT**AGGCTT**
T4: GGCTTAGGCTTA**GGCTTA**
T5: GCTTAGGCTTAG**GCTTAG**
T6: CTTAGGCTTAGG**CTTAGG**

B   Human conditions 30°C

T1 T2 T3 T4 T5 T6

control

TRT-1::FLAG a IPs   over-exposed

C   Human conditions 25°C

RNAse inhibitor:

T1-3 T1-3 T4-6 T4-6 T1-3 T1-3 T4-6 T4-6
 +   -   +   -   +   -   +   -

control

TRT-1::FLAG b IP   FLAG::POT-1 b IP   over-exposed

45

Figure 2.4

D Human conditions 15°C

T1-6

control
FLAG::POT-1 a IP + control
TRT-1::FLAG a IP
RNAse + TRT-1::FLAG a IP
FLAG::POT-1 b IP

over-exposed

E Human conditions 15°C

T1-6

control
TRT-1::FLAG b IP + control
FLAG::POT-1 a IP + control
wildtype IP + control
wildtype
TRT-1::FLAG b
TRT-1::FLAG d
RNAse+ TRT-1::FLAG d
FLAG::POT-1 a
RNAse+ FLAG::POT-1 a
FLAG::POT-1 b
RNAse+ FLAG::POT-1 b
TOM-1ASNARE::FLAG
RNAse + TOM-1ASNARE::FLAG
POT-2::GFP IP
histone::GFP IP

over-exposed

α-FLAG IPs

F Human conditions 15°C   *Tetrahymena* conditions

T1 T2 T3 T4 T5 T6 T1 T2 T3 T4 T5 T6   T1-3 T4-6 T1-3 T4-6

histone::GFP
RNAse + histone::GFP
RNAse + human control
human control
histone::GFP
RNAse + histone::GFP
Tetrahymena control
RNAse + *Tetrahymena* control

over-exposed

G Human conditions 15°C

T4 T5 T6 T4 T5 T6 T4 T5 T6

human control
histone::GFP
histone::GFP; *mrt-1*
histone::GFP; *trt-1*
RNAse + histone::GFP
RNAse + histone::GFP; *mrt-1*
RNAse + histone::GFP; *trt-1*

over-exposed

46

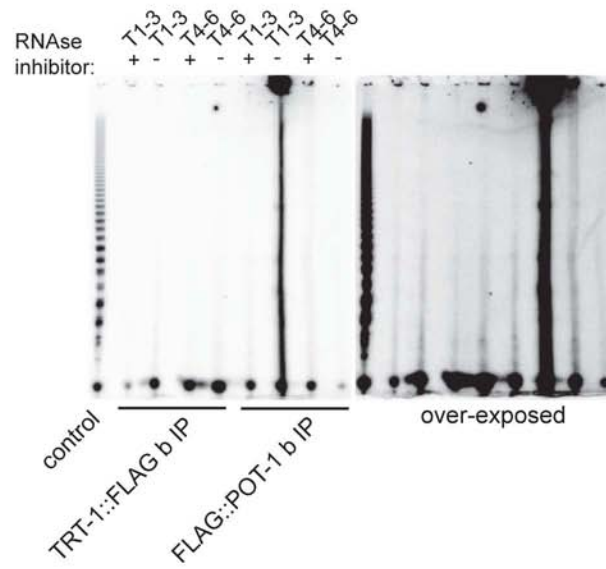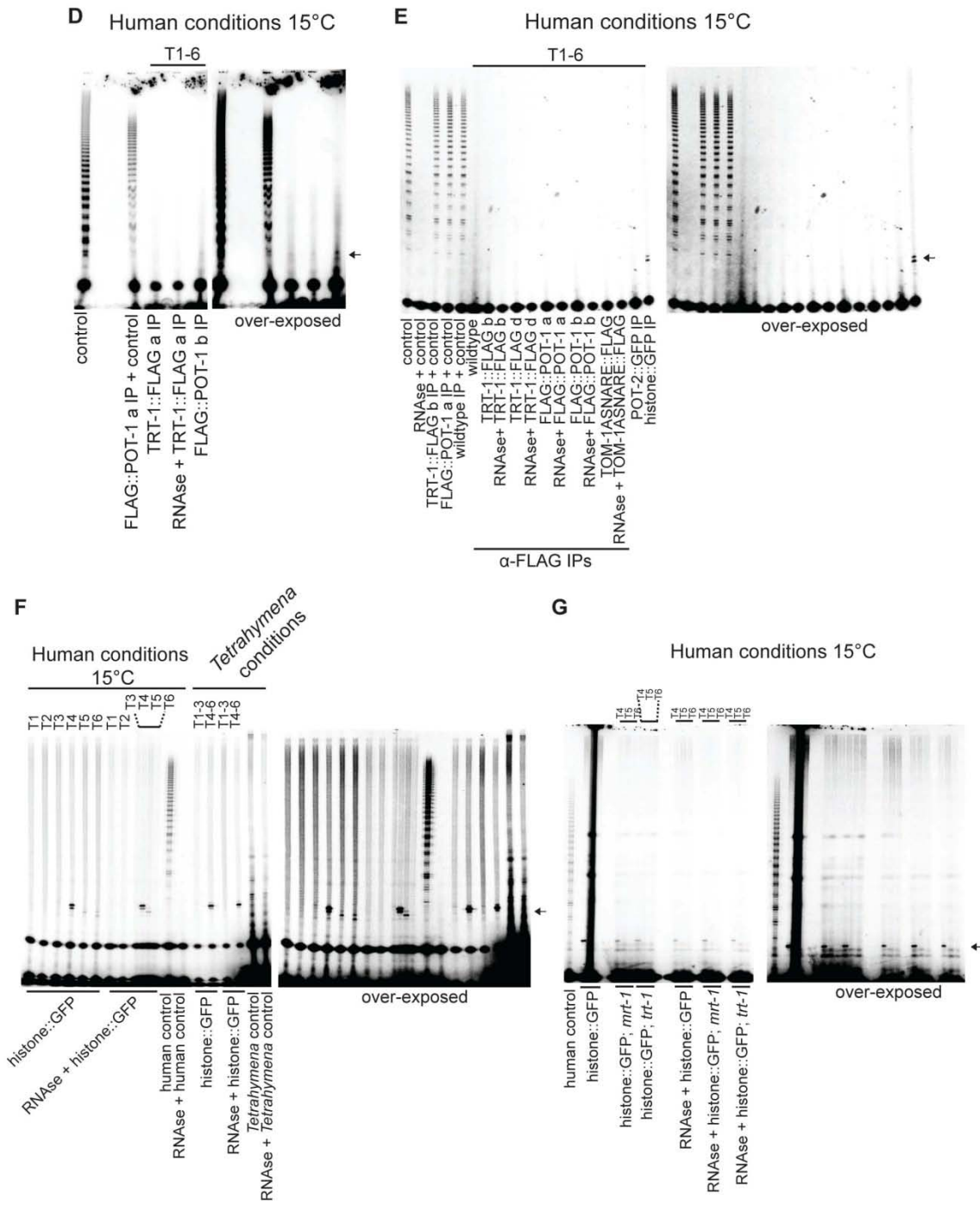**Figure 2.4 Direct telomerase assays with immunoprecipitated proteins.** A) Six telomeric permutations, T1-T6, of the *C. elegans* telomeric repeat TTAGGC. B) Immunoprecipitations from *trt-1::FLAG* extracts using α-FLAG antibodies are tested for the presence of catalytically active telomerase under human telomerase assay conditions. C) Immunoprecipitations from *trt-1::FLAG* and *FLAG::pot-1* extracts using α-FLAG antibodies are tested for the presence of catalytically active telomerase under human telomerase assay conditions with pooled T1, T2, and T3 or T4, T5, and T6 oligos. D) Immunoprecipitations from *trt-1::FLAG* and *FLAG::pot-1* extracts using α-FLAG antibodies are tested for the presence of catalytically active telomerase under human telomerase assay conditions with six pooled oligos. FLAG::POT-1 IP was mixed with control purified human telomerase prior to reaction (2nd lane). E) Immunoprecipitations from wildtype, *trt-1::FLAG, FLAG::pot-1,*and *tom-1SNARE::FLAG; tom-1(nu468)* extracts using α-FLAG antibodies and from *pot-2::GFP* and *histone::GFP* extracts using α-GFP antibodies are tested for the presence of catalytically active telomerase under human telomerase assay conditions with six pooled oligos. IPs were mixed with control purified human telomerase prior to reactions. Putative terminal transferase activity is indicated by arrow on the right. F) Immunoprecipitations from *pot-2::GFP* and *histone::GFP* extracts using α-GFP antibodies were tested for the presence of catalytically active telomerase under human and *Tetrahymena* telomerase assay conditions with single oligos (human) and pooled oligos (*Tetrahymena*). RNAse treatment erodes RNA template and prevents telomerase-mediated oligo extension. Faint laddering similar to telomerase activity is absent in RNAse-treated lanes but present in other lanes (histone::GFP IPs). Putative terminal transferase activity is indicated by arrow on the right. G) Immunoprecipitations from *histone::GFP*, *histone::GFP; mrt-1,* and *histone::GFP; trt-1* extracts using α-GFP antibodies were tested for the presence of catalytically active telomerase under human conditions. Putative terminal transferase activity, which is RNAse-insensitive, is indicated by arrow on the right.

I repeated the assay using human assay conditions at 15°C with several IPs from *trt-1::FLAG, FLAG::pot-1,* and *pot-2::GFP* animals and various positive (*tom-1SNARE::FLAG*) and negative (wildtype, non-transgenic animals) controls to test the above observations. Combining anti-FLAG IPs from *trt-1::FLAG, FLAG::pot-1,* or wildtype animals with telomerase immunoprecipitated from human HEK 293 cells did not impede oligo elongation efficiency, as compared to the control by itself, indicating that our IPs or the buffers do not actually inhibit this reaction (Figure 2.4E). Additionally, neither *FLAG::pot-1* strain yielded IPs with terminal transferase-like activity, as previously observed for the FLAG::POT-1 b IP, suggesting that this activity may be a consequence of a contaminating polymerase (Figure 2.4D & E). Curiously, two small bands were apparent for anti-GFP IPs from *histone::GFP* extracts using all six oligos combined in one reaction (Figure 2.4E). Therefore, I assayed for the presence of telomerase activity with individual telomeric oligos from anti-GFP IPs from *histone::GFP* extracts to determine if there was a preferred substrate for this kind of activity. Indeed, I observed several small bands with T4, T5, and T6, which were resistant to RNAse treatment (Figure 2.4F). This activity was also observed under *Tetrahymena* telomerase activity assay conditions with oligos T4-6 (Figure 2.4F). Curiously, RNAse-sensitive faint laddering bands, reminiscent of distributive telomerase activity, are apparent in anti-GFP IPs under human conditions, suggesting that there may be an RNA template-dependent activity (Figure 2.4F).

To further understand the nature of this activity, I repeated this assay using individual T4, T5, and T6 oligos with anti-GFP IPs from *histone::GFP* animals as well as *histone::GFP; trt-1* and *histone::GFP; mrt-1* animals. I observed activity in all IPs, regardless of RNAse treatment, with the most prominent bands occurring with the T4 oligo (Figure 2.4G). The presence of bands representing oligo extension in every sample suggests contamination. Although the three extracts were prepared separately, thus contamination of all three is unlikely, contaminating polymerase activity may have been introduced during the IPs, which were performed in parallel. Moreover, activity in IPs from *histone::GFP; trt-1* animals indicates that it is not telomerase-mediated.

48

However, the faint ladder seen in IPs from *histone::GFP* animals is absent in IPs from *histone::GFP; trt-1* and *histone::GFP; mrt-1* animals, suggesting that this may indeed be telomerase-mediated (Figure 2.4F). Unfortunately, one of the histone::GFP IP reactions was not properly clarified and thus has contaminating radioactivity that obstructs most of the other two histone::GFP reactions, precluding an analysis of whether the faint ladder appears in these reactions. Therefore, to conclude that telomerase was present in histone::GFP IPs, these experiments must be repeated.

Discussion

While I was not able to definitely conclude whether telomerase activity precipitated with POT-1, POT-2, or even histone, future biochemical efforts may indicate such an interaction. The mammalian shelterin component TPP1 directly recruits telomerase to telomeres via its oligosaccharide/oligonucleotide (OB) fold, but POT1 is not required for this interaction (Abreu *et al.* 2010). However, *C. elegans* POT-1, POT-2 and MRT-1, which harbor OB folds, may participate in such a recruitment event. *Arabidopsis* POT1a interacts directly with the telomerase RNA via its OB folds and is required for telomerase-mediated telomere repeat addition *in vivo* and *in vitro* (Surovtseva *et al.* 2007; Cifuentes-Rojas *et al.* 2010). Tandem affinity purification of Pot1a from *Tetrahymena thermophila* extracts revealed two associated proteins, Tpt1 and Pat1 (Linger *et al.* 2011). Neither protein precipitated telomerase activity *in vitro*. Future analysis of whether any of the four *C. elegans* POT1-derived homologs interact directly with telomerase may reveal insights into how telomerase is recruited to telomeres in worms. In particular, because POT-1 harbors a distinct OB fold from POT-2, POT-3, and MRT-1 (see Chapter 3 and Figure 3.1A for details), and *pot-1* and *pot-2* mutants display telomere phenotypes different from *mrt-1* and *pot-3* mutants, a functional link between any of these proteins and telomerase might prove mechanistic insight into how OB fold-harboring proteins have evolved in their function in telomere maintenance. Even if MRT-1 proves to be dispensable for telomerase recruitment, it

49

may be required for telomere repeat addition by processing telomeric ends via its nuclease activity. The results of the telomerase assays with IPs from *histone::GFP*; *mrt-1* animals suggest this may be the case, but these need to be validated.

Although several proteins are necessary for telomere maintenance *in vivo*, the mechanisms by which they accomplish this feat remain unclear. Co-purification of a protein that yields *in vitro* telomerase activity can indicate several roles in telomere repeat addition for that protein. For example, in addition to the telomerase catalytic and RNA subunits, three genes in budding yeast, *EST1*, *EST3*, and *CDC13*, are required for telomere maintenance *in vivo*, yet they are dispensable for telomere repeat addition *in vitro*, suggesting that they are involved in recruiting telomerase to telomeres, which is unnecessary in an *in vitro* setting (Lingner *et al.* 1997). Moreover, immunoprecipitation of Est1 or Est3 co-purifies telomerase activity (Steiner *et al.* 1996; Hughes *et al.* 2000), indicating that an apparent interaction with telomerase does not guarantee that the protein functions in its assembly or stability. Consistently, mutations altering Est1 binding to the telomerase RNA do not alter *in vitro* telomerase activity, indicating that although Est1 may be a component of the yeast telomerase RNP, it does not necessarily promote its biogenesis (DeZwaan & Freeman 2009). Indeed, addition of extra Est1 to the reaction increased telomere repeat addition in a concentration-dependent manner, indicating that Est1 actually promotes telomerase activity at the substrate (DeZwaan & Freeman 2009). However, the authors suggest that Est1 may still be required for maturation of an effective *in vivo* telomerase RNP but such processing may not be required for *in vitro* activity. Therefore, even if any of our telomeric proteins will prove to successfully precipitate telomerase activity, further detailed assessment is required before we can conclude that these proteins participate in telomerase stability or biogenesis.

Lastly, to definitively show that POT-1 interacts with MRT-1, POT-2, or TRT-1 *in vivo*, POT-1 could be immunoprecipitated from GFP-tagged POT-1 animals deficient for MRT-1, POT-2, or TRT-1. Those IPs should then be compared to IPs from tagged POT-1 animals with

wildtype MRT-1 and POT-2 using anti-MRT-1 or anti-TRT-1 antibodies. Though I made extensive progress in establishing biochemistry in the Ahmed lab, my efforts did not yield attractive results that would be clearly publishable, so I decided to focus on genetic analysis of *pot-1* and *pot-2*, as discussed in the next chapter.

CHAPTER 3:

Telomere length regulation by *C. elegans* POT-1 and POT-2

Human somatic cells have finite replicative lifespans and can enter an irreversible cell cycle arrest, termed senescence, in response to various stresses. Senescence can occur due to progressive shortening of telomeres, which cannot be completely replicated by canonical DNA polymerases (Harley *et al.* 1990). Telomeres are composed of simple TTAGGG repeats in vertebrates and related sequences in other organisms, such as TTAGGC repeats in *C. elegans*. To combat telomere erosion, cells can express the enzyme telomerase, which adds *de novo* telomere repeats to chromosome ends via reverse transcription from an RNA template (Greider & Blackburn 1989). Telomerase is expressed at high levels in germ cells and can be expressed in human somatic cells, but its expression is transient or absent altogether in more differentiated cells (Kim *et al.* 1994; Sharma *et al.* 1995).

The shelterin complex, composed of six mammalian telomere-binding proteins TRF1, TRF2, TIN2, POT1, RAP1 and TPP1, and its associated proteins protect telomeres from nucleases and DNA damage repair mechanisms that can lead to exacerbated telomere shortening or cellular senescence (reviewed in Diotti & Loayza 2011). Shelterin components maintain telomere homeostasis through positive and negative influences on telomere length. The double-stranded telomeric DNA-binding proteins TRF1 and TRF2 have been implicated as negative regulators of telomere length, where removal of TRF1 from telomeres or over-expression of TRF2 yielded telomere elongation or erosion, respectively (Smogorzewska *et al.* 2000; van Steensel & de Lange 1997). TIN2 and TPP1 proteins bridge the interaction between these double-stranded telomere-binding proteins and the single-stranded telomere-binding protein POT1 and

are also considered negative regulators of telomere length, as their depletion results in progressive telomere elongation (Kim *et al.* 1999; Ye & de Lange 2004; Ye *et al.* 2004)

Human POT1 interacts with single-stranded telomeric DNA via two oligonucleotide/oligosaccharide (OB) folds and is primarily considered a negative regulator of telomere length (Ye *et al.* 2004; Kendellen *et al.* 2009; Veldman *et al.* 2004). However, numerous studies have revealed roles for POT1 in both telomere elongation and telomere protection. POT1 over-expression (Armbruster *et al.* 2004; Liu *et al.* 2004) and mutant or splice-variant POT1 expression (Kendellen *et al.* 2009; Armbruster *et al.* 2004; Liu *et al.* 2004; Colgin *et al.* 2003; Loayza & de Lange 2003) can elicit telomere elongation. Additionally, POT1 can inhibit telomere repeat synthesis in the presence of its binding partner TPP1 or promote telomerase processivity *in vitro* in its absence (Kelleher *et al.* 2005; Walne *et al.* 2007).

Both mouse Pot1 homologs promote chromosome end protection, as G-strand overhangs lengthen in Pot1b$^{-/-}$ cells, and end-to-end chromosome fusions occur as a result of telomere deprotection in both Pot1a$^{-/-}$ and Pot1b$^{-/-}$ cells (He *et al.* 2006; He *et al.* 2009; Hockemeyer *et al.* 2006; Hockemeyer *et al.* 2008; Wu *et al.* 2006). However, disparate cellular and telomere phenotypes have been reported. For example, fibroblasts derived from Pot1a$^{-/-}$ mice senesced prematurely in one study (Wu *et al.* 2006) but not in another (Hockemeyer *et al.* 2006). Additionally, Pot1b$^{-/-}$ cells did not prematurely senescence in one study (Hockemeyer *et al.* 2006), but mouse embryonic fibroblasts over-expressing an OB-fold Pot1b mutant exhibited early-onset senescence in another study (He *et al.* 2006). Moreover, telomeres from Pot1b$^{-/-}$ cells have been shown to either shorten or stay the same (He *et al.* 2009; Hockemeyer *et al.* 2006; Hockemeyer *et al.* 2008), whereas Pot1a$^{-/-}$ cells exhibited telomere elongation (Wu *et al.* 2006).

The *C. elegans* genome is predicted to encode four proteins with OB folds homologous to mammalian POT1, including a single protein with an OB1-fold, POT-1, and three proteins with OB2-folds, POT-2, POT-3 and MRT-1 (Figure 3.1A) (Meier *et al.* 2009; Raices *et al.* 2008). Previous work has illustrated that POT-1, also known as CeOB2, and POT-2, also known as

CeOB1, preferentially interact with G- or C-rich single-stranded telomeric DNA *in vitro*, respectively (Raices *et al*. 2008). Additionally, this study reported elongated telomeres for both *pot-1(tm1620)* and *pot-2(tm1400)* mutant strains, although *pot-1(tm1620)* telomeres were distinctive and appeared similar to those of human cells that maintain their telomeres by a telomerase-independent telomere replication pathway termed Alternative Lengthening of Telomeres (ALT).

We previously demonstrated that one of four POT1-derived proteins, MRT-1, is necessary for telomerase-mediated telomere repeat addition *in vivo* (Meier *et al.* 2009). Here we investigate additional roles for POT1-derived proteins in *C. elegans* by studying telomere dynamics in *pot-1* and *pot-2* mutants. I show that POT-1 and POT-2 are negative regulators of telomerase and that epitope-tagged POT-1 can enhance the onset of senescence in a telomerase-deficient background. This synthetic interaction may mimic accelerated telomere shortening and senescence observed in human early-onset aging diseases and suggests that POT1 could be the molecular culprit in some progeric individuals.

POT-1 and POT-2 are negative regulators of telomere extension in vivo

Analysis of *pot-1(tm1620)* and *pot-2(tm1400)* deletion mutant strains provided by Shohei Mitani revealed moderate telomere elongation in the first few generations of growth, and propagation for many generations resulted in unusually long telomeres (Figure 3.1B). However, propagation of *pot-3(ok1530)* strains revealed no overt telomere length changes (Figure 3.1B). Outcrossing of *pot-1* or *pot-2* mutations for 15 generations as heterozygotes, followed by isolation of homozygous mutant *pot-1* or *pot-2* strains, revealed normal telomere lengths in early generations followed by progressive telomere elongation (Figure 3.1C). Therefore, the telomere elongation phenotypes caused by *pot-1* and *pot-2* mutations are recessive and can be eliminated by maintaining the strains as heterozygotes. *pot-1; pot-2* double mutants did not display an enhanced progressive telomere elongation phenotype in comparison to *pot-1* or *pot-2* single

54

mutant controls (Figure 3.1D), suggesting a common function for both gene products in negative regulation of telomere length.

To confirm that the *pot-1(tm1620)* mutation was responsible for the telomere elongation phenotype of outcrossed *pot-1* strains, single-copy transgenes designed to express wildtype POT-1 fused to a fluorescent mCherry protein at its C terminus were created, outcrossed 9 times, and crossed into a *pot-1(tm1620)* background that had been outcrossed 30 times. In contrast to *pot-1(tm1620)* mutants (Figure 3.1C), telomere lengths in independent *pot-1::mCherry*; *pot-1(tm1620)* strains remained constant over many generations (Figure 3.1E), indicating that the progressive telomere elongation phenotype of *pot-1(tm1620)* mutants is caused by the *pot-1* deletion rather than a tightly linked mutation. Moreover, normal telomere dynamics were observed for independently outcrossed *pot-1::mCherry* strains in a wildtype *pot-1* background, indicating that the POT-1::mCherry fusion protein does not perturb the ability of endogenous POT-1 to regulate telomere length (Figure 3.1F).

A single-copy *GFP::pot-2* transgene did not have significant effects on telomere length when endogenous *pot-2* was wildtype but rather promoted smeary, heterogeneous telomeres during early generations of growth when endogenous *pot-2* was mutant (Figure 3.2A). Thus, *GFP::pot-2* failed to rescue the telomere elongation phenotype caused by the *pot-2(tm1400)* mutation. GFP::POT-2 yielded strong yet diffuse GFP fluorescence in the cytoplasm of germ cells and occasionally in the nucleoplasm (Figure 3.2B). Readily quantifiable clear and consistent nuclear foci were only apparent for a minority of animals, where some germ cell nuclei displayed faint GFP::POT-2 foci (Figure 3.2B).

Figure 3.1

Figure 3.1. POT-1 and POT-2 are negative regulators of telomere replication. A) A representation of the four POT-1 homologs in *C.* elegans. Terminal restriction fragment length analysis was performed on DNA collected from consecutive generations of (B) *pot-1(tm1620)*, *pot-2(1400)*, and *pot-3(ok1530)* single mutants, (C) outcrossed *pot-2(1400)* and *pot-1(tm1620)* single mutants, (D) wildtype and *pot-1; pot-2* double mutants (E) outcrossed *pot-1::mCherry*; *pot-1(tm1620)* strains, and (F) outcrossed *pot-1::mCherry* strains.

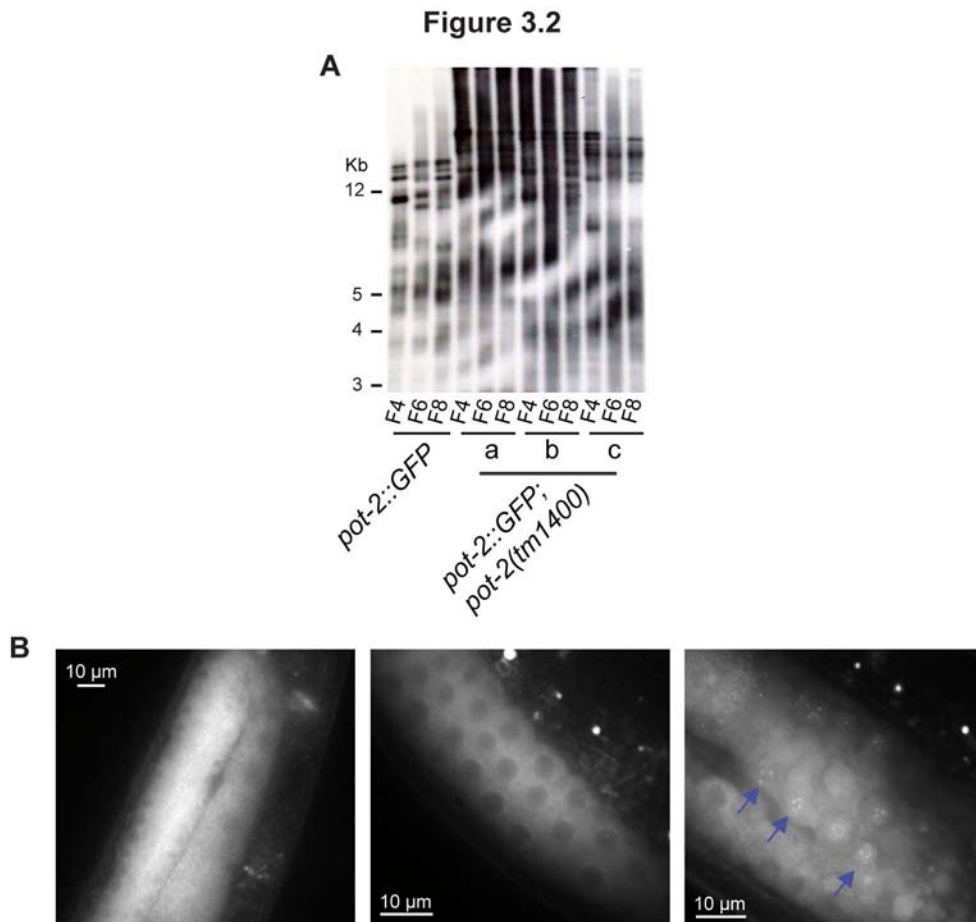**Figure 3.2. The POT-2::GFP construct does not rescue mutant pot-2 phenotypes.** A) DNA was collected from progressive generations of several independent *pot-2::GFP; pot-2(tm1400)* lines and a *pot-2::GFP; pot-2(+)* control line and subjected to terminal restriction fragment length analysis. B) POT-2::GFP is dispersed throughout the germline and occasionally as punctate foci (blue arrows) in germ cell nuclei (bottom panel).

57

POT-1 localizes as punctate foci to C. elegans telomeres in vivo

In contrast to weak and inconsistent GFP::POT-2 foci described above, live imaging of animals possessing *pot-1::mCherry* transgenes revealed strong punctate POT-1::mCherry foci within the nuclei of sperm, some oocytes, and at the nuclear periphery throughout the rest of the germline (Figure 3.3A-C). POT-1::mCherry foci could be robustly quantified in meiotic pachytene nuclei near the bend of germline arms, where the six homologous chromosomes of *C. elegans* are synapsed and in late stages of meiotic recombination (Dernburg *et al*. 1998). Analysis of independent *pot-1::mCherry* transgene insertions, *pot-1::mCherry.B* and *pot-1::mCherry.C*, revealed approximately 12 foci per nucleus (11.82±0.07; 11.87±0.09), which could plausibly correspond to chromosome termini of the six paired homologous chromosomes (Figure 3.3D and F). To confirm that these were telomeric foci, I utilized the end-to-end chromosome fusions *ypT24* and *ypT28*, which can be stably maintained in *C. elegans* due to their holocentric chromosomes (Lowden *et al*. 2008). Strains homozygous for *ypT24* and *ypT28* X-autosome chromosome fusions harbor five homologous chromosomes and 10 chromosome termini. *ypT24* and *ypT28* chromosome fusions were crossed with *pot-1::mCherry* to create *pot-1::mCherry; ypT24* and *pot-1::mCherry; ypT28* strains, and quantification of POT-1 fluorescent foci in these strains revealed approximately 10 meiotic foci per nucleus (9.97±0.10; 9.94±0.09) (Figure 3.3F), indicating that POT-1:mCherry foci correspond to discrete chromosome termini that are not clustered in meiotic pachytene nuclei. Telomere clustering has been reported as chromosomes pair during meiosis (Cooper *et al*. 1998; Yamamoto & Hiraoka 2011), a process that occurs in transition zone nuclei of the *C. elegans* germline, and POT-1::mCherry foci were less discrete at this stage of germ cell development (Figure 3.4), possibly due to rapid chromosome movements as chromosomes pair.
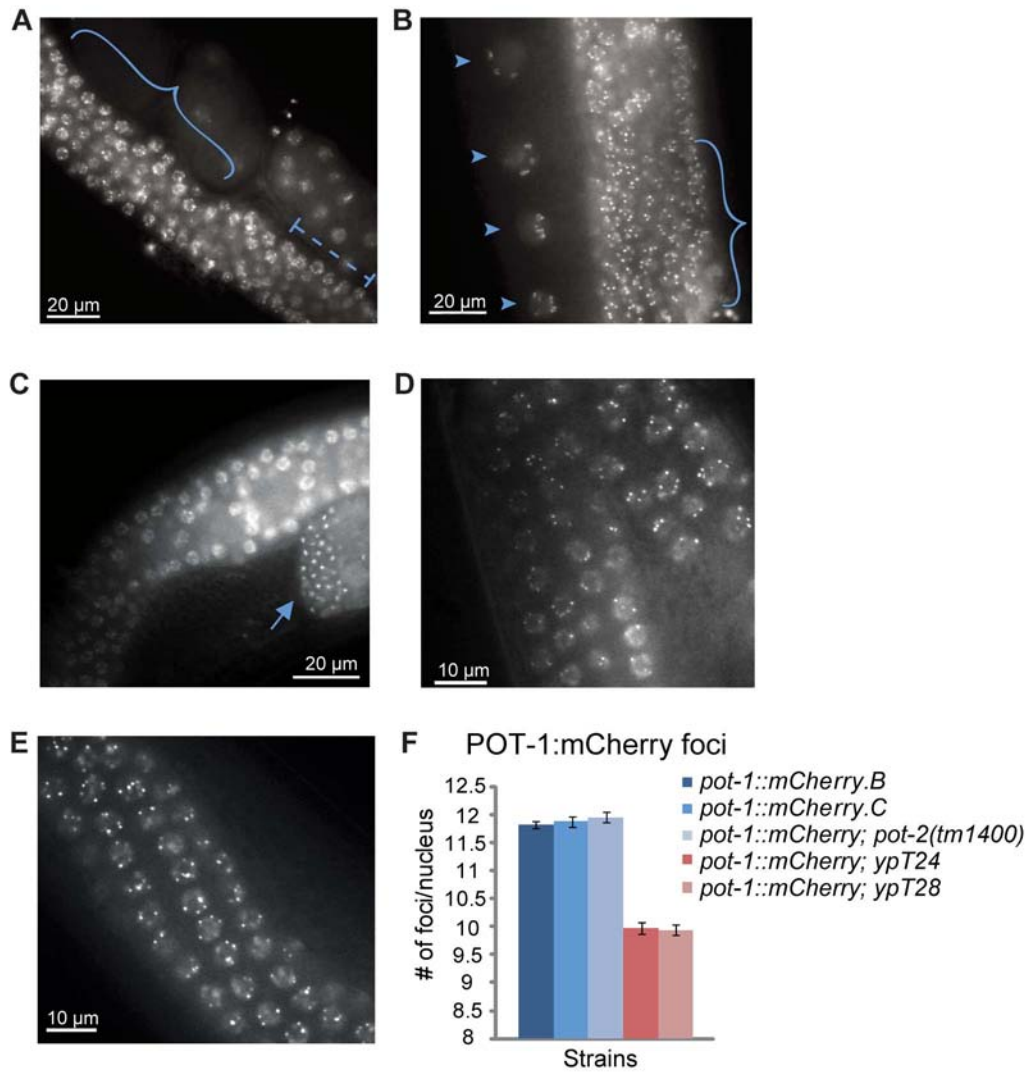
Figure 3.3. POT-1:mCherry localizes to telomeres as punctate foci independent of POT-2.
Live imaging of *pot-1::mCherry* strains revealed germline-specific expression, including meiotic
nuclei (A, B; solid brackets) and mitotic nuclei (A; dashed brackets), oocytes (B; arrow heads),
and sperm (C; arrow). (D) Representative image of *pot-1::mCherry*. (E) Representative image of
pot-1::mCherry; pot-2(tm1400). (F) POT-1:mCherry foci were quantified in the meiotic nuclei of
two independent wildtype strains, *pot-1::mCherry.B* (n=83) and *C* (n=54), in a *pot-2(tm1400)*
mutant strain (n=56), and in the strains *ypT24* (n=30) and *ypT28* (n=51).
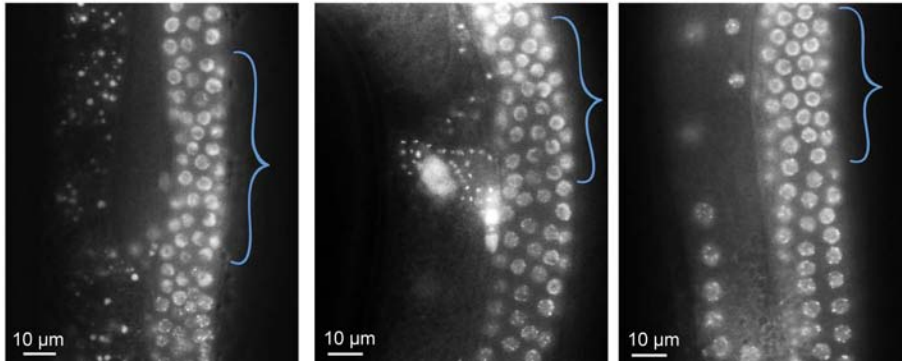
Figure 3.4. POT-1::mCherry localization in transition zone germline nuclei. POT-1::mCherry fluorescence is more diffuse in transition zone nuclei (brackets), where chromosomes begin to pair and enter meiosis.

Lack of an additive telomere elongation phenotype for *pot-1; pot-2* double mutants (Figure 3.1D) suggested a common function for their gene products, so I assessed whether the telomeric localization of POT-1 was affected by POT-2 by quantifying POT-1::mCherry foci in live *pot-1::mCherry*; *pot-2(tm1400)* animals. Approximately 12 foci per meiotic pachytene nucleus were observed when *pot-2* was mutant (11.96±0.09), and the POT-1::mCherry localization pattern was qualitatively similar throughout the germline in wildtype and *pot-2* mutant backgrounds (Figure 3.3E and F). Therefore, POT-2 did not have an obvious effect on the telomeric localization of POT-1.

POT-1 and POT-2 repress telomerase activity at telomeres

To ascertain whether the telomere elongation phenotype of *pot-1* and *pot-2* mutants is mediated by telomerase, I crossed the *pot-1* and *pot-2* mutations into a telomerase-deficient background by constructing double and triple mutants with a null allele of the telomerase reverse transcriptase, *trt-1(ok410)*. Telomeres shortened progressively in the absence of telomerase and *pot-1*, *pot-2* or both *pot-1* and *pot-2* (Figure 3.5A-C). Therefore, telomere elongation of *pot-1* or *pot-2* single mutants depends on telomerase activity.

In the absence of telomerase, canonical DNA polymerases cannot maintain telomere length, resulting in a loss of telomere sequence with each cell division. We asked whether POT-1 or POT-2 affected the rate of telomere erosion in the absence of telomerase by quantifying telomere shortening in *trt-1; pot-1* and *trt-1; pot-2* double mutants as well as in *trt-1; pot-2; pot-1* triple mutants. An enhanced telomere erosion rate was observed for *trt-1; pot-1* mutants (158.9±12.2 bp/generation) in comparison to *trt-1* single mutants (122.2±6.4 bp/generation) (Figure 3.6A) or *trt-1; pot-2* double mutants (122.9±8.8 bp/generation) (Figure 3.5D).

Figure 3.5

A

Kb
12
5
4
3
2
1.6

F5 F7 F9 F11 F13 | F5 F7 F9 F11 F13 | F5 F9 F11 F13 | F7 F9 F11 F13

a   b   c   d

trt-1; pot-1

B

Kb
12
5
4
3
2

F9 F11 F13 | F7 F9 F11 F13 | F7 F9 F13 F15 | F7 F9 F13 F15

a   b   c   d

trt-1; pot-2

C

Kb
12
5
4
3
2

F10 F18 F20 | F10 F18 F20 | F10 F18 F20 | F10 F18 F20 | F10 F18 F20

a   b   c   d   e

trt-1; pot-2; pot-1

D   Telomere erosion rates

P = 0.745
P = 0.005
P = 0.945

# of base pairs lost / generation

200
180
160
140
120
100
80
60
40
20

Strains

- *trt-1(ok410)*
- *trt-1; pot-2*
- *trt-1; pot-1*
- *trt-1; pot-2; pot-1*

E   Trans-generational Lifespan

Percent fertile

100
90
80
70
60
50
40
30
20
10
0

F4 F8 F12 F16 F20 F24 F28 F32 F36 F40 F44 F48 F52 F56 F60 F64 F68 F72 F76 F80 F84

Generations of growth

- *trt-1(ok410)*
- *trt-1; pot-1*
- *trt-1; pot-2; pot-1*

Figure 3.5. POT-1 and POT-2 negatively regulate telomerase-mediated telomere repeat addition. DNA collected from consecutive generations of (A) *trt-1; pot-1*, (B) *trt-1; pot-2*, and (C) *trt-1; pot-1; pot-2* mutant strains was submitted to terminal restriction fragment length analysis, and the rate of their telomere erosion was measured (D). Error bars represent the S.E.M., and *P* values were determined by the Student's t-test (D).
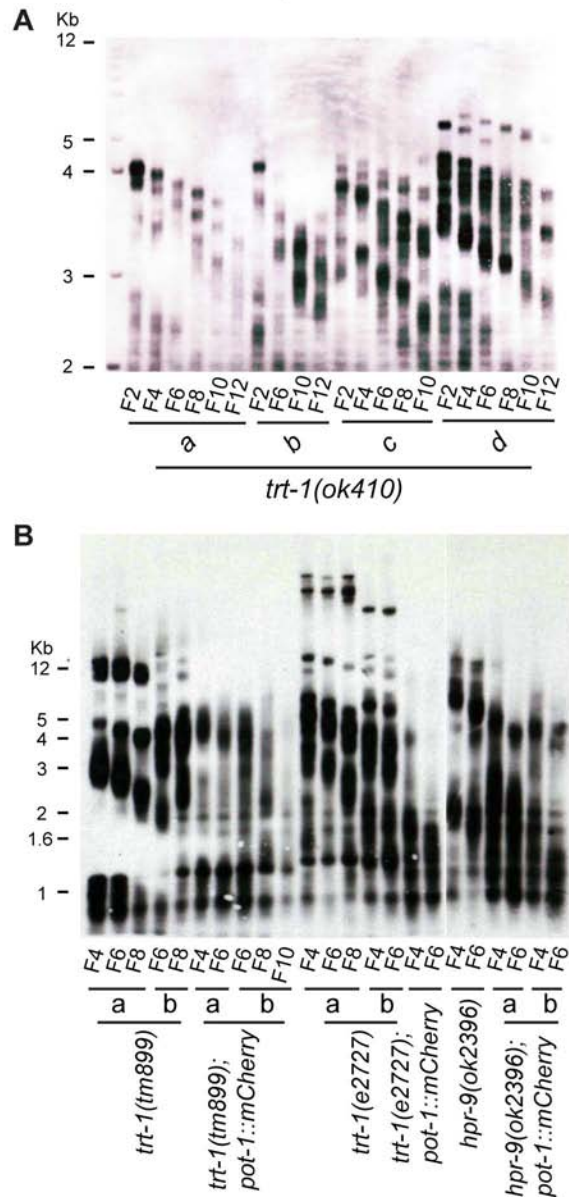
Figure 3.6. Telomerase reverse transcriptase mutants exhibit progressive telomere erosion, which is exacerbated by the presence of a POT-1::mCherry fusion protein. DNA was collected from (A) four independent *trt-1(ok410)* mutant lines and (B) several independent *trt-1(tm899)*, *trt-1(e2727)*, and *hpr-9(ok2396)* single mutants and their respective *pot-1::mCherry* strains and subjected to terminal restriction fragment length analysis.

Therefore, POT-1, but not POT-2, protects telomeres from exacerbated erosion in the absence of telomerase. Moreover, *trt-1; pot-2; pot-1* telomeres shortened at a similar rate (167.7±8.8 bp/generation) to *trt-1; pot-1* telomeres, indicating that POT-2 does not have an obvious telomere protection function in the absence of POT-1 (Figure 3.5C and D).

To study the effects of the modestly exacerbated telomere erosion observed in *pot-1* mutant strains that are deficient for telomerase, the onset of sterility (senescence) was quantified for *trt-1; pot-1* double mutants and *trt-1; pot-2; pot-1* triple mutants (n=40 independent lines per strain). However, both *trt-1; pot-1* double mutants (26.8+/-1.3 generations) and *trt-1; pot-2; pot-1* triple mutants ($\geq$39.7+/-3 generations) exhibited longer trans-generational lifespans in comparison to *trt-1* mutant controls (16.7+/-0.4 generations) ($P<0.001$; Student's t-test) (Figure 3.5E). Additionally, *trt-1; pot-2; pot-1* triple mutants exhibited a significantly longer average trans-generational lifespan than the *trt-1; pot-1* double mutants ($P<0.001$; Student's t-test) (Figure 3.5E). Therefore, although POT-1 represses telomere shortening in the absence of telomerase, deficiency for *pot-1* or both *pot-1* and *pot-2* failed to enhance the onset of senescence in the absence of telomerase.

POT-1::mCherry perturbs telomere stability in the absence of telomerase

To determine if the telomerase reverse transcriptase might affect POT-1 localization, independent *trt-1(ok410); pot-1::mCherry* strains were constructed. Unexpectedly, these strains displayed rapid drops in brood size within six generations and early-onset sterility at approximately 12 generations, which we have not previously observed for many well-outcrossed *C. elegans* strains that are deficient for the telomerase reverse transcriptase or for additional proteins that are required for telomerase-mediated telomere repeat addition *in vivo* (Meier *et al.* 2009; Lowden *et al.* 2008; Ahmed & Hodgkin 2000; Boerckel *et al.* 2000; Meier *et al.* 2006). These results were confirmed by creating *trt-1; pot-1::mCherry* strains using two independent alleles of *trt-1*, *tm899* and *e2727*, as well as matched *trt-1* single mutant controls derived from the

same crosses. *trt-1(tm899); pot-1::mCherry* and *trt-1(e2727); pot-1::mCherry* strains exhibited average trans-generational lifespans of 13+/-0.4 and 12.1+/-0.4 generations, respectively, in comparison to 24.7+/-0.7 and 23+/-0.4 generations for *trt-1(tm899)* and *trt-1(e2727)* single mutant controls, respectively (Figure 3.7A) (*P*<0.001 for both *trt-1; pot-1::mCherry* genotypes in comparison to *trt-1* controls; n=40 strains per genotype; Student's t-test). Therefore, expression of the *pot-1::mCherry* transgene enhances the onset of senescence for *C. elegans* strains that are deficient for *trt-1*.

In addition to *trt-1*, telomerase fails to add *de novo* telomeric repeats to telomeres in mutants that are deficient for subunits of the 9-1-1 DNA damage response signaling complex (HPR-9 / MRT-2 / HUS-1) (Ahmed & Hodgkin 2000; Meier *et al.* 2006; Hofmann *et al.* 2000), its clamp loader HPR-17 (Boerckel *et al.* 2000), or the nuclease MRT-1 (Meier *et al.* 2009). To determine if the former DNA damage response proteins might promote the early-onset sterility phenotype of *pot-1::mCherry* strains that are deficient for telomerase, the *pot-1::mCherry* transgene was crossed onto *hpr-9*, *mrt-2*, *hpr-17* and *mrt-1* mutant backgrounds. These strains were created using novel alleles of *hpr-17* and *mrt-2,* which were identified in screens for *C. elegans* mutants exhibiting progressive sterility, as well as a deletion allele of *hpr-9* that causes progressive telomere erosion and end-to-end chromosome fusions (See Chapter 1). *pot-1::mCherry* strains deficient for any of the above DNA damage response mutations also exhibited an accelerated time-to-sterility in comparison to single DNA damage response mutant controls (Figure 3.7A). *pot-1::mCherry* mutant doubles with *hpr-9(ok2396), mrt-2(yp8), hpr-17(yp7), mrt-1(e2661), and mrt-1(yp2)* were fertile for 11.1±0.5, 15.9±0.4, 11.8±0.4, 14.2±0.4, and 11±0.4 generations as compared to 24±0.5, 20.5±0.9, 19.8±0.4, 19.5±0.7, and 23.1±1 generations for *hpr-9(ok2396), mrt-2(yp8), hpr-17(yp7), mrt-1(e2661), and mrt-1(yp2)* single mutants, respectively (*P*<0.001 for all comparisons; Student's t-test) (Figure 3.7A).

Figure 3.7

A Trans-generational Lifespan

Legend:
- trt-1(tm899)
- trt-1(tm899); pot-1::mCherry
- trt-1(e2727)
- trt-1(e2727); pot-1::mCherry
- hpr-9(ok2396)
- hpr-9(ok2396); pot-1::mCherry
- hpr-17(yp7)
- hpr-17(yp7); pot-1::mCherry
- mrt-2(yp8)
- mrt-2(yp8); pot-1::mCherry
- mrt-1(e2661)
- mrt-1(e2661); pot-1::mCherry
- mrt-1(yp2)
- mrt-1(yp2); pot-1::mCherry

B Trans-generational Lifespan

Legend:
- trt-1(tm899)
- trt-1(tm899); pot-1::mCherry
- trt-1(tm899); FLAG::pot-1
- trt-1(tm899); pot-2::GFP
- trt-1(tm899); ttTi5605

C *trt-1(tm899); pot-1::mCherry* / *trt-1(tm899); pot-2::GFP*

D *trt-1(tm899); pot-1::mCherry* / *trt-1(tm899)*

E trt-1(ok410); pot-1::mCherry   10 μm

F trt-1(tm899); pot-1::mCherry   10 μm

G hpr-17(yp7); pot-1::mCherry   10 μm

H hpr-9(ok2396); pot-1::mCherry   10 μm

I mrt-2(yp8); pot-1::mCherry   10 μm

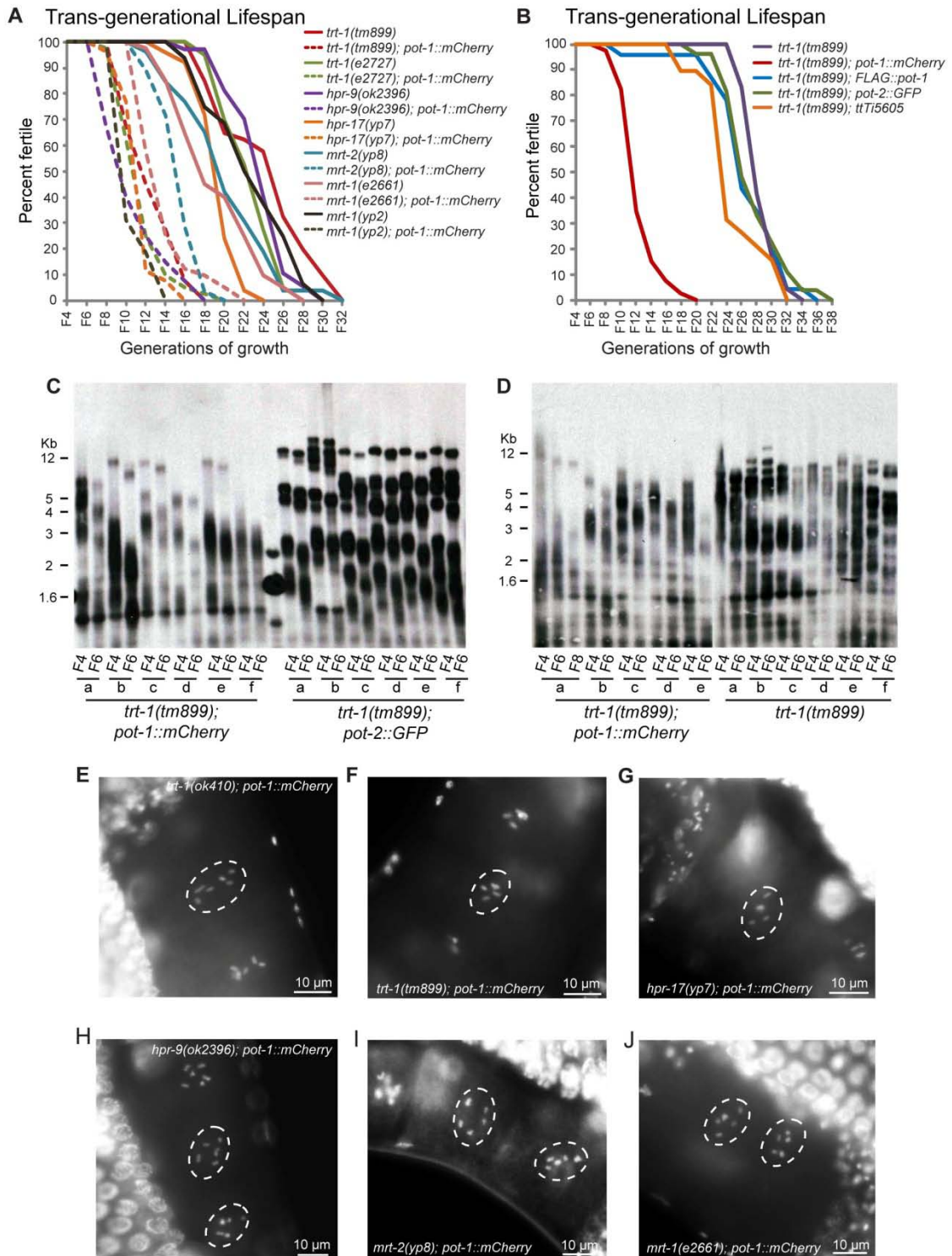**J** mrt-1(e2661); pot-1::mCherry   10 μm

67

Figure 3.7. POT-1::mCherry exacerbates telomere loss in telomere maintenance-defective mutants. (A) Trans-generational lifespan is reduced in telomere maintenance-defective *pot-1::mCherry* mutants as compared to telomere maintenance-defective single mutants. (B) The *pot-1::mCherry* transgene, but not other transgenes, exacerbate senescence of telomerase mutants. Telomere maintenance-defective *pot-1::mCherry* mutants exhibit smeary telomeres that are shorter than matched telomerase-deficient *pot-2::GFP* strains (C) or telomerase mutants alone (D). (E-J) Telomere maintenance-deficient *pot-1::mCherry* mutants exhibit end-to-end fusions. White dashed lines surround unfused chromosomes in early generation, wildtype brood size *trt-1; pot-1::mCherry* (E) and fused chromosomes in later-generation, low broodsize *trt-1; pot-1::mCherry* (F), *hpr-17; pot-1::mCherry* (G), *hpr-9; pot-1::mCherry* (H), *mrt-2; pot-1::mCherry* (I), and *mrt-1; pot-1::mCherry* (J).

These results mimic those of *trt-1; pot-1::mCherry* strains and are consistent with the

model that *hpr-9*, *mrt-2*, *hpr-17,* and *mrt-1* are deficient for telomerase-mediated telomere repeat

addition (Meier *et al.* 2009; Ahmed & Hodgkin 2000; Boerckel *et al.* 2000; Hofmann *et al.* 2002),

and that the DNA damage response functions of these genes do not promote the rapid senescence

phenotype caused transgenic *pot-1::mCherry*. Finally, all *trt-1; pot-1::mCherry* strains, as well as

pot-1::mCherry strains with mutant DNA damage response complex genes, exhibited normal

meiotic localization of POT-1::mCherry in early generations (Figure 3.8A-F).

To confirm that POT-1::mCherry is responsible for the enhanced onset of senescence

phenotype in the absence of telomerase, I constructed double mutants between *trt-1(tm899)* and

an N-terminally tagged POT-1 construct, *FLAG::pot-1*, or the previously mentioned *pot-2::GFP*

construct, both of which were integrated at the same locus on Chromosome *II* as the *pot-*

1::mCherry transgene. The *Mos1* transposon insertion, *ttTi5605* (Frokjaer-Jensen *et al.* 2008),

which was excised to create the single-copy insertions *pot-1::mCherry*, *FLAG::pot-1* and *pot-*

2::GFP, was also used as a control (Figure 3.9). These control strains did not exhibit an

exacerbated onset of sterility in comparison to *trt-1(tm899)* single mutant controls, whereas *trt-*

1(tm899); pot-1::mCherry strains constructed concurrently with the above controls became

rapidly sterile (Figure 3.7B). These results indicate that specific expression of the *pot-1::mCherry*

transgene drives early-onset senescence when telomerase is deficient.

Southern blotting revealed that telomeric DNA of telomerase-deficient *pot-1::mCherry*

strains was more smeary and predominantly shorter than DNA from telomerase single mutant

controls (Figure 3.7C and D; Supplementary Figure 3.7B). A precise rate of telomere erosion was

difficult to obtain for telomerase-deficient *pot-1::mCherry* strains due to a lack of discrete

telomere bands and rapid drops in brood size that typically prevented collection of adequate

amounts of DNA for telomere length analysis in later generations. Short telomeres appeared

rapidly in *pot-1::mCherry* animals defective for telomerase-mediated telomere maintenance. As

telomeric circles (t-circles) have been associated with rapid telomere deletion events (Tomaska *et*

al. 2009; Wang et *al.* 2004), I assayed for the presence of t-circles in several *pot-1::mCherry; trt-1* lines using two-dimensional gel electrophoresis (Raices *et al.* 2008; Wang *et al.* 2006). T-circles were observed for three of six *trt-1* single mutant samples and for two of six *pot-1::mCherry; trt-1* double mutant samples analyzed (Figure 3.10, as well as longer exposures of these and other blots, data not shown). Therefore, *pot-1::mCherry; trt-1* strains did not possess higher levels of t-circles than *trt-1* controls, suggesting that rapid telomere deletion events mediated by t-circle generation may not account for their rapid senescence phenotype. Although single-stranded telomeric DNA was observed below the arcs on the former 2D gels, a consistent increase was not observed for *pot-1::mCherry* strains in comparison to telomerase single mutant controls (Figure 3.10), suggesting that extensive resection of 5' ends of chromosome termini does not occur as a consequence of the mCherry tag (Pitt & Cooper 2010).

Late-generation telomerase-deficient *C. elegans* strains likely become sterile as a consequence of an accumulation of end-to-end chromosome fusions (Lowden *et al.* 2008; Meier *et al.* 2006). A decrease in chromosome number was apparent in oocytes of telomere maintenance-defective *pot-1::mCherry* strains at generations concomitant with drops in brood size (Figure 3.7E-J), as observed with late-generation *trt-1(ok410)* controls displaying similar levels of fertility (Table 1). Moreover, drops in POT-1::mCherry foci accompanied chromosome end-to-end fusions (*mrt-2; pot-1::mCherry* = 8.84±0.16, n=43; *hpr-9; pot-1::mCherry* = 7.98±0.17, n=55). Thus, POT-1::mCherry exacerbates the time-to-sterility by driving early onset telomere fusions. In addition, long telomeric bands did not appear in Southern blots of late-generation *trt-1; pot-1::mCherry* strains (Figure 3.7C and D; Figure 3.6B), so premature uncapping and fusion of long telomeres is unlikely to be responsible for early-onset senescence. Instead, the end-to-end fusions that arise in *trt-1; pot-1::mCherry* strains are likely to be caused by critical telomere shortening, as observed for telomerase single mutant controls (Lowden *et al.* 2008; Lowden *et al.* 2011).
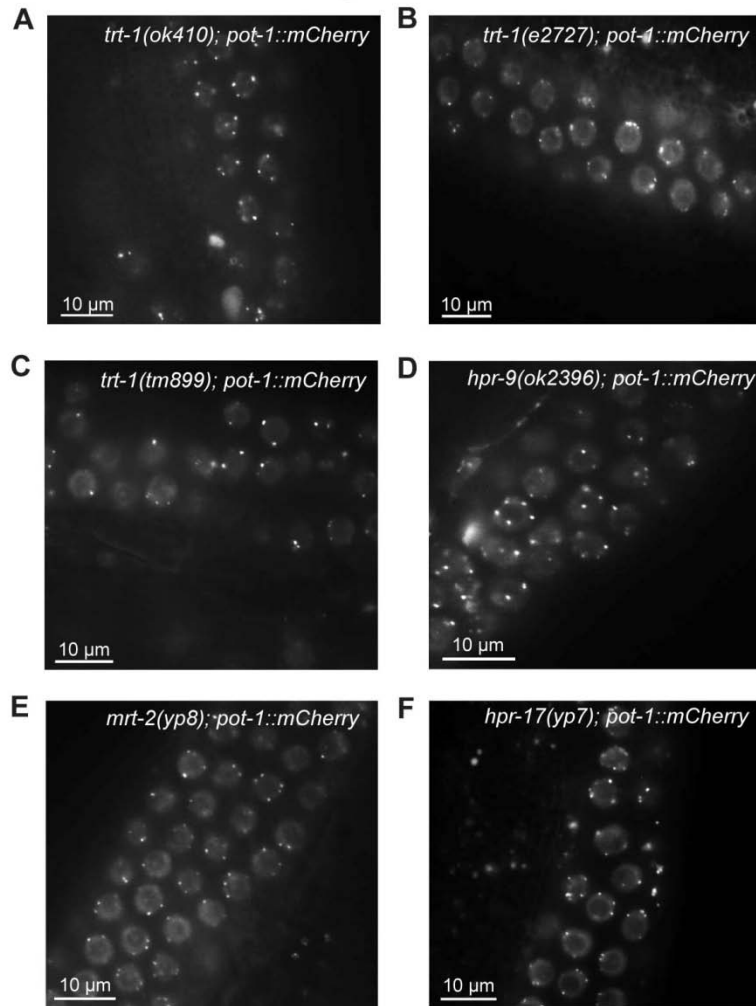
70

Figure 3.8

Figure 3.8. POT-1::mCherry localization in several telomere maintenance-defective mutants. POT-1::mCherry localizes as punctate foci to germline nuclei irrespective of telomerase-mediated telomere repeat addition.

Figure 3.9
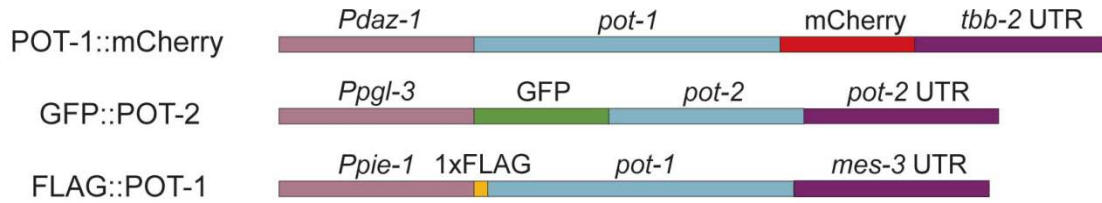
Figure 3.9. Schematic representation of the transgenes constructed.

Table 1.

	Strain	# of chromosomes per oocyte
	wildtype	5.95±0.03
Early-generation	*trt-1(ok410)*	5.96±0.03
	trt-1(tm899); pot-1::mCherry a	5.93±0.04
	trt-1(tm899); pot-1::mCherry b	5.92±0.04
Middle-generation	*trt-1(e2727)*	5.0±0
	hpr-9(ok2396); pot-1::mCherry	5.23±0.09
	mrt-2(yp8); pot-1::mCherry	5.15±0.11
Late-generation	*trt-1(e2727)*	4.83±0.08
	trt-1(tm899); pot-1::mCherry	5.0±0.12
	hpr-17(yp7); pot-1::mCherry	4.69±0.13

Table 1. Haploid number of chromosomes per oocyte in early-, middle- and late-generation strains.

Figure 3.10
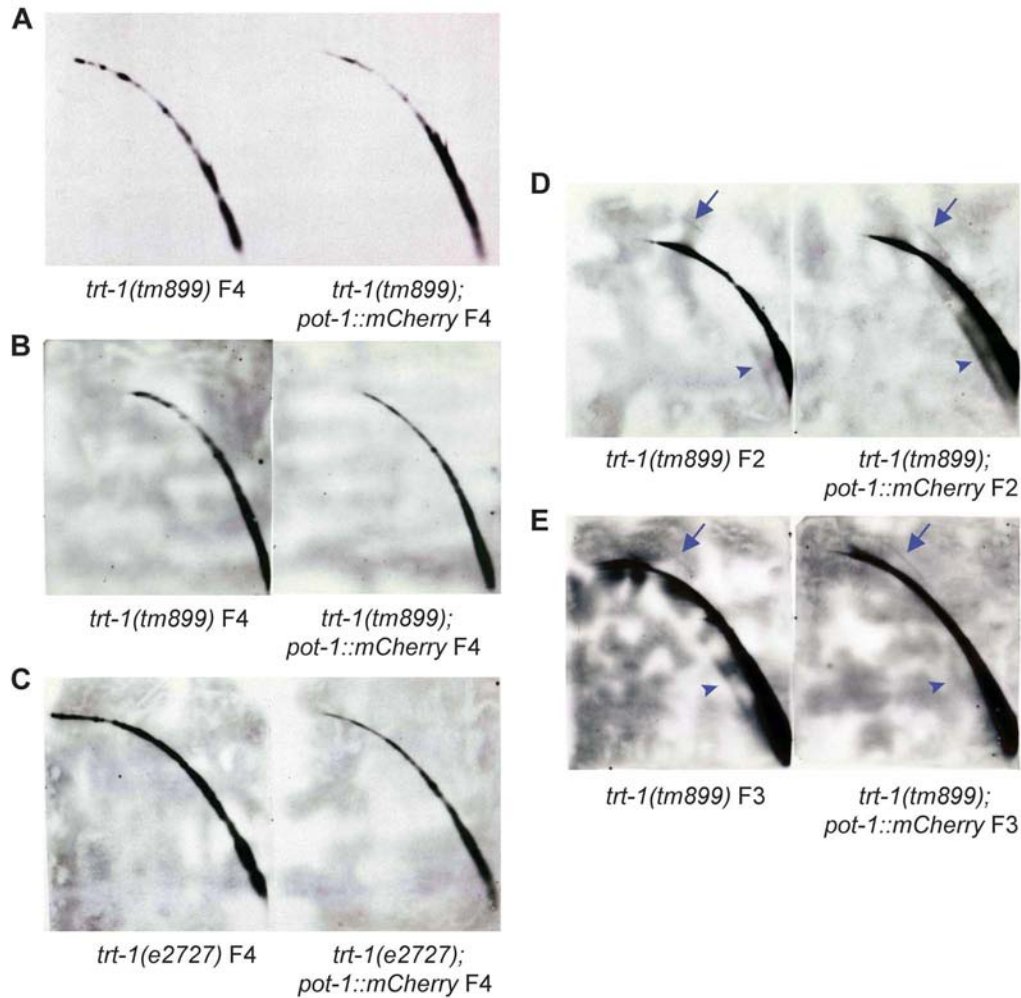
Figure 3.10. Telomerase-deficient pot-1::mCherry mutants do not exhibit higher levels of telomeric circles than telomerase mutants alone. DNA was collected from the fourth generation of several independent telomerase-deficient *pot-1::mCherry* lines and *pot-1::mCherry* only lines (A-C), from F2s (D) and F3s (E), where only ~1/4th of the "*trt-1(tm899)*" animals were homozygous for *trt-1(tm899)* and ~1/16th of the "*trt-1(tm899); pot-1::mCherry*" animals were homozygous for *trt-1(tm899); pot-1::mCherry* in the F2, and subjected to two-dimensional telomere analysis. Telomeric circles (blue arrows) and single-stranded telomeric DNA (arrow heads) can be seen in (D) and (E).

Discussion

POT1 is a multifunctional telomere capping protein, and the presence of four *C. elegans* genes derived from POT1 provides an opportunity to better understand the functions of POT1 in telomere biology. Here I show that *C. elegans* POT-1 and POT-2 single-stranded telomere-binding proteins negatively regulate telomerase-mediated telomere repeat addition. Similar telomere elongation dynamics were observed for *pot-1* and *pot-2* mutants, as well as for *pot-1; pot-2* double mutants. Although POT-1 and POT-2 have been proposed to play distinct roles at telomeres based on their differential affinities for single-stranded G- or C-rich telomeric DNA *in vitro* (Raices *et al.* 2008), my results suggest that these proteins may function together to repress telomerase, even though POT-1 localization to telomeres was not perturbed by mutation of *pot-2*.

POT-1 and POT-2 do have distinct effects on telomere biology, as deficiency for *pot-1* but not *pot-2* modestly increased the rate of telomere erosion in *trt-1* mutants by ~30%, suggesting a telomere capping function of POT-1. POT-1 is the sole POT1-derived *C. elegans* protein with an OB1 fold (Figure 3.1A) and can interact with non-terminal segments of single-stranded telomeric oligonucleotides *in vitro* (Raices *et al.* 2008). Thus, POT-1 may be well positioned to prevent resection of the 5' end of the C-rich strand of the telomere. Consistent with our observations, mammalian POT1 has been shown to protect the 5' end of the telomeric C-strand, which could be subjected to aberrant processing or resection in the absence of POT-1 (Hockemeyer *et al.* 2005). In contrast, the OB2 fold of POT-2 is predicted to interact with the 3' end of single-stranded telomeric overhangs (Raices *et al.* 2008), which could be less relevant to protection or processing of telomeres in the absence of telomerase.

Neither *pot-1* nor *pot-2* mutations strongly enhanced the senescence phenotype of telomerase mutants. Indeed, we observed a longer trans-generational lifespan for *trt-1; pot-1* double mutants vs. *trt-1* single mutants although *trt-1; pot-1* telomeres erode modestly faster. We speculate that mutation of *pot-1* could promote the activity of a telomerase-independent telomere maintenance pathway that extends the proliferative lifespan of *trt-1* mutants. However, these

74

telomerase-deficient strains do not develop a full-blown telomerase-independent telomere maintenance phenotype (ALT) that allows them to escape senescence indefinitely. Consistent with the extended proliferative lifespans of *trt-1; pot-1* double mutants, POT-1 (CeOB2) has been previously proposed to repress telomerase-independent telomere maintenance (Raices *et al.* 2008). Alternatively, although well-outcrossed *pot-1* or *pot-2* mutations with normal telomere lengths were used to construct double mutants with *trt-1*, longer telomeres were detected in some early generation double mutants (Fig. 3.5A and B) in comparison to *trt-1* single mutant controls (Fig. 3.1C and Fig. 3.6A), potentially promoting longer trans-generational lifespans.

Synthetic effects with *pot-1* mutants in the context of a telomerase deficiency have been reported in mice, where Pot1b mutants that are haploinsufficient for telomerase exhibit severe abnormalities, reminiscent of the human disease Dyskeratosis Congenita (DC), in comparison to Pot1b single mutant controls (He *et al.* 2009; Hockemeyer *et al.* 2008). Moreover, Pot1b mutants that are completely deficient for telomerase display dramatically reduced viability due to depletion of hematopoietic stem cells (He *et al.* 2009; Hockemeyer *et al.* 2008; Wang *et al.* 2011), a common ailment in DC patients. In contrast, *C. elegans trt-1; pot-1* double mutants and *trt-1; pot-2; pot-1* triple mutants failed to exacerbate senescence of telomerase mutants. Mutation of a third *C. elegans* POT1-derived OB-fold protein, MRT-1, mimics telomerase deficiency and fails to exacerbate the rate of telomere erosion or the time-to-sterility in *trt-1* mutants (Meier *et al.* 2009).

The modest effects of deficiency for *pot-1* or *pot-2* are at odds with phenotypes reported for mutation of *S. pombe pot1*, which results in an immediate and complete loss of telomeric DNA in the presence of telomerase (Baumann & Cech 2001). Similarly, rapid shortening of *P. patens* Δ*pot1* telomeres is accompanied by chromosomal end-to-end fusions and developmental defects (Shakirov *et al*. 2010). Moreover, *Arabidopsis thaliana* Pot2 truncation mutants exhibit strong dysfunctional telomere phenotypes (Shakirov *et al.* 2005; Surovtseva *et al.* 2007). Therefore, the four genes with POT1 OB-fold domains in *C. elegans* may possess some functions

75

of ancestral POT1, but single and double mutant strains of *pot-1*, *pot-2*, *pot-3* and *mrt-1* that have been studied thus far lack the strong 'deprotection of chromosome termini' phenotype that can be observed in other organisms.

Although deficiency for *C. elegans* POT proteins does not reduce trans-generational lifespan of telomerase mutants, I illustrate that addition of a relatively small C-terminal tag to POT-1 can significantly accelerate the onset of senescence in the absence of telomerase. Expression of POT-1::mCherry shortened trans-generational lifespan of telomerase mutants by ~50% (Figure 3.7A), and led to fertility deficits caused by telomere fusions in earlier generations than observed for single mutant controls (Figure 3.11). This accelerated senescence phenotype contrasts with stark drops in telomere length that cause sudden and rapid lethality or sterility when Pot1 is deficient some species (Baumann & Cech 2001; Shakirov *et al*. 2010; Shakirov *et al.* 2005; Surovtseva *et al.* 2007; Pitt & Cooper 2010). The effect of POT-1::mCherry on telomere stability was complemented by the presence of telomerase, where telomere lengths were normal (Figure 3.1E and F). Similar to my observations, *S. cerevisiae rad52, sgs1, slx5,* and *slx8* mutants senesce prematurely when telomerase is absent but display normal telomere lengths when telomerase is active (Azam *et al.* 2006; Johnson *et al.* 2001; Lowell *et al.* 2003). These proteins repress senescence of telomerase mutants by promoting telomere maintenance via recombination (Azam *et al.* 2006; Burgess *et al*. 2007; Lee *et al*. 2007; Nagai *et al*. 2011). Thus, addition of a carboxy-terminal mCherry tag to *C. elegans* POT-1 could promote premature senescence in the absence of telomerase by disrupting a telomere maintenance mechanism involving recombination between sister chromatids. However, the deleterious *pot-1::mCherry* phenotype did not depend on several DNA damage signaling factors that are likely to interact with *C. elegans* telomeres (Figure 3.7A) and promote sister chromatid-mediated homologous recombination *in vivo* (Azam *et al.* 2006; Burgess *et al*. 2007; Lee *et al*. 2007; Nagai *et al*. 2011; Harris *et al*. 2006).

Figure 3.11

Figure 3.11

A — trt-1(tm899) / trt-1(tm899); pot-1::mCherry

B — trt-1(e2727) / trt-1(e2727); pot-1::mCherry

C — hpr-17(yp7) / hpr-17(yp7); pot-1::mCherry

D — mrt-2(yp8) / mrt-2(yp8); pot-1::mCherry

E — hpr-9(ok2396) / hpr-9(ok2396); pot-1::mCherry

F — mrt-1(e2661) / mrt-1(e2661); pot-1::mCherry

Legend: wildtype, large, medium, small, very small, sterile
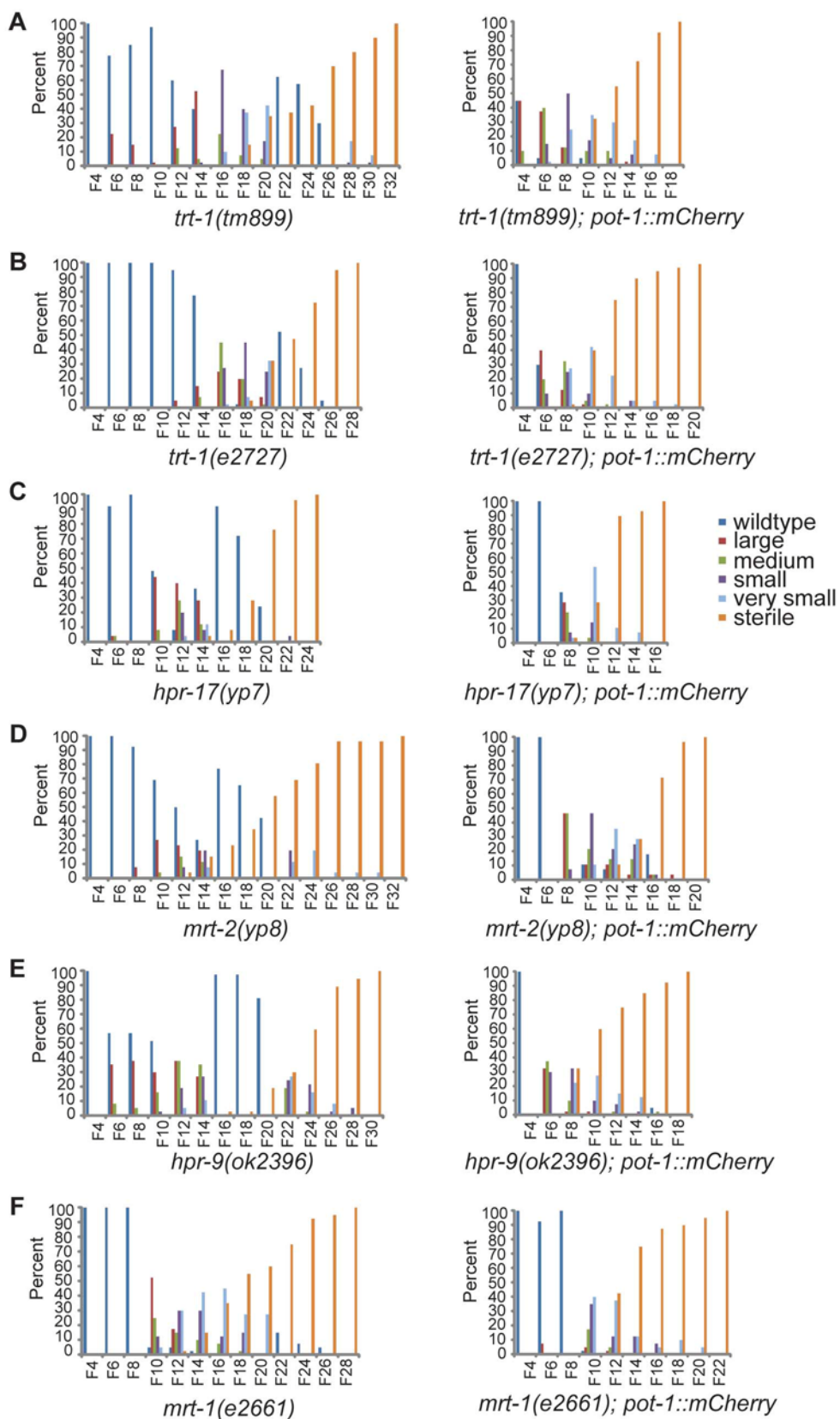
Figure 3.11. The brood size of several telomere maintenance-defective mutants decreases progressively. Brood size at each generation is shown for (A) *trt-1(tm899)* (left, n=40) and *trt-1(tm899); pot-1::mCherry* (right, n=40), (B) *trt-1(e2727)* (left, n=40) and *trt-1(e2727); pot-1::mCherry* (right, n=40), (C) *hpr-17(yp7)* (left, n=25) and *hpr-17(yp7); pot-1::mCherry* (right, n=26), (D) *mrt-2(yp8)* (left, n=26) and *mrt-2(yp8); pot-1::mCherry* (right, n=28), (E) *hpr-9(ok2396)* (left, n=37) and *hpr-9(ok2396); pot-1::mCherry* (right, n=40), and (F) *mrt-1(e2661)* (left, n=40) and *mrt-1(e2661); pot-1::mCherry* (right, n=40).

Premature senescence is also observed for telomerase-deficient *S. cerevisiae* yeast harboring mutations in Ku genes, which encode for proteins that mediate non-homologous end joining and protect the 3' telomeric overhang (Gravel *et al.* 1998). However, yeast Ku mutants exhibit short telomeres when telomerase is wildtype (Boulton & Jackson 1996), and structure-guided mutagenesis experiments have failed to separate this phenotype from premature senescence when telomerase is dysfunctional (Bertuch & Lundblad 2003; Ribes-Zamora *et al.* 2007). In contrast, transgenic POT-1::mCherry did not have an obvious effect on telomere length in *C. elegans* when telomerase was wildtype.

Rapid telomere shortening events have been observed in the presence of wildtype telomerase in mammalian cells. Expression of the reverse transcriptase subunit of telomerase in telomerase-deficient ALT cells with long telomeres restores telomerase activity and promotes rapid telomere shortening, albeit down to wildtype lengths (Ford *et al.* 2001). Similarly, over-expression of the RNA subunit of telomerase in human cells leads to long telomeres that are subjected to rapid telomere shortening, termed telomere trimming, which may be a mechanism for maintaining normal telomere lengths (Pickett *et al.* 2009; Pickett *et al.* 2011). Rapid telomere shortening has also been reported in the presence of a mutant mammalian TRF2 protein lacking its basic domain, TRF2ΔB, which elicits a rapid loss of duplex telomeric DNA and senescence in human and mouse cells (Wang *et al.* 2004). Elongated telomeres and TRF2ΔB induce telomere shortening in the presence of telomerase, unlike the *pot-1::mCherry*-induced effects reported in this study. Thus, if a telomere trimming mechanism is promoted by transgenic POT-1::mCherry, these aberrant shortening events can be readily mended by telomerase. Two-dimensional gel electrophoresis analysis of telomeric DNA from mammalian cells with long telomeres or those expressing TRF2ΔB has revealed t-circles, although TRF2ΔB lines with short telomeres could not be analyzed for t-circles, which cannot be resolved at short sizes. Consistently, detection of t-circles from wildtype *C. elegans* strains, which typically harbor telomeres of 4-9 kb in length, was rare, whereas t-circles were readily observed in *pot-1(tm1620)* and *pot-2(tm1400)* mutants,

which exhibit much longer telomeres (Raices *et al*. 2008). Therefore, the shorter telomere lengths of our strains (<12 kb) could have prevented the detection of t-circles in either *trt-1* single mutants or *pot-1::mCherry; trt-1* double mutants (Figure 3.10), even if telomere rapid deletion via t-circle formation was occurring.

Maintaining proper telomere homeostasis is clinically relevant. Not only does telomere length correlate with age (reviewed in Aubert & Lansdorp 2008), but mutations in RNA and reverse transcriptase subunits of telomerase and associated proteins can cause lethal human diseases such as pulmonary fibrosis and DC, which can affect lung or lymphatic systems (Walne *et al.* 2007; Armanios *et al.* 2007; Vulliamy *et al.* 2008; Vulliamy *et al*. 2005; Walne *et al*. 2008; reviewed in Shtessel & Ahmed 2011). Familial transmission of such mutations results in genetic anticipation, where presentation or disease onset at younger ages occurs in successive generations, due to telomerase dysfunction in germ cells and inheritance of shortened telomeres. A severe form of DC can be caused by missense mutations in the telomere capping protein TIN2, encoded by the *TINF2* gene (Savage *et al*. 2008; Vulliamy *et al.* 2006; Yang *et al.* 2011). *TINF2* patients exhibit more severe disease symptoms than humans who are haploinsufficient for telomerase holoenzyme components. Although most *TINF2* mutations arise *de novo* and cause death at an early age, one individual with a milder array of symptoms was reported to pass on his *TINF2* mutation to two daughters, who exhibited disease symptoms at an earlier age than he did (Walne *et al*. 2008). This single rare case suggests that *TINF2* mutations can cause genetic anticipation and are likely to disrupt telomerase activity in human germ cells.

A significant amount of effort has been dedicated to discerning the mechanisms by which these *TINF2* mutations induce dysfunction. *In vitro* telomerase activity has been shown to be unperturbed by these *TINF2* mutations, but telomerase recruitment to telomeres, mediated predominantly by TPP1, is abrogated (Yang *et al.* 2011). In addition, sister telomere cohesion mediated by HP1γ binding to TIN2 promotes telomerase access to the telomere and is dysfunctional in *TINF2* patients (Houghtaling *et al.* 2012). Moreover, only one of over 20

identified *TINF2* mutations was shown to significantly reduce TIN2 association with TRF1, a canonical telomere-binding protein and known TIN2 binding partner (Sasa *et al.* 2011; Xin & Ly 2012), indicating that *TINF2* mutations drive severe telomere dysfunction without disrupting associations with other shelterin subunits.

The above results suggest that *TINF2* mutations drive dysfunction through perturbing telomerase-mediated telomere repeat addition, and rare biallelic inactivation of telomerase results in strong deficiency for telomerase and causes severe DC-like symptoms of Hoyeraal-Hreidarsson syndrome patients (Walne *et al.* 2008; Savage *et al.* 2008; Sasa *et al.* 2011; Marrone *et al.* 2007). However, the relatively modest effects of mutant TIN2 proteins on telomere length in telomerase-proficient cell lines suggest that gaps remain in understanding precisely how *TINF2* mutations drive disease (Kim *et al.* 1999; Yang *et al.* 2011; Canudas *et al.* 2011; Kim *et al.* 2008). Our study suggests that the severity of *TINF2* mutations could be partially explained by effects that occur in cells that are deficient for telomerase.

Telomere biology has been implicated in distinct human genetic disorders that cause premature aging, such as Werner syndrome and Hutchinson-Gilford Progeria syndrome (HGPS), where telomerase-negative fibroblasts display accelerated telomere shortening accompanied by early-onset senescence (Faragher *et al.* 1993; Huang *et al.* 2008). *Lamin A* mutations cause HGPS (De Sandre-Giovannoli *et al.* 2003; Eriksson *et al.* 2003), and WRN helicase mutations are the predominant cause of classical Werner syndrome (reviewed in Hisama *et al.* 2006). However, *Lamin A* mutations can also cause atypical Werner syndrome, suggesting a mechanistic link between these premature aging disorders (Chen *et al.* 2003; Doh *et al.* 2009; Renard *et al.* 2009). Werner syndrome lymphocytes that can express telomerase *in vivo* do not display premature senescence *in vitro* (James *et al.* 2000), and expression of telomerase can rescue premature senescence of Werner syndrome or HGPS fibroblasts (Benson *et al.* 2010; Wyllie *et al.* 2000). Thus, the effects of these mutations on telomere length may only occur in the absence of telomerase, although formal tests of these possibilities in human stem cells from Werner or HGPS

patients have not been conducted (Decker *et al.* 2009). Further evidence that short telomeres are likely to contribute to Werner and Bloom syndromes comes from studies of mice deficient for WRN or the related RecQ helicase BLM, whose age-related pathologies are exacerbated by deficiency for telomerase (Chang *et al.* 2004; Du *et al.* 2004).

POT1 has been shown to cooperate with WRN at human telomeres (Arnoult *et al.* 2009; Opresko *et al.* 2005), and we speculate that the effects of our POT-1::mCherry transgene may mimic the effects of Werner or HGPS mutations by exacerbating telomere erosion in cells that are deficient for telomerase. Although telomere dysfunction is not the sole defect in these rare disorders, it could be a major factor that contributes to precocious aging. Almost twenty percent of Werner patients remain molecularly undefined (Chen *et al.* 2003), and identification of missense mutations in genes that encode canonical telomere binding proteins, such as POT1, in these patients could lead to elegant tests of the ability of such mutations to cause accelerated telomere erosion and senescence in telomerase-negative rather than telomerase-positive cells. This scenario would clearly establish a role for telomere biology in classically defined syndromes of premature aging.

MATERIALS AND METHODS

Strains

Unless noted otherwise, all strains were cultured at 20°C on Nematode Growth Medium (NGM) plates seeded with *E. coli* OP50. Strains used include Bristol N2 wild type, *dpy-5(e61) I*, *dpy-14 I*, *unc-55 I*, *unc-13 I*, *daf-8 I*, *trt-1(ok410) I*, *trt-1(tm899)*, *trt-1(e2727)*, *mrt-1(e2661)*, *unc-55(e402) I*, *unc-29(e193) I*, *hpr-17(yp7) II*, *pot-2(tm1400) II*, *rol-6(e187) II*, *rol-1 II*, *dpy-1 III*, *unc-93 III*, *dpy-17(e164) III*, *pot-1(tm1620) III*, *unc-32(e189) III*, *vab-7 III*, *dpy-18 III*, *hpr-9(ok2396) III*, and *mrt-2(yp8) III*, *unc-64 III*.

The *pot-1* mutation was outcrossed versus an outcrossed stock of *dpy-17, unc-32*. *pot-2* and *pot-1::mCherry* lines were outcrossed versus outcrossed stocks of *rol-6* or *unc-52*, respectively. Freshly isolated homozygous F2 lines were established for analysis.

To create *pot-1; pot-2* double mutants, a *pot-1; unc-52* double mutant and a *dpy-17, unc-32, pot-2* triple mutant were first created, phenotypically wildtype progeny of *unc-52 / pot-2*; *pot-1 / dpy-17, unc-32* heterozygotes were selected, and the strains that segregated only phenotypically wildtype F3 progeny were retained for analysis.

To create the *trt-1; pot-1* and *trt-1; pot-2* double mutants, *dpy-5, unc-55; pot-1, dpy-5, unc-55; pot-2, trt-1; unc-32, dpy-17,* and *trt-1; unc-52* mutants were generated. Phenotypically wildtype progeny of *dpy-5, unc-55 / trt-1; pot-1 / dpy-17, unc-32* or *dpy-5, unc-55 trt-1; pot-2 / unc-52* heterozygotes were selected, and the strains that segregated only phenotypically wildtype F3 progeny were retained for analysis.

To create the *trt-1; pot-2; pot-1* triple mutant, *trt-1; pot-2; dpy-17 unc-32* and *trt-1; unc-52; pot-1* triple mutants were first created, phenotypically wildtype progeny were selected from *trt-1; pot-2*

/ unc-52; pot-1 / dpy-17 unc-32 heterozygotes, and the strains that segregated only phenotypically wildtype F3 progeny were retained for analysis.

To place the *ypIn2 pot-1::mCherry* transgene into the *pot-1* mutant background, *ypIn2; dpy-17, unc-32* hermaphrodites were crossed to *rol-6 / +; pot-1 / dpy-17, unc-32* males, and phenotypically wildtype F2 progeny were singled from *rol-6 / ypIn2; pot-1 / dpy-17, unc-32* F1, and F2 that segregated only phenotypically wildtype F3 progeny were retained for analysis. *ypIn2 pot-1::mCherry* was placed into the *pot-2* mutant background analogously, where *ypIn2 pot-1::mCherry, unc-52* hermaphrodites were crossed to *rol-6 / +; pot-2 / unc-52* males and phenotypically wildtype F2 progeny were selected. Transgenes were placed into the *trt-1* mutant background analogously, where *dpy-5, unc-55; ypIn2* hermaphrodites were crossed to *trt-1 / dpy-5, unc-55; rol-6 / +* males prior to selecting for loss of marker mutations.

Terminal restriction fragment length analysis

C. elegans genomic DNA was isolated using Gentra Puregene reagents (Qiagen), digested with Hinf*I* enzyme (NEB), and separated on a 0.6% agarose gel at 1.5 V/cm. Southern blotting was performed using the DIG Wash and Block Buffer Set (Roche) following the manufacturer's instructions. A telomere probe, corresponding to the *C. elegans* telomeric repeat TTAGGC, was synthesized and labeled with digoxigenin (DIG)-dUTPs using the PCR DIG Probe Synthesis Kit (Roche) following the manufacturer's instructions.

Transgene construction

All transgene constructs were made using the *MosI*-mediated single-copy insertion system that allows for the incorporation of a single copy of a transgene into one specific locus in the *C. elegans* genome (Frokjaer-Jensen *et al*. 2008). Briefly, the *pot-1::mCherry* transgene was constructed using the Invitrogen Gateway Cloning kit using the positive selection marker *Cb-unc-119(+),* a germ line-specific promoter *daz-1*, full-length genomic *pot-1* sequence lacking a stop

84

codon, *mCherry* sequence, and the *tbb-2* 3' UTR. An extrachromosomal array consisting of this construct, *Pglh-2::Mos1 transposase*, and three fluorescent *mCherry* negative selection markers was introduced into *Mos-1(ttTi5605); unc-119* worms via microinjection into the germline of young adults. Progeny of injected animals were screened for loss of the Unc phenotype and for the presence of mCherry fluorescence, suggesting successful transformation of the injected extrachromosomal array. Lines with successful transformants were further propagated and progeny were screened for loss of co-injection *mCherry* fluorescence markers but continued rescue of the Unc phenotype, indicating successful integration of the construct. Genomic DNA prepared from these lines was tested by PCR and DNA sequencing to confirm the presence of a single-copy insertion in the *Mos-1(ttTi5605)* insertion site on chromosome *II*. PCR was performed on cDNA created from RNA of transgenic strains to confirm transgene expression. *GFP::pot-2* (*pgl-3* promoter, GFP lacking a stop codon, full-length genomic *pot-2* sequence, *pot-2* 3' UTR), *FLAG::pot-1* (*pie-1* promoter, 1xFLAG epitope, full-length genomic *pot-1* sequence with a stop, *mes-3* 3' UTR), *trt-1::FLAG* (*pgl-3* or *pie-1* promoters, full-length genomic *trt-1* sequence, FLAG, *tbb-2* or *mes-3* 3' UTRs), and *FLAG::pot-1* (*pie-1* promoter, FLAG lacking a stop codon, full-length genomic *pot-1* sequence with a stop, *mes-3* 3' UTR) transgenes were constructed analogously. Single-copy transgene insertions were designated *ypIn2 (Pdaz-1::pot-1::mCherry::tbb-2utr)*, *ypIn3 (Pdaz-1::pot-1::mCherry::tbb-2utr)*, *ypIn4 (Ppgl-3::GFP::pot-2)*, and *ypIn5 (Ppie-1::1xFLAG::pot-1::mes-3utr)*.

DAPI staining

One-day-old adult worms were soaked in 150 µL of a 400 ng/mL DAPI in ethanol solution for 30 minutes or until evaporated, rehydrated in 2 mLs M9 solution overnight at 4°C, and mounted in 5 µL of fresh NPG/glycerol medium. Chromosome counts were performed under 100X magnification using a Nikon Eclipse E800 microscope.

POT-1::mCherry foci quantification

Live one-day-old adult worms were mounted onto 2% agarose pads in 5 µL tetramisole and Z stacks were taken within 2 hours of mounting under 100X magnification and X excitation wavelength using a Nikon Eclipse E800 microscope. Foci were quantified by manually scanning through compiled Z stacks.

Interstrand Crosslink Agent Exposure

Cisplatin: A 3.3 mM stock of cisplatin (1 mg/mL stock; APP Pharmaceuticals) was obtained from University of North Carolina—Chapel Hill hospitals, the appropriate amounts to attain desire final concentrations were aliquoted onto 5.5 mL NGM agar plates seeded with bacteria, and plates were allowed to dry overnight at room temperature. One-day-old young adults were singled onto dried plates and allowed to lay eggs for 48 hours before removal. To quantify drug sensitivity, embryonic lethality was calculated as the number of unhatched eggs divided by the total number of eggs laid (hatched + unhatched).

UV-TMP: Trimethyl psoralen (TMP) (Sigma T-6137) was suspended in acetone at a final concentration of 0.5 mg/mL and stored at -20°C wrapped in foil. Fifty young adults were placed into 2 mL S basal solution, 40 µL 0.5 mg/mL TMP was added to the worm+S basal mix, and worms were incubated at RT for 1 hour. Using a pipet, 15 worms were removed from the TMP solution and placed into a 40-µL S basal drop residing on a small petri dish lid resting on top of a UV meter . Worms were irradiated with UVA using a hand-held lamp for 5-30 seconds at 7-8 J/s (where indicated), then droplets were transferred to the edge of fresh NGM plates, and worms were allowed to crawl away from the solution before singling. Worms were singled onto fresh NGM plates for 48 hours and then transferred onto fresh plates for an additional 24 hrs before removal. To quantify drug sensitivity, embryonic lethality was calculated as the number of unhatched eggs divided by the total number of eggs laid (hatched + unhatched) on both plates.

Ionizing Radiation Exposure

One-day-old young adults were exposed to 0 or 60 Gy of ionizing radiation from a cesium source, singled and allowed to lay eggs for 36 hr, transferred to a new plate and allowed to lay eggs for an additional 24 hr before worms were removed. Embryonic lethality was calculated as a measure of drug sensitivity as described above.

Biochemistry

1) Liquid Culture. L1-stage worms were harvested from six freshly-starved 100 mm agarose plates and added, along with concentrated HB101 bacteria, to 500 mL S medium supplemented with 5 mL 10,000 U/ mL penicillin (Cellgro), 10 mg/ mL streptomycin (Cellgro) and 10,000 U/ mL nystatin (Sigma) in a 2.8 L fernbach flask. After 3 days of growth at 20°C, adult worms were harvested through a 35 µM nitex filter. Worms left in the filter were washed once with M9, 1X lysis buffer (50 mM HEPES pH 7.4, 1 mM EGTA, 1 mM $MgCl_2$, 100 mM KCl, 10% glycerol, 0.05% NP-40) and 1X lysis buffer containing a complete Mini, EDTA-free protease inhibitor cocktail tablet (Roche; 1 tablet/12 mL). Worms were centrifuged at 800 g for 2 minutes between washes. A 1:1 mix of worms:lysis buffer was slowly pipetted into liquid nitrogen then ground to a fine powder in a mortar and pestle.

2) Extract Preparation. Thawed ground worm powder was sonicated using a Branson sonication tip for 3 minutes (15 seconds on, 45 seconds off) at 30% amplitude and for 30 seconds at 40% amplitude. Samples were cooled in an ice bath for 2 minutes in between each minute of sonication. Sonicated samples were centrifuged in a Sorvall Ultra80 centrifuge, using a TH-641 rotor, for 11.5K RPM for 10 minutes, then the supernatant was centrifuged at 29K RPM for 20 minutes. The supernatant was frozen in liquid nitrogen in 1- mL aliquots and stored at −80°C.

3) Immunoprecipitation. One hundred microliters of FLAG antibody-conjugated agarose beads (Sigma F2426) were washed twice with 1 mL PBST, once with 1 mL PBS, twice with 1 mL 0.1 M glycine and twice with 1 mL ice cold lysis buffer with 0.1 mM DTT. Beads were centrifuged

at 4°C at 4K RPM for 2 minutes between washes. Beads were rotated for 2 hours at 4°C with 1 mL of clarified extract. Beads were briefly rinsed twice then washed three times, by rotating for 5 minutes at 4°C, with 1 mL 0.1 mM DTT lysis buffer. Beads were incubated with 9 µL of 600 µg/mL FLAG peptide at 4°C for 1 hour in Protein LoBind tubes (Epindorf). Supernatant was transferred to fresh tubes and mixed with equal volume 2X Laemmli sample buffer and stored at −20°C.

4) Western blotting. Samples were analyzed by 12% SDS-PAGE (0.1% SDS). The nitrocellulose membrane was blocked at RT in 5% milk/TBST for 1 hour then incubated with either HRP-conjugated 1° anti-FLAG antibody (Sigma A8592), 1° anti-FLAG antibody (Sigma F3165) followed by a 2° HRP-conjugated anti-mouse antibody, or a 1° anti-GFP antibody (Santa Cruz, sc-9996) followed by a 2° HRP-conjugated anti-mouse antibody. Primary antibodies were used at a 1:500 dilution in TBST overnight at 4°C, and secondary antibodies were used at a 1:10,000 dilution in TBST for 30 minutes at RT. Membrane was washed four times for 10 minutes with TBST shaking at RT then incubated with 2 mL HRP substrate (Amersham) for 5 minutes prior to exposure to film.

Direct telomerase assays

Human conditions: Twenty-six-microliter reactions comprising 10 of µL IP/extract, 1 µL of 25 µM telomere oligo, and 13 µL of reaction mix (6.25 µL 200 mM Tris-Cl, pH 8, 0.625 µL 2M KCl, 0.625 µL 40mM $MgCl_2$, 0.875 µL 142 mM β-mercaptoethanol (made fresh each time), 0.8 µL 31.35 mM spermidine, 0.625 µL 20 mM dATP/dTTP/dCTP mix, 0.73 µL 100 µM dGTP, 2.5 µL 3.3 µM ^{32}P-dGTP) were incubated at 15°C, 20°C or 30°C (where indicated) for 1 hour. One reaction volume of phenol/chloroform was added to each reaction, then tubes were vortexed and centrifuged at 13K RPM for 2 minutes. The top, aqueous layer was removed, one reaction volume of isoamyl alcohol/chloroform was added to each tube, then tubes were vortexed and centrifuged at 13K RPM for 2 minutes. The top layer was transferred to a fresh tube, and the isoamyl

alcohol/chloroform step was repeated. Eighty microliters of ethanol precipitation mix (composed of 3.5 µL 5M NH$_4$OAc, 2 µL 5 µg/µL glycogen, 75 µL 100% EtOH) was added to each tube, vortexed, and stored at -80°C for 10 minutes. Supernatant was discarded, pellet was washed with 60 µL 70% EtOH, supernatant was discarded again, and pellet was dried in a vacuum for 30 minutes. Pellet was resuspended in 6 µL loading buffer (80% formamide, 0.5X TBE, 4 mM EDTA, 0.01% bromo phenol blue, 0.01% xylene cyanol, up to final volume ddH$_2$O), boiled for 3 minutes, and loaded onto an 8% polyacrylamide gel. Samples were resolved at 675V for 50 minutes.

Tetrahymena conditions: Twenty-microliter reactions comprising 10 µL of IP/extract, 2 µL of 25 µM telomere oligo, and 8 µL of reaction mix (2 µL of 10X telomerase buffer [1 µL 1M DTT, 10 µL 1M Tris, pH 8.3, 2.5 µL 100 mM MgCl$_2$, 6.5 µL ddH$_2$O], 1 µL 2mM dTTP/dATP/dCTP mix, 0.2 µL 1mM dGTP, 3 µL ddH$_2$O, 1.7 µL ^{32}P-dGTP) were incubated at 20°C for 1 hour. One reaction volume of phenol/chloroform was added, and precipitation and cleaning steps were performed as for the human conditions.

REFERENCES

Abreu E, Aritonovska E, Reichenbach P, Cristofari G, Culp B, Terns RM, Lingner J, Terns MP. TIN2-tethered TPP1 recruits human telomerase to telomeres in vivo. Mol Cell Biol. 2010 Jun;30(12):2971-82.

Agarwal AK, Fryns JP, Auchus RJ, Garg A. Zinc metalloproteinase, ZMPSTE24, is mutated in mandibuloacral dysplasia. Hum Mol Genet. 2003 Aug 15;12(16):1995-2001.

Ahmed S, Hodgkin J. MRT-2 checkpoint protein is required for germline immortality and telomere replication in C. elegans. Nature. 2000 Jan 13;403(6766):159-64.

Aigner S, Lingner J, Goodrich KJ, Grosshans CA, Shevchenko A, Mann M, Cech TR. Euplotes telomerase contains an La motif protein produced by apparent translational frameshifting. EMBO J. 2000 Nov 15;19(22):6230-9.

Allsopp RC, Vaziri H, Patterson C, Goldstein S, Younglai EV, Futcher AB, Greider CW, Harley CB. Telomere length predicts replicative capacity of human fibroblasts. Proc Natl Acad Sci U S A. 1992 Nov 1;89(21):10114-8.

Alter BP, Rosenberg PS, Giri N, Baerlocher GM, Lansdorp PM, Savage SA. Telomere length is associated with disease severity and declines with age in dyskeratosis congenita. Haematologica. 2012 Mar;97(3):353-9.

Anderson BH, Kasher PR, Mayer J, Szynkiewicz M, Jenkinson EM, Bhaskar SS, Urquhart JE, Daly SB, Dickerson JE, O'Sullivan J, Leibundgut EO, Muter J, Abdel-Salem GM, Babul-Hirji R, Baxter P, Berger A, Bonafé L, Brunstom-Hernandez JE, Buckard JA, Chitayat D, Chong WK, Cordelli DM, Ferreira P, Fluss J, Forrest EH, Franzoni E, Garone C, Hammans SR, Houge G, Hughes I, Jacquemont S, Jeannet PY, Jefferson RJ, Kumar R, Kutschke G, Lundberg S, Lourenço CM, Mehta R, Naidu S, Nischal KK, Nunes L, Ounap K, Philippart M, Prabhakar P, Risen SR, Schiffmann R, Soh C, Stephenson JB, Stewart H, Stone J, Tolmie JL, van der Knaap MS, Vieira JP, Vilain CN, Wakeling EL, Wermenbol V, Whitney A, Lovell SC, Meyer S, Livingston JH, Baerlocher GM, Black GC, Rice GI, Crow YJ. Mutations in CTC1, encoding conserved telomere maintenance component 1, cause Coats plus. Nat Genet. 2012 Jan 22;44(3):338-42.

Armanios MY, Chen JJ, Cogan JD, Alder JK, Ingersoll RG, Markin C, Lawson WE, Xie M, Vulto I, Phillips JA 3rd, Lansdorp PM, Greider CW, Loyd JE. Telomerase mutations in families with idiopathic pulmonary fibrosis. N Eng J Med 2007; 356:1317-26.

Armanios M, Chen JL, Chang YP, Brodsky RA, Hawkins A, Griffin CA, et al. Haploinsufficiency of telomerase reverse transcriptase leads to anticipation in autosomal dominant dyskeratosis congenita. Proc Natl Acad Sci USA 2005; 102:15960-4.

Armbruster BN, Linardic CM, Veldman T, Bansal NP, Downie DL, Counter CM. Rescue of an hTERT mutant defective in telomere elongation by fusion with hPot1. Mol Cell Biol. 2004 Apr;24(8):3552-61.

Arnoult N, Saintome C, Ourliac-Garnier I, Riou JF, Londoño-Vallejo A. Human POT1 is required for efficient telomere C-rich strand replication in the absence of WRN. Genes Dev. 2009 Dec 15;23(24):2915-24.

Aubert G, Lansdorp PM. Telomeres and aging. Physiol Rev. 2008 Apr;88(2):557-79.

Azam M, Lee JY, Abraham V, Chanoux R, Schoenly KA, Johnson FB. Evidence that the S.cerevisiae Sgs1 protein facilitates recombinational repair of telomeres during senescence. Nucleic Acids Res. 2006 Jan 20;34(2):506-16.

Baird DM, Davis T, Rowson J, Jones CJ, Kipling D. Normal telomere erosion rates at the single cell level in Werner syndrome fibroblast cells. Hum Mol Genet. 2004 Jul 15;13(14):1515-24.

Basel-Vanagaite L, Dokal I, Tamary H, Avigdor A, Garty BZ, Volkov A, Vulliamy T. Expanding the clinical phenotype of autosomal dominant dyskeratosis congenita caused by TERT mutations. Haematologica. 2008 Jun;93(6):943-4.

Baumann P, Cech TR. Pot1, the putative telomere end-binding protein in fission yeast and humans. Science. 2001 May 11;292(5519):1171-5.

Baynton K, Otterlei M, Bjørås M, von Kobbe C, Bohr VA, Seeberg E. WRN interacts physically and functionally with the recombination mediator protein RAD52. J Biol Chem. 2003 Sep 19;278(38):36476-86.

Benson EK, Lee SW, Aaronson SA. Role of progerin-induced telomere dysfunction in HGPS premature cellular senescence. J Cell Sci. 2010 Aug 1;123(Pt 15):2605-12.

Bertrand AT, Chikhaoui K, Yaou RB, Bonne G. Clinical and genetic heterogeneity in laminopathies. Biochem Soc Trans. 2011 Dec;39(6):1687-92.

Bertuch AA, Lundblad V. The Ku heterodimer performs separable activities at double-strand breaks and chromosome termini. Mol Cell Biol. 2003 Nov;23(22):8202-15.

Blackburn EH, Gall JG. A tandemly repeated sequence at the termini of the extrachromosomal ribosomal RNA genes in Tetrahymena. J Mol Biol. 1978 Mar 25;120(1):33-53.

Bodnar AG, Ouellette M, Frolkis M, Holt SE, Chiu CP, Morin GB, Harley CB, Shay JW, Lichtsteiner S, Wright WE. Extension of life-span by introduction of telomerase into normal human cells. Science. 1998 Jan 16;279(5349):349-52.

Boerckel J, Walker D, Ahmed S. The Caenorhabditis elegans Rad17 homolog HPR-17 is required for telomere replication. Genetics. 2007 May;176(1):703-9.

Boulton SJ, Jackson SP. Identification of a Saccharomyces cerevisiae Ku80 homologue: roles in DNA double strand break rejoining and in telomeric maintenance. Nucleic Acids Res. 1996 Dec 1;24(23):4639-48.

Burgess RC, Rahman S, Lisby M, Rothstein R, Zhao X. The Slx5-Slx8 complex affects sumoylation of DNA repair proteins and negatively regulates recombination. Mol Cell Biol. 2007 Sep;27(17):6153-62.

Calado RT, Regal JA, Kleiner DE, Schrump DS, Peterson NR, Pons V, et al. A spectrum of severe familial liver disorders associate with telomerase mutations. PLoS One. 2009;4:1–9.

Caspari T, Dahlen M, Kanter-Smoler G, Lindsay HD, Hofmann K, Papadimitriou K, Sunnerhagen P, Carr AM. Characterization of Schizosaccharomyces pombe Hus1: a PCNA-related protein that associates with Rad1 and Rad9. Mol Cell Biol. 2000 Feb;20(4):1254-62.

Chang S, Multani AS, Cabrera NG, Naylor ML, Laud P, Lombard D, Pathak S, Guarente L, DePinho RA. Essential role of limiting telomeres in the pathogenesis of Werner syndrome. Nat Genet. 2004 Aug;36(8):877-82.

Chen JL, Greider CW. Determinants in mammalian telomerase RNA that mediate enzyme processivity and cross-species incompatibility. EMBO J. 2003 Jan 15;22(2):304-14.

Chen L, Lee L, Kudlow BA, Dos Santos HG, Sletvold O, Shafeghati Y, Botha EG, Garg A, Hanson NB, Martin GM, Mian IS, Kennedy BK, Oshima J. LMNA mutations in atypical Werner's syndrome. Lancet. 2003 Aug 9;362(9382):440-5.

Chen MJ, Lin YT, Lieberman HB, Chen G, Lee EY. ATM-dependent phosphorylation of human Rad9 is required for ionizing radiation-induced checkpoint activation. J Biol Chem. 2001 May 11;276(19):16580-6.

Cheung I, Schertzer M, Baross A, Rose AM, Lansdorp PM, Baird DM. Strain-specific telomere length revealed by single telomere length analysis in Caenorhabditis elegans. Nucleic Acids Res. 2004 Jun 24;32(11):3383-91.

Cheung I, Schertzer M, Rose A, Lansdorp PM. High incidence of rapid telomere loss in telomerase-deficient Caenorhabditis elegans. Nucleic Acids Res. 2006 Jan 10;34(1):96-103.

Chiu CP, Dragowska W, Kim NW, Vaziri H, Yui J, Thomas TE, Harley CB, Lansdorp PM. Differential expression of telomerase activity in hematopoietic progenitors from adult human bone marrow. Stem Cells. 1996 Mar;14(2):239-48.

Cifuentes-Rojas C, Kannan K, Tseng L, Shippen DE. Two RNA subunits and POT1a are components of Arabidopsis telomerase. Proc Natl Acad Sci U S A. 2011 Jan 4;108(1):73-78.

Cimprich KA, Cortez D. ATR: an essential regulator of genome integrity. Nat Rev Mol Cell Biol. 2008 Aug;9(8):616-27.

Clericuzio C, Harutyunyan K, Jin W, Erickson RP, Irvine AD, McLean WH, Wen Y, Bagatell R, Griffin TA, Shwayder TA, Plon SE, Wang LL. Identification of a novel C16orf57 mutation in Athabaskan patients with Poikiloderma with Neutropenia. Am J Med Genet A. 2011 Feb;155A(2):337-42.
Collins K. The biogenesis and regulation of telomerase holoenzymes. Nat Rev Mol Cell Biol. 2006 Jul;7(7):484-94.

Collins K, Kobayashi R, Greider CW. Purification of Tetrahymena telomerase and cloning of genes encoding the two protein components of the enzyme. Cell. 1995 Jun 2;81(5):677-86.

Constantinou A, Tarsounas M, Karow JK, Brosh RM, Bohr VA, Hickson ID, West SC. Werner's syndrome protein (WRN) migrates Holliday junctions and co-localizes with RPA upon replication arrest. EMBO Rep. 2000 Jul;1(1):80-4.
Cooper MP, Machwe A, Orren DK, Brosh RM, Ramsden D, Bohr VA. Ku complex interacts with and stimulates the Werner protein. Genes Dev. 2000 Apr 15;14(8):907-12.

Cooper JP, Watanabe Y, Nurse P. Fission yeast Taz1 protein is required for meiotic telomere clustering and recombination. Nature. 1998 Apr 23;392(6678):828-31.

Crow YJ, McMenamin J, Haenggeli CA, Hadley DM, Tirupathi S, Treacy EP, Zuberi SM, Browne BH, Tolmie JL, Stephenson JB. Coats' plus: a progressive familial syndrome of bilateral Coats' disease, characteristic cerebral calcification, leukoencephalopathy, slow pre- and post-natal linear growth and defects of bone marrow and integument. Neuropediatrics. 2004 Feb;35(1):10-9.

Dahlen M, Olsson T, Kanter-Smoler G, Ramne A, Sunnerhagen P. Regulation of telomere length by checkpoint genes in Schizosaccharomyces pombe. Mol Biol Cell. 1998 Mar;9(3):611-21.

Decker ML, Chavez E, Vulto I, Lansdorp PM. Telomere length in Hutchinson-Gilford progeria syndrome. Mech Ageing Dev. 2009 Jun;130(6):377-83.

Déjardin J, Kingston RE. Purification of proteins associated with specific genomic Loci. Cell. 2009 Jan 9;136(1):175-86.

Dernburg AF, Zalevsky J, Colaiácovo MP, Villeneuve AM. Transgene-mediated cosuppression in the C. elegans germ line. Genes Dev. 2000 Jul 1;14(13):1578-83.

Dernburg AF, McDonald K, Moulder G, Barstead R, Dresser M, Villeneuve AM. Meiotic recombination in C. elegans initiates by a conserved mechanism and is dispensable for homologous chromosome synapsis. Cell. 1998 Aug 7;94(3):387-98.

DeZwaan DC, Freeman BC. The conserved Est1 protein stimulates telomerase DNA extension activity. Proc Natl Acad Sci U S A. 2009 Oct 13;106(41):17337-42.

Diaz de Leon A, Cronkhite JT, Katzenstein AL, Godwin JD, Raghu G, Glazer CS, Rosenblatt RL, Girod CE, Garrity ER, Xing C, Garcia CK. Telomere lengths, pulmonary fibrosis and telomerase (TERT) mutations. PLoS One. 2010 May 19;5(5):e10680.

Diotti R, Loayza D. Shelterin complex and associated factors at human telomeres. Nucleus. 2011 Mar-Apr;2(2):119-35.

Doh YJ, Kim HK, Jung ED, Choi SH, Kim JG, Kim BW, Lee IK. Novel LMNA gene mutation in a patient with Atypical Werner's Syndrome. Korean J Intern Med. 2009 Mar;24(1):68-72.

Dokal I. Dyskeratosis congenita. Hematology Am Soc Hematol Educ Program. 2011;2011:480-6.

Du X, Shen J, Kugan N, Furth EE, Lombard DB, Cheung C, Pak S, Luo G, Pignolo RJ, DePinho RA, Guarente L, Johnson FB. Telomere shortening exposes functions for the mouse Werner and Bloom syndrome genes. Mol Cell Biol. 2004 Oct;24(19):8437-46.

Ellis NA, German J. Molecular genetics of Bloom's syndrome. Hum Mol Genet. 1996;5 Spec No:1457-63.

Eriksson M, Brown WT, Gordon LB, Glynn MW, Singer J, Scott L, Erdos MR, Robbins CM, Moses TY, Berglund P, Dutra A, Pak E, Durkin S, Csoka AB, Boehnke M, Glover TW, Collins FS. Recurrent de novo point mutations in lamin A cause Hutchinson-Gilford progeria syndrome. Nature. 2003 May 15;423(6937):293-8.

Faragher RG, Kill IR, Hunter JA, Pope FM, Tannock C, Shall S. The gene responsible for Werner syndrome may be a cell division "counting" gene. Proc Natl Acad Sci U S A. 1993 Dec 15;90(24):12030-4.

Fay, D. and Bender, A. SNPs: Introduction and two-point mapping (September 25, 2008), *WormBook*, ed. The *C. elegans* Research Community, WormBook, doi/10.1895/wormbook.1.93.2

Ford LP, Zou Y, Pongracz K, Gryaznov SM, Shay JW, Wright WE. Telomerase can inhibit the recombination-based pathway of telomere maintenance in human cells. J Biol Chem. 2001 276:32198-203.

Francia S, Weiss RS, Hande MP, Freire R, d'Adda di Fagagna F. Telomere and telomerase modulation by the mammalian Rad9/Rad1/Hus1 DNA-damage-checkpoint complex. Curr Biol. 2006 Aug 8;16(15):1551-8.

Frøkjaer-Jensen C, Davis MW, Hopkins CE, Newman BJ, Thummel JM, Olesen SP, Grunnet M, Jorgensen EM. Single-copy insertion of transgenes in Caenorhabditis elegans. Nat Genet. 2008 Nov;40(11):1375-83.

Fry M, Loeb LA. Human werner syndrome DNA helicase unwinds tetrahelical structures of the fragile X syndrome repeat sequence d(CGG)n. J Biol Chem. 1999 Apr 30;274(18):12797-802.

Fu D, Collins K. Purification of human telomerase complexes identifies factors involved in telomerase biogenesis and telomere length regulation. Mol Cell. 2007 Dec 14;28(5):773-85.

Ghosh A, Rossi ML, Aulds J, Croteau D, Bohr VA. Telomeric D-loops containing 8-oxo-2'-deoxyguanosine are preferred substrates for Werner and Bloom syndrome helicases and are bound by POT1. J Biol Chem. 2009 Nov 6;284(45):31074-84.

Goldman F, Bouarich R, Kulkarni S, Freeman S, Du HY, Harrington L, Mason PJ, Londoño-Vallejo A, Bessler M. The effect of TERC haploinsufficiency on the inheritance of telomere length. Proc Natl Acad Sci U S A. 2005 Nov 22;102(47):17119-24.

Gray MD, Shen JC, Kamath-Loeb AS, Blank A, Sopher BL, Martin GM, Oshima J, Loeb LA. The Werner syndrome protein is a DNA helicase. Nat Genet. 1997 Sep;17(1):100-3.
Gravel S, Larrivée M, Labrecque P, Wellinger RJ. Yeast Ku as a regulator of chromosomal DNA end structure. Science. 1998 May 1;280(5364):741-4.

Greider CW, Blackburn EH. Identification of a specific telomere terminal transferase activity in Tetrahymena extracts. Cell. 1985 Dec;43(2 Pt 1):405-13.

Greider CW, Blackburn EH. A telomeric sequence in the RNA of Tetrahymena telomerase required for telomere repeat synthesis. Nature. 1989 Jan 26;337(6205):331-7.

Griffith JD, Comeau L, Rosenfield S, Stansel RM, Bianchi A, Moss H, de Lange T. Mammalian telomeres end in a large duplex loop. Cell. 1999 May 14;97(4):503-14.

Hagelstrom RT, Blagoev KB, Niedernhofer LJ, Goodwin EH, Bailey SM. Hyper telomere recombination accelerates replicative senescence and may promote premature aging. Proc Natl Acad Sci U S A. 2010 Sep 7;107(36):15768-73.

Hardy CF, Sussel L, Shore D. A RAP1-interacting protein involved in transcriptional silencing and telomere length regulation. Genes Dev. 1992 May;6(5):801-14.

Harley CB, Futcher AB, Greider CW. Telomeres shorten during ageing of human fibroblasts. Nature. 1990 May 31;345(6274):458-60.

Harris J, Lowden M, Clejan I, Tzoneva M, Thomas JH, Hodgkin J, Ahmed S. Mutator phenotype of Caenorhabditis elegans DNA damage checkpoint mutants. Genetics. 2006 Oct;174(2):601-16.

He H, Multani AS, Cosme-Blanco W, Tahara H, Ma J, Pathak S, Deng Y, Chang S. POT1b protects telomeres from end-to-end chromosomal fusions and aberrant homologous recombination. EMBO J. 2006 Nov 1;25(21):5180-90.

He H, Wang Y, Guo X, Ramchandani S, Ma J, Shen MF, Garcia DA, Deng Y, Multani AS, You MJ, Chang S. Pot1b deletion and telomerase haploinsufficiency in mice initiate an ATR-dependent DNA damage response and elicit phenotypes resembling dyskeratosis congenita. Mol Cell Biol. 2009 Jan;29(1):229-40.

Heiss NS, Knight SW, Vulliamy TJ, Klauck SM, Wiemann S, Mason PJ, Poustka A, Dokal I. X-linked dyskeratosis congenita is caused by mutations in a highly conserved gene with putative nucleolar functions. Nat Genet. 1998 May;19(1):32-8.

Hemann MT, Strong MA, Hao LY, Greider CW. The shortest telomere, not average telomere length, is critical for cell viability and chromosome stability. Cell. 2001 Oct 5;107(1):67-77.

Hisama FM, Bohr VA, Oshima J. WRN's tenth anniversary. Sci Aging Knowledge Environ. 2006 Jun 28;2006(10):pe18.

Hockemeyer D, Daniels JP, Takai H, de Lange T. Recent expansion of the telomeric complex in rodents: Two distinct POT1 proteins protect mouse telomeres. Cell. 2006 Jul 14;126(1):63-77.

Hockemeyer D, Palm W, Wang RC, Couto SS, de Lange T. Engineered telomere degradation models dyskeratosis congenita. Genes Dev. 2008 Jul 1;22(13):1773-85.

Hockemeyer D, Sfeir AJ, Shay JW, Wright WE, de Lange T. POT1 protects telomeres from a transient DNA damage response and determines how human chromosomes end. EMBO J. 2005 Jul 20;24(14):2667-78.

Hofmann ER, Milstein S, Boulton SJ, Ye M, Hofmann JJ, Stergiou L, Gartner A, Vidal M, Hengartner MO. Caenorhabditis elegans HUS-1 is a DNA damage checkpoint protein required for genome stability and EGL-1-mediated apoptosis. Curr Biol. 2002 Nov 19;12(22):1908-18.

Hopkins KM, Auerbach W, Wang XY, Hande MP, Hang H, Wolgemuth DJ, Joyner AL, Lieberman HB. Deletion of mouse rad9 causes abnormal cellular responses to DNA damage, genomic instability, and embryonic lethality. Mol Cell Biol. 2004 Aug;24(16):7235-48.

Hou YY, Toh MT, Wang X. NBS1 deficiency promotes genome instability by affecting DNA damage signaling pathway and impairing telomere integrity. Cell Biochem Funct. 2012 Apr;30(3):233-42.

Houghtaling BR, Canudas S, Smith S. A role for sister telomere cohesion in telomere elongation by telomerase. Cell Cycle. 2012 Jan 1;11(1):19-25.

Huang S, Lee L, Hanson NB, Lenaerts C, Hoehn H, Poot M, Rubin CD, Chen DF, Yang CC, Juch H, Dorn T, Spiegel R, Oral EA, Abid M, Battisti C, Lucci-Cordisco E, Neri G, Steed EH, Kidd A, Isley W, Showalter D, Vittone JL, Konstantinow A, Ring J, Meyer P, Wenger SL, von Herbay A, Wollina U, Schuelke M, Huizenga CR, Leistritz DF, Martin GM, Mian IS, Oshima J. The spectrum of WRN mutations in Werner syndrome patients. Hum Mutat. 2006 Jun;27(6):558-67.

Huang S, Li B, Gray MD, Oshima J, Mian IS, Campisi J. The premature ageing syndrome protein, WRN, is a 3'-->5' exonuclease. Nat Genet. 1998 Oct;20(2):114-6.

Huang S, Risques RA, Martin GM, Rabinovitch PS, Oshima J. Accelerated telomere shortening and replicative senescence in human fibroblasts overexpressing mutant and wild-type lamin A. Exp Cell Res. 2008 Jan 1;314(1):82-91.

Hughes TR, Evans SK, Weilbaecher RG, Lundblad V. The Est3 protein is a subunit of yeast telomerase. Curr Biol. 2000 Jun 29;10(13):809-12.

Ishikawa N, Nakamura K, Izumiyama-Shimomura N, Aida J, Ishii A, Goto M, Ishikawa Y, Asaka R, Matsuura M, Hatamochi A, Kuroiwa M, Takubo K. Accelerated in vivo epidermal telomere loss in Werner syndrome. Aging (Albany NY). 2011 Apr;3(4):417-29.

James SE, Faragher RG, Burke JF, Shall S, Mayne LV. Werner's syndrome T lymphocytes display a normal in vitro life-span. Mech Ageing Dev. 2000 Dec 20;121(1-3):139-49.

Johnson FB, Marciniak RA, McVey M, Stewart SA, Hahn WC, Guarente L. The Saccharomyces cerevisiae WRN homolog Sgs1p participates in telomere maintenance in cells lacking telomerase. EMBO J. 2001 Feb 15;20(4):905-13.

Kanoh J, Ishikawa F. spRap1 and spRif1, recruited to telomeres by Taz1, are essential for telomere function in fission yeast. Curr Biol. 2001 Oct 16;11(20):1624-30.

Karlseder J, Smogorzewska A, de Lange T. Senescence induced by altered telomere state, not telomere loss. Science. 2002 Mar 29;295(5564):2446-9.

Kendellen MF, Barrientos KS, Counter CM. POT1 association with TRF2 regulates telomere length. Mol Cell Biol. 2009 Oct;29(20):5611-9.

Kilian A, Bowtell DD, Abud HE, Hime GR, Venter DJ, Keese PK, Duncan EL, Reddel RR, Jefferson RA. Isolation of a candidate human telomerase catalytic subunit gene, which reveals complex splicing patterns in different cell types. Hum Mol Genet. 1997 Nov;6(12):2011-9.

Kim SH, Beausejour C, Davalos AR, Kaminker P, Heo SJ, Campisi J. TIN2 mediates functions of TRF2 at human telomeres. J Biol Chem. 2004 Oct 15;279(42):43799-804.

Kim M, Xu L, Blackburn EH. Catalytically active human telomerase mutants with allele-specific biological properties. Exp Cell Res. 2003 Aug 15;288(2):277-87.

Kim SH, Kaminker P, Campisi J. TIN2, a new regulator of telomere length in human cells. Nat Genet. 1999 Dec;23(4):405-12.

Kim NW, Piatyszek MA, Prowse KR, Harley CB, West MD, Ho PL, Coviello GM, Wright WE, Weinrich SL, Shay JW. Specific association of human telomerase activity with immortal cells and cancer. Science. 1994 Dec 23;266(5193):2011-5.

Kipling D, Cooke HJ. Hypervariable ultra-long telomeres in mice. Nature. 1990 Sep 27;347(6291):400-2.

Kitao S, Ohsugi I, Ichikawa K, Goto M, Furuichi Y, Shimamoto A. Cloning of two new human helicase genes of the RecQ family: biological significance of multiple species in higher eukaryotes. Genomics. 1998 Dec 15;54(3):443-52.

Kitao S, Shimamoto A, Goto M, Miller RW, Smithson WA, Lindor NM, Furuichi Y. Mutations in RECQL4 cause a subset of cases of Rothmund-Thomson syndrome. Nat Genet. 1999 May;22(1):82-4.

Klobutcher LA, Swanton MT, Donini P, Prescott DM. All gene-sized DNA molecules in four species of hypotrichs have the same terminal sequence and an unusual 3' terminus. Proc Natl Acad Sci U S A. 1981 May;78(5):3015-9.

Knight SW, Heiss NS, Vulliamy TJ, Aalfs CM, McMahon C, Richmond P, Jones A, Hennekam RC, Poustka A, Mason PJ, Dokal I. Unexplained aplastic anaemia, immunodeficiency, and cerebellar hypoplasia (Hoyeraal-Hreidarsson syndrome) due to mutations in the dyskeratosis congenita gene, DKC1. Br J Haematol. 1999 Nov;107(2):335-9.

Kolquist KA, Ellisen LW, Counter CM, Meyerson M, Tan LK, Weinberg RA, Haber DA, Gerald WL. Expression of TERT in early premalignant lesions and a subset of cells in normal tissues. Nat Genet. 1998 Jun;19(2):182-6.

Larizza L, Roversi G, Volpi L. Rothmund-Thomson syndrome. Orphanet J Rare Dis. 2010 Jan 29;5:2.

Lebel M, Leder P. A deletion within the murine Werner syndrome helicase induces sensitivity to inhibitors of topoisomerase and loss of cellular proliferative capacity. Proc Natl Acad Sci U S A. 1998 Oct 27;95(22):13097-102.

Lee HW, Blasco MA, Gottlieb GJ, Horner JW 2nd, Greider CW, DePinho RA. Essential role of mouse telomerase in highly proliferative organs. Nature. 1998 Apr 9;392(6676):569-74.

Lee JY, Kozak M, Martin JD, Pennock E, Johnson FB. Evidence that a RecQ helicase slows senescence by resolving recombining telomeres. PLoS Biol. 2007 Jun;5(6):e160

Lei M, Zaug AJ, Podell ER, Cech TR. Switching human telomerase on and off with hPOT1 protein in vitro. J Biol Chem. 2005 May 27;280(21):20449-56.

Levy MZ, Allsopp RC, Futcher AB, Greider CW, Harley CB. Telomere end-replication problem and cell aging. J Mol Biol. 1992 Jun 20;225(4):951-60.

Li B, Comai L. Functional interaction between Ku and the werner syndrome protein in DNA end processing. J Biol Chem. 2000 Sep 15;275(37):28349-52.

Li B, Jog SP, Reddy S, Comai L. WRN controls formation of extrachromosomal telomeric circles and is required for TRF2DeltaB-mediated telomere shortening. Mol Cell Biol. 2008 Mar;28(6):1892-904.

Li B, de Lange T. Rap1 affects the length and heterogeneity of human telomeres. Mol Biol Cell. 2003 Dec;14(12):5060-8.

Li B, Oestreich S, de Lange T. Identification of human Rap1: implications for telomere evolution. Cell. 2000 May 26;101(5):471-83.

Linger BR, Morin GB, Price CM. The Pot1a-associated proteins Tpt1 and Pat1 coordinate telomere protection and length regulation in Tetrahymena. Mol Biol Cell. 2011 Nov;22(21):4161-70.

Lingner J, Cech TR. Purification of telomerase from Euplotes aediculatus: requirement of a primer 3' overhang. Proc Natl Acad Sci U S A. 1996 Oct 1;93(20):10712-7.

Lingner J, Cech TR, Hughes TR, Lundblad V. Three Ever Shorter Telomere (EST) genes are dispensable for in vitro yeast telomerase activity. Proc Natl Acad Sci U S A. 1997 Oct 14;94(21):11190-5.

Liu D, Safari A, O'Connor MS, Chan DW, Laegeler A, Qin J, Songyang Z. PTOP interacts with POT1 and regulates its localization to telomeres. Nat Cell Biol. 2004 Jul;6(7):673-80.

Loayza D, De Lange T. POT1 as a terminal transducer of TRF1 telomere length control. Nature. 2003 Jun 26;423(6943):1013-8.

Lombard DB, Beard C, Johnson B, Marciniak RA, Dausman J, Bronson R, Buhlmann JE, Lipman R, Curry R, Sharpe A, Jaenisch R, Guarente L. Mutations in the WRN gene in mice accelerate mortality in a p53-null background. Mol Cell Biol. 2000 May;20(9):3286-91.

Longhese MP. DNA damage response at functional and dysfunctional telomeres. Genes Dev. 2008 Jan 15;22(2):125-40.

Longhese MP, Paciotti V, Neecke H, Lucchini G. Checkpoint proteins influence telomeric silencing and length maintenance in budding yeast. Genetics. 2000 Aug;155(4):1577-91.

Lowden MR, Flibotte S, Moerman DG, Ahmed S. DNA synthesis generates terminal duplications that seal end-to-end chromosome fusions. Science. 2011 Apr 22;332(6028):468-71.

Lowden MR, Meier B, Lee TW, Hall J, Ahmed S. End joining at Caenorhabditis elegans telomeres. Genetics. 2008 Oct;180(2):741-54.

Lowell JE, Roughton AI, Lundblad V, Pillus L. Telomerase-independent proliferation is influenced by cell type in Saccharomyces cerevisiae. Genetics. 2003 Jul;164(3):909-21.

Lue NF, Bosoy D, Moriarty TJ, Autexier C, Altman B, Leng S. Telomerase can act as a template- and RNA-independent terminal transferase. Proc Natl Acad Sci U S A. 2005 Jul 12;102(28):9778-83.

Lydall D, Weinert T. Yeast checkpoint genes in DNA damage processing: implications for repair and arrest. Science. 1995 Dec 1;270(5241):1488-91.

Machwe A, Lozada E, Wold MS, Li GM, Orren DK. Molecular cooperation between the Werner syndrome protein and replication protein A in relation to replication fork blockage. J Biol Chem. 2011 Feb 4;286(5):3497-508.

Maizels N. Dynamic roles for G4 DNA in the biology of eukaryotic cells. Nat Struct Mol Biol. 2006 Dec;13(12):1055-9.

Marrone A, Walne A, Tamary H, Masunari Y, Kirwan M, Beswick R, Vulliamy T, Dokal I. Telomerase reverse-transcriptase homozygous mutations in autosomal recessive dyskeratosis congenita and Hoyeraal-Hreidarsson syndrome. Blood. 2007 Dec 15;110(13):4198-205.

Mason DX, Autexier C, Greider CW. Tetrahymena proteins p80 and p95 are not core telomerase components. Proc Natl Acad Sci U S A. 2001 Oct 23;98(22):12368-73.

Masutomi K, Possemato R, Wong JM, Currier JL, Tothova Z, Manola JB, Ganesan S, Lansdorp PM, Collins K, Hahn WC. The telomerase reverse transcriptase regulates chromatin state and DNA damage responses. Proc Natl Acad Sci U S A. 2005 Jun 7;102(23):8222-7.

McClintock B. The Behavior in Successive Nuclear Divisions of a Chromosome Broken at Meiosis. Proc Natl Acad Sci U S A. 1939 Aug;25(8):405-16.

Meier B, Barber LJ, Liu Y, Shtessel L, Boulton SJ, Gartner A, Ahmed S. The MRT-1 nuclease is required for DNA crosslink repair and telomerase activity in vivo in Caenorhabditis elegans. EMBO J. 2009 Nov 18;28(22):3549-63.

Meier B, Clejan I, Liu Y, Lowden M, Gartner A, Hodgkin J, Ahmed S. trt-1 is the Caenorhabditis elegans catalytic subunit of telomerase. PLoS Genet. 2006 Feb;2(2):e18.

Miller MC, Collins K. The Tetrahymena p80/p95 complex is required for proper telomere length maintenance and micronuclear genome stability. Mol Cell. 2000 Oct;6(4):827-37.

Mitchell JR, Cheng J, Collins K. A box H/ACA small nucleolar RNA-like domain at the human telomerase RNA 3' end. Mol Cell Biol. 1999 Jan;19(1):567-76.

Mitchell JR, Wood E, Collins K. A telomerase component is defective in the human disease dyskeratosis congenita. Nature. 1999 Dec 2;402(6761):551-5.

Miyake Y, Nakamura M, Nabetani A, Shimamura S, Tamura M, Yonehara S, Saito M, Ishikawa F. RPA-like mammalian Ctc1-Stn1-Ten1 complex binds to single-stranded DNA and protects telomeres independently of the Pot1 pathway. Mol Cell. 2009 Oct 23;36(2):193-206.

Moyzis RK, Buckingham JM, Cram LS, Dani M, Deaven LL, Jones MD, Meyne J, Ratliff RL, Wu JR. A highly conserved repetitive DNA sequence, (TTAGGG)n, present at the telomeres of human chromosomes. Proc Natl Acad Sci U S A. 1988 Sep;85(18):6622-6.

Muftuoglu M, Oshima J, von Kobbe C, Cheng WH, Leistritz DF, Bohr VA. The clinical characteristics of Werner syndrome: molecular and biochemical diagnosis. Hum Genet. 2008 Nov;124(4):369-77.

Murray AW, Schultes NP, Szostak JW. Chromosome length controls mitotic chromosome segregation in yeast. Cell. 1986 May 23;45(4):529-36.

Nabetani A, Yokoyama O, Ishikawa F. Localization of hRad9, hHus1, hRad1, and hRad17 and caffeine-sensitive DNA replication at the alternative lengthening of telomeres-associated promyelocytic leukemia body. J Biol Chem. 2004 Jun 11;279(24):25849-57.

Nagai S, Davoodi N, Gasser SM. Nuclear organization in genome stability: SUMO connections. Cell Res. 2011 Mar;21(3):474-85.

Nakamura TM, Moser BA, Russell P. Telomere binding of checkpoint sensor and DNA repair proteins contributes to maintenance of functional fission yeast telomeres. Genetics. 2002 Aug;161(4):1437-52.

O'Connor MS, Safari A, Liu D, Qin J, Songyang Z. The human Rap1 protein complex and modulation of telomere length. J Biol Chem. 2004 Jul 2;279(27):28585-91.

O'Connor MS, Safari A, Xin H, Liu D, Songyang Z. A critical role for TPP1 and TIN2 interaction in high-order telomeric complex assembly. Proc Natl Acad Sci U S A. 2006 Aug 8;103(32):11874-9.

Opresko PL, Mason PA, Podell ER, Lei M, Hickson ID, Cech TR, Bohr VA. POT1 stimulates RecQ helicases WRN and BLM to unwind telomeric DNA substrates. J Biol Chem. 2005 Sep 16;280(37):32069-80.

Opresko PL, Otterlei M, Graakjaer J, Bruheim P, Dawut L, Kølvraa S, May A, Seidman MM, Bohr VA. The Werner syndrome helicase and exonuclease cooperate to resolve telomeric D loops in a manner regulated by TRF1 and TRF2. Mol Cell. 2004 Jun 18;14(6):763-74.

Opresko PL, von Kobbe C, Laine JP, Harrigan J, Hickson ID, Bohr VA. Telomere-binding protein TRF2 binds to and stimulates the Werner and Bloom syndrome helicases. J Biol Chem. 2002 Oct 25;277(43):41110-9.

Opresko PL, Mason PA, Podell ER, Lei M, Hickson ID, Cech TR, Bohr VA. POT1 stimulates RecQ helicases WRN and BLM to unwind telomeric DNA substrates. J Biol Chem. 2005 Sep 16;280(37):32069-80.

Oshima J, Yu CE, Piussan C, Klein G, Jabkowski J, Balci S, Miki T, Nakura J, Ogihara T, Ells J, Smith M, Melaragno MI, Fraccaro M, Scappaticci S, Matthews J, Ouais S, Jarzebowicz A, Schellenberg GD, Martin GM. Homozygous and compound heterozygous mutations at the Werner syndrome locus. Hum Mol Genet. 1996 Dec;5(12):1909-13.

Pandita RK, Sharma GG, Laszlo A, Hopkins KM, Davey S, Chakhparonian M, Gupta A, Wellinger RJ, Zhang J, Powell SN, Roti Roti JL, Lieberman HB, Pandita TK. Mammalian Rad9 plays a role in telomere stability, S- and G2-phase-specific cell survival, and homologous recombinational repair. Mol Cell Biol. 2006 Mar;26(5):1850-64.

Parrilla-Castellar ER, Arlander SJ, Karnitz L. Dial 9-1-1 for DNA damage: the Rad9-Hus1-Rad1 (9-1-1) clamp complex. DNA Repair (Amst). 2004 Aug-Sep;3(8-9):1009-14.

Patro BS, Frøhlich R, Bohr VA, Stevnsner T. WRN helicase regulates the ATR-CHK1-induced S-phase checkpoint pathway in response to topoisomerase-I-DNA covalent complexes. J Cell Sci. 2011 Dec 1;124(Pt 23):3967-79.
Phillips LG, Sale JE. The Werner's Syndrome protein collaborates with REV1 to promote replication fork progression on damaged DNA. DNA Repair (Amst). 2010 Oct 5;9(10):1064-72.

Pichierri P, Nicolai S, Cignolo L, Bignami M, Franchitto A. The RAD9-RAD1-HUS1 (9.1.1) complex interacts with WRN and is crucial to regulate its response to replication fork stalling. Oncogene. 2011 Oct 17. doi: 10.1038/onc.2011.468.

Pickett HA, Cesare AJ, Johnston RL, Neumann AA, Reddel RR. Control of telomere length by a trimming mechanism that involves generation of t-circles. EMBO J. 2009 Apr 8;28(7):799-809.

Pickett HA, Henson JD, Au AY, Neumann AA, Reddel RR. Normal mammalian cells negatively regulate telomere length by telomere trimming. Hum Mol Genet. 2011 Dec 1;20(23):4684-92

Pitt CW, Cooper JP. Pot1 inactivation leads to rampant telomere resection and loss in one cell cycle. Nucleic Acids Res. 2010 Nov;38(20):6968-75.

Prowse KR, Greider CW. Developmental and tissue-specific regulation of mouse telomerase and telomere length. Proc Natl Acad Sci U S A. 1995 May 23;92(11):4818-22.

Raices M, Verdun RE, Compton SA, Haggblom CI, Griffith JD, Dillin A, Karlseder J. C. elegans telomeres contain G-strand and C-strand overhangs that are bound by distinct proteins. Cell. 2008 Mar 7;132(5):745-57.

Renard D, Fourcade G, Milhaud D, Bessis D, Esteves-Vieira V, Boyer A, Roll P, Bourgeois P, Levy N, De Sandre-Giovannoli A. Novel LMNA mutation in atypical Werner syndrome presenting with ischemic disease. Stroke. 2009 Feb;40(2):e11-4.

Ribes-Zamora A, Mihalek I, Lichtarge O, Bertuch AA. Distinct faces of the Ku heterodimer mediate DNA repair and telomeric functions. Nat Struct Mol Biol. 2007 Apr;14(4):301-7.

Richards EJ, Ausubel FM. Isolation of a higher eukaryotic telomere from Arabidopsis thaliana. Cell. 1988 Apr 8;53(1):127-36.

Richter T, Saretzki G, Nelson G, Melcher M, Olijslagers S, von Zglinicki T. TRF2 overexpression diminishes repair of telomeric single-strand breaks and accelerates telomere shortening in human fibroblasts. Mech Ageing Dev. 2007 Apr;128(4):340-5.

Riha K, Fajkus J, Siroky J, Vyskot B. Developmental control of telomere lengths and telomerase activity in plants. Plant Cell. 1998 Oct;10(10):1691-8.

Ropp JD, Donahue CJ, Wolfgang-Kimball D, Hooley JJ, Chin JY, Hoffman RA, Cuthbertson RA, Bauer KD. Aequorea green fluorescent protein analysis by flow cytometry. Cytometry. 1995 Dec 1;21(4):309-17.

Saito RM, Perreault A, Peach B, Satterlee JS, van den Heuvel S. The CDC-14 phosphatase controls developmental cell-cycle arrest in C. elegans. Nat Cell Biol. 2004 Aug;6(8):777-83.

De Sandre-Giovannoli A, Bernard R, Cau P, Navarro C, Amiel J, Boccaccio I, Lyonnet S, Stewart CL, Munnich A, Le Merrer M, Lévy N. Lamin a truncation in Hutchinson-Gilford progeria. Science. 2003 Jun 27;300(5628):2055.

Sarper N, Zengin E, Kılıç SÇ. A child with severe form of dyskeratosis congenita and TINF2 mutation of shelterin complex. Pediatr Blood Cancer. 2010 Dec 1;55(6):1185-6.

Sasa G, Ribes-Zamora A, Nelson N, Bertuch A. Three novel truncating TINF2 mutations causing severe dyskeratosis congenita in early childhood. Clin Genet. 2012 May;81(5):470-8.

Savage SA. Connecting complex disorders through biology. Nat Genet. 2012 Feb 27;44(3):238-40.

Savage SA, Giri N, Baerlocher GM, Orr N, Lansdorp PM, Alter BP. TINF2, a component of the shelterin telomere protection complex, is mutated in dyskeratosis congenita. Am J Hum Genet. 2008 Feb;82(2):501-9.

Schulz VP, Zakian VA, Ogburn CE, McKay J, Jarzebowicz AA, Edland SD, Martin GM. Accelerated loss of telomeric repeats may not explain accelerated replicative decline of Werner syndrome cells. Hum Genet. 1996 Jun;97(6):750-4.

Sfeir AJ, Chai W, Shay JW, Wright WE. Telomere-end processing the terminal nucleotides of human chromosomes. Mol Cell. 2005 Apr 1;18(1):131-8.

Shackleton S, Smallwood DT, Clayton P, Wilson LC, Agarwal AK, Garg A, Trembath RC. Compound heterozygous ZMPSTE24 mutations reduce prelamin A processing and result in a severe progeroid phenotype. J Med Genet. 2005 Jun;42(6):e36.

Shakirov EV, Perroud PF, Nelson AD, Cannell ME, Quatrano RS, Shippen DE. Protection of Telomeres 1 is required for telomere integrity in the moss Physcomitrella patens. Plant Cell. 2010 Jun;22(6):1838-48.

Shakirov EV, Surovtseva YV, Osbun N, Shippen DE. The Arabidopsis Pot1 and Pot2 proteins function in telomere length homeostasis and chromosome end protection. Mol Cell Biol. 2005 Sep;25(17):7725-33.
Shampay J, Szostak JW, Blackburn EH. DNA sequences of telomeres maintained in yeast. Nature. 1984 Jul 12-18;310(5973):154-7.
Sharma HW, Sokoloski JA, Perez JR, Maltese JY, Sartorelli AC, Stein CA, Nichols G, Khaled Z, Telang NT, Narayanan R. Differentiation of immortal cells inhibits telomerase activity. Proc Natl Acad Sci U S A. 1995 Dec 19;92(26):12343-6.

Shay JW, Wright WE. Role of telomeres and telomerase in cancer. Semin Cancer Biol. 2011 Dec;21(6):349-53.

Shtessel L, Ahmed S. Telomere dysfunction in human bone marrow failure syndromes. Nucleus. 2011 Jan-Feb;2(1):24-9.

Silverman J, Takai H, Buonomo SB, Eisenhaber F, de Lange T. Human Rif1, ortholog of a yeast telomeric protein, is regulated by ATM and 53BP1 and functions in the S-phase checkpoint. Genes Dev. 2004 Sep 1;18(17):2108-19.

Smogorzewska A, van Steensel B, Bianchi A, Oelmann S, Schaefer MR, Schnapp G, de Lange T. Control of human telomere length by TRF1 and TRF2. Mol Cell Biol. 2000 Mar;20(5):1659-68.

Sogabe Y, Yasuda M, Yokoyama Y, Tamura A, Negishi I, Ohnishi K, Shinozaki T, Ishikawa O. Genetic analyses of two cases of Werner's syndrome. Eur J Dermatol. 2004 Nov-Dec;14(6):379-82.

van Steensel B, de Lange T. Control of telomere length by the human telomeric protein TRF1. Nature. 1997 Feb 20;385(6618):740-3.

St Onge RP, Udell CM, Casselman R, Davey S. The human G2 checkpoint control protein hRAD9 is a nuclear phosphoprotein that forms complexes with hRAD1 and hHUS1. Mol Biol Cell. 1999 Jun;10(6):1985-95.

Steiner BR, Hidaka K, Futcher B. Association of the Est1 protein with telomerase activity in yeast. Proc Natl Acad Sci U S A. 1996 Apr 2;93(7):2817-21.

Surovtseva YV, Shakirov EV, Vespa L, Osbun N, Song X, Shippen DE. Arabidopsis POT1 associates with the telomerase RNP and is required for telomere maintenance. EMBO J. 2007 Aug 8;26(15):3653-61.

Szostak JW, Blackburn EH. Cloning yeast telomeres on linear plasmid vectors. Cell. 1982 May;29(1):245-55.

Takai KK, Kibe T, Donigian JR, Frescas D, de Lange T. Telomere protection by TPP1/POT1 requires tethering to TIN2. Mol Cell. 2011 Nov 18;44(4):647-59.

Tomaska L, Nosek J, Kramara J, Griffith JD. Telomeric circles: universal players in telomere maintenance? Nat Struct Mol Biol. 2009 Oct;16(10):1010-5.

Touzot F, Callebaut I, Soulier J, Gaillard L, Azerrad C, Durandy A, Fischer A, de Villartay JP, Revy P. Function of Apollo (SNM1B) at telomere highlighted by a splice variant identified in a patient with Hoyeraal-Hreidarsson syndrome. Proc Natl Acad Sci U S A. 2010 Jun 1;107(22):10097-102.

Touzot F, Gaillard L, Vasquez N, Le Guen T, Bertrand Y, Bourhis J, Leblanc T, Fischer A, Soulier J, de Villartay JP, Revy P. Heterogeneous telomere defects in patients with severe forms of dyskeratosis congenita. J Allergy Clin Immunol. 2012 Feb;129(2):473-82

Tsakiri KD, Cronkhite JT, Kuan PJ, Xing C, Raghu G, Weissler JC, et al. Adult-onset pulmonary fibrosis caused by mutations in telomerase. Proc Natl Acad Sci USA. 2007;104:7552–7557.

Venteicher AS, Abreu EB, Meng Z, McCann KE, Terns RM, Veenstra TD, Terns MP, Artandi SE. A human telomerase holoenzyme protein required for Cajal body localization and telomere synthesis. Science. 2009 Jan 30;323(5914):644-8.

Venteicher AS, Meng Z, Mason PJ, Veenstra TD, Artandi SE. Identification of ATPases pontin and reptin as telomerase components essential for holoenzyme assembly. Cell. 2008 Mar 21;132(6):945-57.

Veldman T, Etheridge KT, Counter CM. Loss of hPot1 function leads to telomere instability and a cut-like phenotype. Curr Biol. 2004 Dec 29;14(24):2264-70.

Volpi L, Roversi G, Colombo EA, Leijsten N, Concolino D, Calabria A, Mencarelli MA, Fimiani M, Macciardi F, Pfundt R, Schoenmakers EF, Larizza L. Targeted next-generation sequencing appoints c16orf57 as clericuzio-type poikiloderma with neutropenia gene. Am J Hum Genet. 2010 Jan;86(1):72-6.

Vulliamy T, Beswick R, Kirwan M, Marrone A, Digweed M, Walne A, Dokal I. Mutations in the telomerase component NHP2 cause the premature ageing syndrome dyskeratosis congenita. Proc Natl Acad Sci USA 2008; 105:8073-8.

Vulliamy T, Marrone A, Dokal I, Mason PJ. Association between aplastic anaemia and mutations in telomerase RNA. Lancet. 2002 Jun 22;359(9324):2168-70.

Vulliamy T, Marrone A, Goldman F, Dearlove A, Bessler M, Mason PJ, Dokal I. The RNA component of telomerase is mutated in autosomal dominant dyskeratosis congenita. Nature. 2001 Sep 27;413(6854):432-5.

Vulliamy TJ, Marrone A, Knight SW, Walne A, Mason PJ, Dokal I. Mutations in dyskeratosis congenita: their impact on telomere length and the diversity of clinical presentation. Blood. 2006 Apr 1;107(7):2680-5.

Vulliamy T, Marrone A, Szydlo R, Walne A, Mason PJ, Dokal I. Disease anticipation is associated with progressive telomere shortening in families with dyskeratosis congenita due tomutations in TERC. Nat Genet 2004;36:447-9.

Vulliamy TJ, Walne A, Baskaradas A, Mason PJ, Marrone A, Dokal I. Mutations in the reverse transcriptase component of telomerase (TERT) in patients with bone marrow failure. Blood Cells Mol Dis. 2005; 34:257-63.

Walne AJ, Vulliamy T, Beswick R, Kirwan M, Dokal I. Mutations in C16orf57 and normal-length telomeres unify a subset of patients with dyskeratosis congenita, poikiloderma with neutropenia and Rothmund-Thomson syndrome. Hum Mol Genet. 2010 Nov 15;19(22):4453-61.

Walne AJ, Vulliamy T, Beswick R, Kirwan M, Dokal I. TINF2 mutations result in very short telomeres: analysis of a large cohort of patients with dyskeratosis congenita and related bone marrow failure syndromes. Blood 2008; 112:3594-600.

Walne AJ, Vulliamy T, Marrone A, Beswick R, Kirwan M, Masunari Y, Al-Qurashi FH, Aljurf M, Dokal I. Genetic heterogeneity in autosomal recessive dyskeratosis congenita with one subtype due to mutations in the telomerase-associated protein NOP10. Hum Mol Genet. 2007; 16:1619-29.

Wang Y, Shen MF, Chang S. Essential roles for Pot1b in HSC self-renewal and survival. Blood. 2011 Dec 1;118(23):6068-77.

Wang RC, Smogorzewska A, de Lange T. Homologous recombination generates T-loop-sized deletions at human telomeres. Cell. 2004 Oct 29;119(3):355-68.

Watson JM, Shippen DE. Telomere rapid deletion regulates telomere length in Arabidopsis thaliana. Mol Cell Biol. 2007 Mar;27(5):1706-15.

Weinert TA, Hartwell LH. The RAD9 gene controls the cell cycle response to DNA damage in Saccharomyces cerevisiae. Science. 1988 Jul 15;241(4863):317-22.

Weiss RS, Enoch T, Leder P. Inactivation of mouse Hus1 results in genomic instability and impaired responses to genotoxic stress. Genes Dev. 2000 Aug 1;14(15):1886-98.

Wicks SR, Yeh RT, Gish WR, Waterston RH, Plasterk RH. Rapid gene mapping in Caenorhabditis elegans using a high density polymorphism map. Nat Genet. 2001 Jun;28(2):160-4.

Wicky C, Villeneuve AM, Lauper N, Codourey L, Tobler H, Müller F. Telomeric repeats (TTAGGC)n are sufficient for chromosome capping function in Caenorhabditis elegans. Proc Natl Acad Sci U S A. 1996 Aug 20;93(17):8983-8.

Witkin KL, Collins K. Holoenzyme proteins required for the physiological assembly and activity of telomerase. Genes Dev. 2004 May 15;18(10):1107-18.

Witkin KL, Prathapam R, Collins K. Positive and negative regulation of Tetrahymena telomerase holoenzyme. Mol Cell Biol. 2007 Mar;27(6):2074-83.

Wu L, Multani AS, He H, Cosme-Blanco W, Deng Y, Deng JM, Bachilo O, Pathak S, Tahara H, Bailey SM, Deng Y, Behringer RR, Chang S. Pot1 deficiency initiates DNA damage checkpoint activation and aberrant homologous recombination at telomeres. Cell. 2006 Jul 14;126(1):49-62.

Wyllie FS, Jones CJ, Skinner JW, Haughton MF, Wallis C, Wynford-Thomas D, Faragher RG, Kipling D. Telomerase prevents the accelerated cell ageing of Werner syndrome fibroblasts. Nat Genet. 2000 Jan;24(1):16-7.

Xin H, Liu D, Wan M, Safari A, Kim H, Sun W, O'Connor MS, Songyang Z. TPP1 is a homologue of ciliate TEBP-beta and interacts with POT1 to recruit telomerase. Nature. 2007 Feb 1;445(7127):559-62.

Xin ZT, Ly H. Characterization of interactions between naturally mutated forms of the TIN2 protein and its known protein partners of the shelterin complex. Clin Genet. 2011 Dec 30.

Xu L, Blackburn EH. Human Rif1 protein binds aberrant telomeres and aligns along anaphase midzone microtubules. J Cell Biol. 2004 Dec 6;167(5):819-30.

Yamaguchi H, Baerlocher GM, Lansdorp PM, Chanock SJ, Nunez O, Sloand E, Young NS. Mutations of the human telomerase RNA gene (TERC) in aplastic anemia and myelodysplastic syndrome. Blood. 2003 Aug 1;102(3):916-8.

Yamaguchi H, Calado RT, Ly H, Kajigaya S, Baerlocher GM, Chanock SJ, Lansdorp PM, Young NS. Mutations in TERT, the gene for telomerase reverse transcriptase, in aplastic anemia. N Engl J Med. 2005 Apr 7;352(14):1413-24.

Yamamoto A, Hiraoka Y. How do meiotic chromosomes meet their homologous partners?: lessons from fission yeast. Bioessays. 2001 Jun;23(6):526-33.

Yang D, He Q, Kim H, Ma W, Songyang Z. TIN2 protein dyskeratosis congenita missense mutants are defective in association with telomerase. J Biol Chem. 2011 Jul 1;286(26):23022-30.

Ye JZ, Donigian JR, van Overbeek M, Loayza D, Luo Y, Krutchinsky AN, Chait BT, de Lange T. TIN2 binds TRF1 and TRF2 simultaneously and stabilizes the TRF2 complex on telomeres. J Biol Chem. 2004 Nov 5;279(45):47264-71.

Ye JZ, Hockemeyer D, Krutchinsky AN, Loayza D, Hooper SM, Chait BT, de Lange T. POT1-interacting protein PIP1: a telomere length regulator that recruits POT1 to the TIN2/TRF1 complex. Genes Dev. 2004 Jul 15;18(14):1649-54.

Ye JZ, de Lange T. TIN2 is a tankyrase 1 PARP modulator in the TRF1 telomere length control complex. Nat Genet. 2004 Jun;36(6):618-23.

Yu CE, Oshima J, Fu YH, Wijsman EM, Hisama F, Alisch R, Matthews S, Nakura J, Miki T, Ouais S, Martin GM, Mulligan J, Schellenberg GD. Positional cloning of the Werner's syndrome gene. Science. 1996 Apr 12;272(5259):258-62.

Zahn TR, Angleson JK, MacMorris MA, Domke E, Hutton JF, Schwartz C, Hutton JC. Dense core vesicle dynamics in Caenorhabditis elegans neurons and the role of kinesin UNC-104. Traffic. 2004 Jul;5(7):544-59.

Zhong F, Savage SA, Shkreli M, Giri N, Jessop L, Myers T, Chen R, Alter BP, Artandi SE. Disruption of telomerase trafficking by TCAB1 mutation causes dyskeratosis congenita. Genes Dev. 2011 Jan 1;25(1):11-6.

Zhu L, Hathcock KS, Hande P, Lansdorp PM, Seldin MF, Hodes RJ. Telomere length regulation in mice is linked to a novel chromosome locus. Proc Natl Acad Sci U S A. 1998 Jul 21;95(15):8648-53.

Zou L, Elledge SJ. Sensing DNA damage through ATRIP recognition of RPA-ssDNA complexes. Science. 2003 Jun 6;300(5625):1542-8.